Diversity of transduction mechanisms in receptor neurons of the main olfactory epithelium in *Xenopus laevis* tadpoles

PhD Thesis

in partial fulfillment of the requirements
for the degree of Doctor of Philosophy (PhD)
in the Graduate Program Neurosciences
at the Georg-August University Göttingen
Faculty of Biology

submitted by
Ivan Manzini

born in
Bolzano, Italy

Göttingen 2002

Advisor, first member of FAC: Prof. Dr. Dr. Detlev Schild
Second member of FAC: Prof. Dr. Friedrich-Wilhelm Schürmann
Third member of FAC: Prof. Dr. Walter Stühmer

Date of submission of the PhD Thesis: December 12th , 2002

Day of Thesis Defense (Disputation): January 29th , 2003

Herewith I declare, that I prepared the PhD Thesis
'Diversity of transduction mechanisms in receptor neurons of the main olfactory epithelium in *Xenopus laevis* tadpoles'
on my own and with no other sources and aids than quoted.

Göttingen, December 12th , 2002

....
Ivan Manzini

CONTENTS

3. Results   38

Summary

The results of this thesis can be split into five major parts.

1) A thorough comparison of two preparations of olfactory receptor neurons (ORNs) was made using the patch-clamp technique. A slice preparation of the olfactory epithelium of *Xenopus laevis* tadpoles was used to record odorant responses of ORNs, and these responses were compared to odorant responses recorded in isolated ORNs. The maximum recording time in the slice was considerably longer than in isolated ORNs, which is essential when many odorants are to be tested. No odorant-induced responses could be obtained from isolated ORNs recorded in the on-cell mode, while recordings in the slice (on-cell and whole-cell) as well as previously reported perforated-patch recordings in isolated ORNs of the same species (Vogler and Schild, 1999) were successful, though qualitatively different. In the slice preparation, amino acids as well as an extract from *Spirulina* algae always induced excitatory responses, while in the previous study on isolated ORNs, responses were either excitatory or inhibitory. The results of this study show that ORNs obtained with different preparation techniques can give markedly different responses upon the application of odorants. This information is important for future studies on odorant transduction as well as for the interpretation of past studies on odorant responses of ORNs. Furthermore, the experiments indicate that the slice preparation combined with the on-cell configuration of the patch-clamp technique is the method of choice for testing many odorants on a large number of individual ORNs.

2) Using the patch-clamp technique and calcium imaging it was shown in a clear and unambiguous way that a number of amino acids are transduced through a cAMP-independent pathway in the main olfactory epithelium of *Xenopus laevis* tadpoles. Both amino acids and pharmacological agents activating the cAMP pathway (forskolin and pCPT-cAMP) proved to be potent stimuli for ORNs in a mucosa slice of *Xenopus laevis* tadpoles. Interestingly, the ensemble of ORNs that was activated by amino acids differed markedly from the ensemble of ORNs activated by forskolin and pCPT-cAMP. Therefore, we conclude that ORNs of *Xenopus laevis* tadpoles have both cAMP-dependent and cAMP-independent olfactory

transduction pathways and that a number of amino acids are transduced in a cAMP-independent way.

3) The differential processing of cAMP-mediated stimuli on one hand and amino acid stimuli on the other was further elucidated by calcium imaging of olfactory bulb neurons using a novel nose-olfactory bulb preparation of *Xenopus laevis* tadpoles. The projection pattern of amino acid-sensitive ORNs to the olfactory bulb (OB) differed markedly from the projection pattern of ORNs sensitive to cAMP pathway activators. Olfactory bulb neurons activated by amino acids were located laterally compared to those activated by pharmacological agents activating the cAMP-pathway (forskolin, IBMX and pCPT-cAMP), and only a small proportion responded to both stimuli. We therefore conclude that amino acid- and cAMP-mediated responses are processed differentially at the level of the OB.

4) Using the patch-clamp technique and calcium imaging technique the response spectra to amino acids of a number of ORNs could be determined. The calcium imaging technique resulted to be the method of choice to determine the specificity profiles of ORNs. The advantage of calcium imaging compared to the patch-clamp technique is the possibility of simultaneously testing many ORNs in a slice for their responsiveness to amino acids. The data so far obtained are auspicious but more experiments have to be performed to be able to thoroughly classify individual ORNs regarding their response spectra to amino acids.

5) Futhermore, the results show for the first time that ORNs possess transporter systems that expel xenobiotics across the plasma membrane. Using calcein and calcium-indicator dyes as xenobiotics it could be demonstrated that ORNs appear to express the multidrug resistance P-glycoprotein (MDR1) and multidrug resistance-associated proteins (MRP). This endows ORNs with the capability of transporting a large number of substrates including calcium-indicator dyes and calcein across their plasma membranes. Conversely, blocking P-glycoprotein and MRP increases the net uptake of these dyes. This was crucial for the feasibility of calcium imaging experiments in mucosa slices. It was necessary to block these transporters in order to be able to load the ORNs with calcium-indicator dyes and to carry out the imaging experiments.

Publishing note:

The results of this thesis are/will be published in the following papers:

-Manzini I, Peters F, Schild D (2002) Odorant responses of *Xenopus laevis* tadpole olfactory neurons: a comparison between preparations. J Neurosci Methods 121: 159-167

-Manzini I, Rössler W, Schild D (2002) cAMP-independent responses of olfactory neurons in *Xenopus laevis* tadpoles and their projection onto olfactory bulb neurons. J Physiol (Lond) 545: 475-484

-Manzini I, Schild D (2003) Multidrug resistance transporters in the olfactory receptor neurons of *Xenopus laevis* tadpoles. J Physiol (Lond) 546: 375-385

-Manzini I, Schild D. cAMP-independent olfactory transduction of amino acids in *Xenopus laevis* tadpoles. (under revision)

1. Introduction

1.1 The sense of smell

The sense of smell is an ancient sense. Early in evolution a common chemical sense endowed primitive organisms with the ability to locate food or avoid harmful substances. This "first sense" was fundamental for the progress of evolution. From this ancient chemical sense the senses of smell and taste developed. To date the sense of smell is of major importance for survival of most species. It is of fundamental importance to identify food, predators and it is crucial for reproduction. For us humans, it is certainly not as important as for most other species, at least at first sight. Most of us would probably rely more on vision and hearing than on the sense of smell. We very often do not realize its importance until we lose it. It is believed that we have about 1000 genes encoding odorant receptors, this is about 1% of the genes of our genome. This staggering number of receptors reflects the crucial importance of the sense of smell. There is strong evidence that the sense of smell influences mood, memory, mate choice, emotions, the endocrine system, and the immune system. Most anosmic people suffer from depression and their quality of life is severely affected. At the moment, there is little that can be done to help them as the sense of smell, despite the progress made in the last decade, is still poorly understood.

1.2 The organization of the olfactory system

Odorants are the natural stimuli of olfactory receptor neurons (ORNs). Depending on the different animal species, they reach the peripheral olfactory system via air or via water. The ORNs are located in the olfactory epithelium (Figure 1), where they are in direct contact with the animal's environment. The olfactory epithelium is build up by three principal cell types: ORNs, sustentacular cells and basal cells. It is covered by a layer of mucus produced primarily by the olfactory glands (Bowman's glands) and the sustentacular cells (for reviews, see Getchell *et al*. 1984; Getchell, 1986; Gold, 1999; Schild and Restrepo, 1998).

Olfactory receptor neurons are bipolar neurons, with a small soma, a single dendrite which ends with an olfactory knob bearing cilia or microvilli and an axon projecting to the olfactory

bulb (OB). The highly specialized cilia or microvilli are the site of initiation of olfactory transduction (Schild and Restrepo, 1998).

Sustentacular cells are supportive cells sharing common features with glia. Their principal task is to isolate ORNs electrically and to produce constituents of the mucus. They were also reported to contain detoxifying enzymes such as P450-like enzymes and UDP glucuronosyl transferase (UGT; Okano and Takagi, 1974; Getchell, 1986; Lazard *et al.* 1991).

The basal cells are precursors of new ORNs. Olfactory receptor neurons are exposed to the environment and therefore in direct contact with cytotoxic substances. That is probably the reason of their relatively short lifetime, not longer than a few months on the average. The basal cells are therefore of crucial importance in the maintenance of the sense of smell (Ronnett and Moon, 2002).

The axons of ORNs terminate in glomeruli in the OB (Figure 1) forming glutamatergic synapses with dentrites of mitral cells, the output neurons of the OB. The mitral cells also form synapses with interneurons, the so-called periglomerular cells, located in the vicinity of the glomeruli. The GABAergic granule cells are another type of interneurons forming synaptic contacts with mitral cells. The axons of mitral cells leave the OB via the lateral olfactory tract and convey the olfactory signals to higher cerebral structures, mainly to the limbic system and the neocortex (Scott, 1986; Nezlin and Schild, 2000).

1.3 The molecular mechanisms of odor perception

Before reaching the ORNs, odorants have to pass through an aqueous mucus barrier toward the cilia of the ORNs. The main protein constituents of the mucus are odorant-binding proteins (OBPs). Odorant-binding proteins are believed to transport odorants through the mucus to the olfactory receptors (ORs; Pelosi, 1996). Alternatively or additionally, OBPs may act as scavangers and remove odorants from the olfactory epithelium (Ronnett and Moon, 2002). The interactions between odorants and the elements of the mucus are so-called perireceptor events (for a detailed overview see Pelosi, 1996).
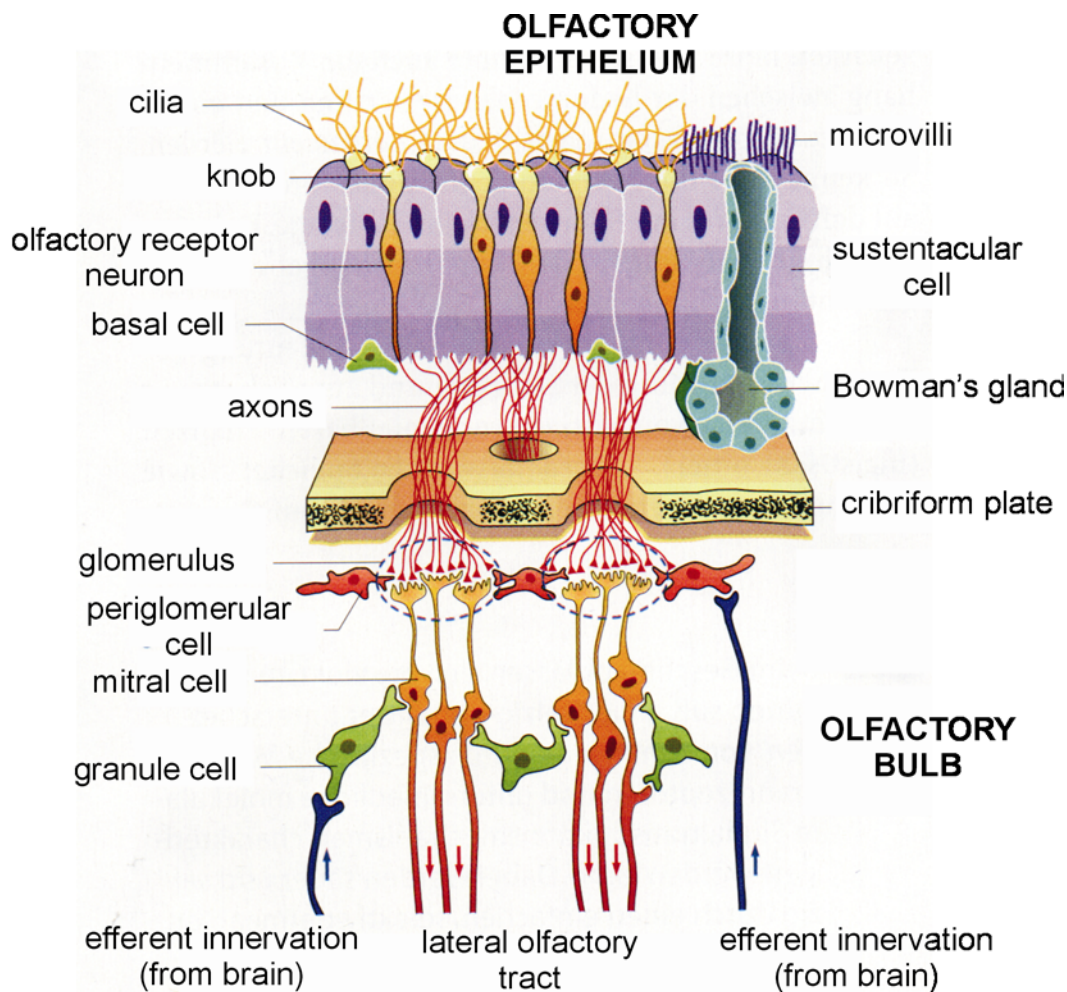
Figure 1. Schematic organization of the olfactory epithelium and the olfactory bulb
[modified from Schmidt, Thews, Lang (2000); In "Physiologie des Menschen", page 322; 27th edition; Berlin Heidelberg New York: Springer Verlag]

1.3.1 Transduction mechanisms in ORNs

Olfactory signal transduction is initiated when odorants bind to ORs situated in the ciliary membrane of ORNs (Buck and Axel, 1991). The question of whether all ORs couple to one or more transduction cascades has been debated over years (Schild and Restrepo, 1998; Gold, 1999) and to date this question has not been unambiguously answered. In many systems the so-called adenosine 3',5'-cyclic monophosphate (cAMP)-transduction pathway has been shown to be predominant (Belluscio *et al.* 1998; Gold, 1999; Wong *et al.* 2000). The cAMP-pathway was first described by Pace and coworkers (1985) and its molecular constituents

have been studied in detail (see Figure 2). Upon binding of the odorant molecule to the receptor protein the guanosine nucleotide-binding protein G_{olf} activates the type III adenylate cyclase, which in turn converts adenosine tri-phosphate (ATP) into cAMP. cAMP directly gates a cation channel (g_{cn}) permeable for sodium, potassium and calcium. The gating of these channels accounts for the initial component of the odor-induced electrical response of the ORN. The concomitant rising calcium concentration in the cytoplasm activates a channel permeable for chloride ions ($g_{Cl(Ca)}$). The resulting chloride current further depolarizes the membrane because the equilibrium potential for chloride in ORNs is less negative than the resting membrane potential. The termination of the cAMP-mediated odorant response takes place, firstly, because of the detachment of the odor molecule from the receptor protein and, secondly, by activation of an intracellularly located calcium-dependent phosphodiesterase and a cAMP-dependent protein kinase. The phosphodiesterase transforms cAMP to adenosine monophosphate (AMP) and the protein kinase phosphorylates and inactivates the receptor protein (Boekhoff *et al.* 1992; Boekhoff and Breer, 1992; Schild and Restrepo, 1998).

The above described cAMP-mediated transduction pathway leads to a depolarizing receptor potential, thus increasing the basal action potential firing rate of the ORNs. In some species, the application of odorants resulted in a hyperpolarizing receptor potential and a decrease of the basal spiking rate of ORNs (Michel and Ache, 1994; Morales *et al.* 1994, 1995; Kang and Caprio, 1995). The transduction events underlying these odorant responses cannot be explained by the above described cAMP-mediated cascade. In lobster, it has been shown that excitatory and inhibitory pathways coexist in single ORNs (Michel and Ache, 1994). These individual observations show that ORNs of at least some species possess more than one transduction pathway.

In ORNs of lobster (Michel and Ache, 1994) and in the vomeronasal organs of rat (Inamura *et al.* 1997) and mouse (Holy *et al.* 2000) the existence of transduction mechanisms other than the cAMP-mediated one has been clearly shown. In these cases a transduction mechanism with inositol 1,4,5,-tris-phosphate (IP$_3$) as second messenger has been suggested. There is evidence for many other transduction mechanisms. In the chilian toad (*Caudiverera caudiverbera*) a hyperpolarizing and thus inhibitory calcium-dependent potassium channel seems to be of crucial importance (Morales *et al.* 1994). Others have described ion channels directly gated by odorant molecules (Labarca *et al.* 1988) and even receptor and second messenger-independent transduction mechanisms have been proposed (Kashiwayanagi and
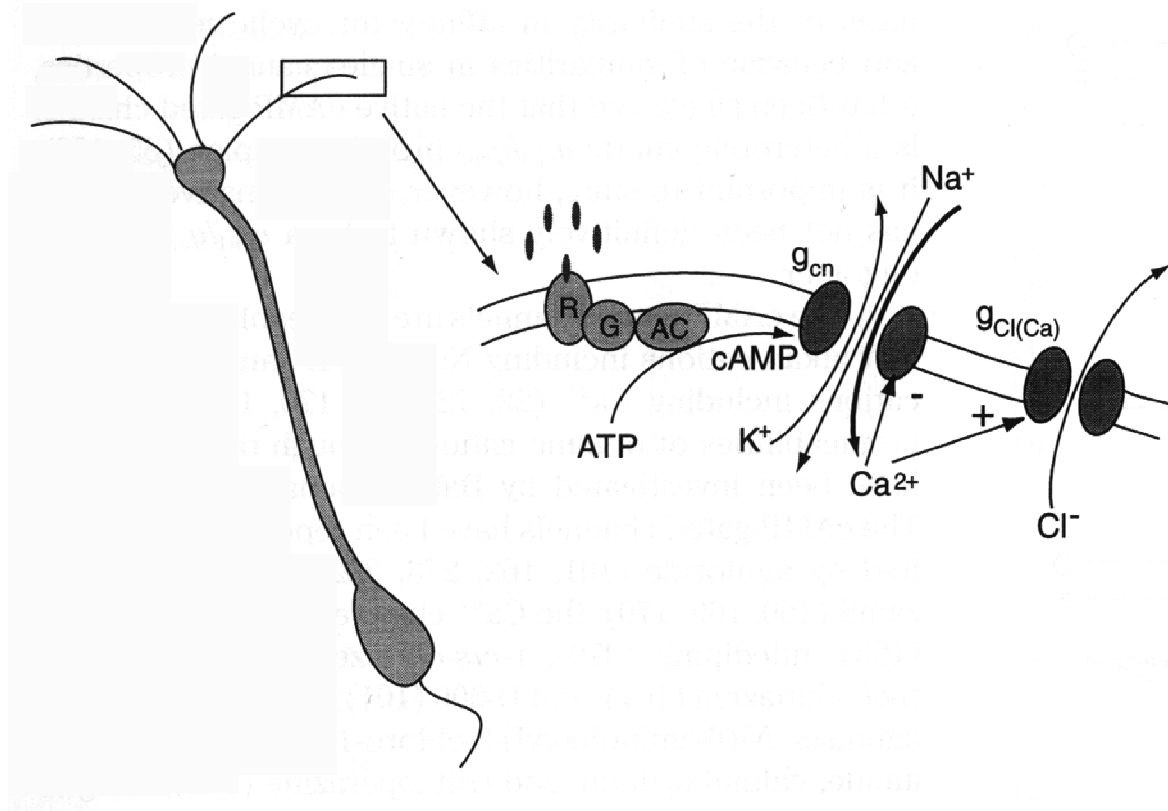
Figure 2. Schematic diagram of the cAMP-mediated transduction cascade of an ORN
Schematic drawing of an ORN (left). The elements of the transduction cascade reside in the cilia membrane. A model of the cAMP pathway is shown on right. R, receptor; G, G protein; AC, adenylate cyclase; g_{cn}, cyclic nucleotide-activated conductance; $g_{cl(Ca)}$, Ca^{2+}-activated Cl^- conductance. [modified from Schild and Restrepo, 1998]

Kurihara, 1996). Moreover, nitric oxide (NO) and carbon monoxide (CO) have been suggested to play a role in olfactory transduction (Broillet and Firestein, 1996; Morales and Bacigalupo, 1996; Schild and Restrepo, 1998). These gaseous messengers are membrane permeable and stimulate the soluble form of guanylate cyclase in many cell systems (Dawson and Snyder, 1994). For a detailed survey of the actual knowledge on olfactory transduction mechanisms see Schild and Restrepo (1998); Zufall and Munger (2001); Ronnett and Moon (2002) and references therein.

Despite the tremendous work done and the continuous enhancement of the investigation methods during the last decade, to date there are no studies that give clear and unambiguous evidence for cAMP-independent transduction in ORNs in the main olfactory epithelium of a vertebrate.

1.3.2 The transformation of local graded receptor potentials into spike trains in ORNs

Olfactory receptor neurons are relatively small neurons with a small membrane capacitance, a high membrane resistance and a relatively long time constant (Schild and Restrepo, 1998). Owing to these properties ORNs can be significantly excited by very small currents. Despite this high sensibility ORNs are very well protected against "false alarms", i.e. spontaneous, casual, not odorant determined openings of its transduction channels. One explanation for this protection mechanism is the long membrane time constant (up to 100 ms) of ORNs. The membrane can be regarded as a first-order low-pass filter. It rejects "high"-frequency noise (Lowe and Gold, 1993).

The amplitude of a receptor potential depends on the number of odorant molecules that bind to ORs of an ORN. Binding of few or maybe only one odorant molecule can excite an ORN and trigger an action potential (Menini *et al.* 1995). Below I briefly summarize the events leading to an action potential taking a *Xenopus laevis* ORN as an example (Figure 3). The receptor potentials are generated in the cilia and are then propagated electrotonically along the dendrite to the soma. If such a potential is strong enough to depolarize the ORN above threshold (about −50 mV), voltage-gated sodium channels (g_{Na}) are activated and an action potential is initiated (Schild, 1989). The strong depolarisation, which reaches also the soma and the proximal dendrite, activates voltage-gated calcium channels (g_{Ca}; high-voltage-activated [HVA]) if the membrane potential reaches −30 mV (Schild *et al.* 1994). The following calcium influx opens a calcium-dependent potassium channel ($g_{K(Ca)}$). These channels together with the voltage-gated potassium channels (g_K) repolarize the membrane and lead to a termination of the action potential, that now runs toward the OB along the axon. For further information about the organization of the neuronal network of the olfactory system see Shipley and Ennis (1996).
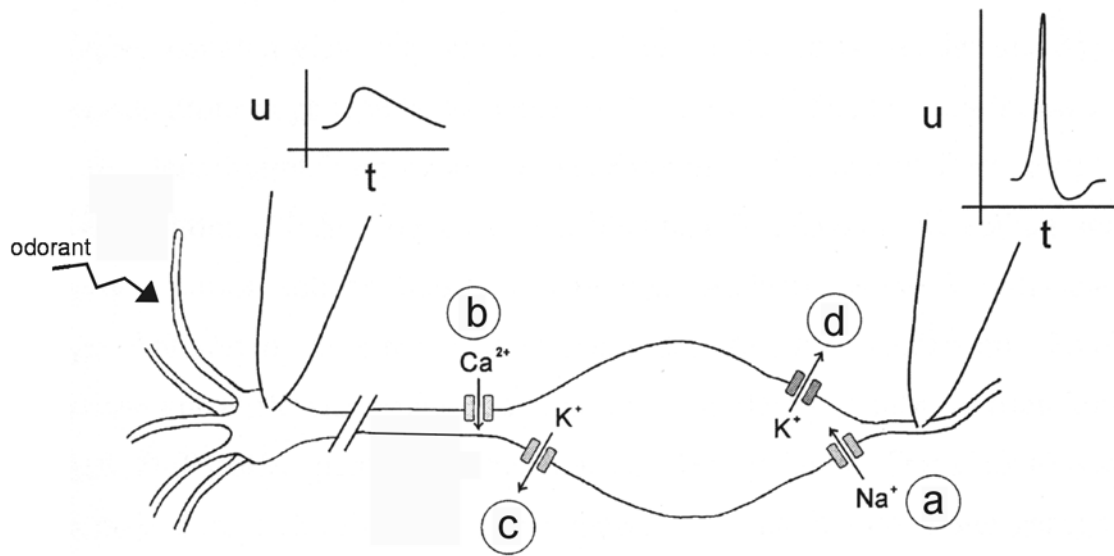
Figure 3. Schematic representation of the transformation of a receptor potential into an action potential in an ORN
For a detailed description see text (page 6). (a): voltage gated sodium channel. (b) voltage gated calcium channel. (c): calcium activated potassium channel. (d): voltage gated potassium channel. On the dendritic knob and the axon two patch pipettes and a recorded receptor potential and an action potential are represented for clarity. u: potential; t: time.

1.4 Odor coding in ORNs

In vertebrates, ORs are encoded by as many as 1000 genes (Mombaerts, 1999). Among different species the number of OR genes vary considerable. In humans the estimated size of the receptor gene family ranges from 500 to 1000 (Mombaerts, 1999), in *Xenopus laevis* the number of receptor genes is reported to be much smaller (Mezler *et al.* 1999, 2001). At present it is generally believed that an ORN expresses one or few different ORs (Rawson and Restrepo, 1995; Kashiwayanagi *et al.* 1996; Buck, 1996, Malnic *et al.* 1999).

Olfactory systems are able to detect and to differentiate among many kinds of odors. Olfactory receptor neurons encode qualitative, quantitative, temporal and spatial information about odors. One odorant can be detected by multiple ORs and one OR can recognize many odorants. To date it is not completely clear which characteristics of an odorant molecule (functional group, charge or size) are crucial for their binding to an OR. However, it is known that different odorant molecules are detected by different OR combinations, i.e. different

odors have different receptor codes which are projected to the OB and then to higher brain areas (Malnic *et al.* 1999).

A coexistence of several transduction pathways in one ORN could be crucial in the modulation of such a receptor code. It has been shown that different transduction pathways coexist in ORNs of lobster (Ache, 1994; Michel and Ache, 1994) and rat (Noé and Breer, 1998; Vogl *et al.* 2000). Especially the existence of inhibitory and excitatory transduction pathways in one ORN (see Michel and Ache, 1994) could be very important in this context.

1.5 Goal of the thesis

Most studies of the function of ORNs have been performed using preparations of isolated cells. In the last few years some research groups began to use slice preparations of the olfactory epithelium. To date it has not been investigated whether these different preparation techniques may influence the response behaviour of ORNs.

It is known that in aquatic species, including tadpoles of *Xenopus laevis* (Vogler and Schild, 1999), amino acids are potent olfactory stimuli. Amino acids can elicit excitatory as well as inhibitory responses, but their transduction mechanisms are not yet known.

Whether odorants are transduced by only one or more than one second messenger has been a long-standing question in olfactory research. Despite the tremendous work done in the last decade, only the so-called cAMP transduction pathway has been completely unraveled by now. Although the simple view of cAMP as the only second messenger in olfaction had to be abandoned it is still a widespread opinion that in the main olfactory epithelium of vertebrates cAMP is the sole second messenger of primary importance.

The purpose of this thesis was to investigate the following questions using tadpoles of *Xenopus laevis* as experimental animals:

1. How does the preparation method of the ORNs (isolated ORNs or ORNs in the slice) affect the outcome of the investigations and which of the two is the best method to study the odorant responsiveness of ORNs?

2. How are amino acids transduced in ORNs of the main olfactory epithelium, and is there one or more than one transduction pathway in *Xenopus laevis* tadpoles?

3. How do ORNs that are sensitive to different odorants project to the olfactory bulb?

2. Materials and Methods

2.1 The experimental animal - *Xenopus laevis*

Xenopus laevis is an amphibian of the order Anura and has a natural geographic range along the African Rift Valley, south of the Sahara Desert. As an invasive species it now occupies freshwater areas all over the world. *Xenopus laevis* lives in warm, stagnant grassland ponds as well as in streams in arid and semi-arid regions. The adult frog is a scavenger and eats living, dead, or dying arthropods and other pieces of organic waste, whereas the tadpoles feed on small organic particles, such as algae. To locate food it uses predominantly its acute sense of smell. It spends most of its time underwater and comes to surface to breathe. Respiration is predominantly through its well developed lungs, there is little cutaneous respiration (Avila and Frye, 1977; Simmonds 1985; Tinsley *et al.* 1996; Nieuwkoop and Faber, 1956).

Xenopus laevis, especially at its larval stages, is an excellent model system to study the olfactory system. The husbandry and breeding of this species is relatively easy and, as it is a poikilothermal animal, all experiments can be carried out at room temperature. Tadpoles of *Xenopus laevis* do not have a lamina cribrosa and therefore the olfactory mucosa is not separated from the olfactory bulb by a bony structure. This is a further advantage of this experimental animal, as it is possible to make nose-olfactory bulb preparations without particular difficulies (see section 2.2.3 for a detailed description of this preparation).

The adult frogs were obtained from a commercial supplier (Kaehler, Hamburg, Germany) and held in aquaria (water temperature 20 °C). They were fed with Pondstick food (Tetra Pond, Melle, Germany) and small pieces of bovine heart. The frogs were induced to breed by giving them injections of human chorionic gonadotropin (Sigma, Deisenhofen, Germany) into the dorsal lymph sac. The breeding pairs were housed together overnight, and the next morning the embryos were collected and put in separate aquaria (water temperature 20 °C). The tadpoles were fed with algae (Dose Aquaristik, Bonn, Germany).

For the experiments tadpoles (see Figure 4) of developmental stages 48 to 54 (staged after Nieuwkoop and Faber, 1956) were used. The tadpoles reached the stage 48 approximately after two weeks and after about five weeks they reached the stage 54. At stage 55 they start metamorphosis, which ends at stage 66 after about 8 weeks (Nieuwkoop and Faber, 1956).
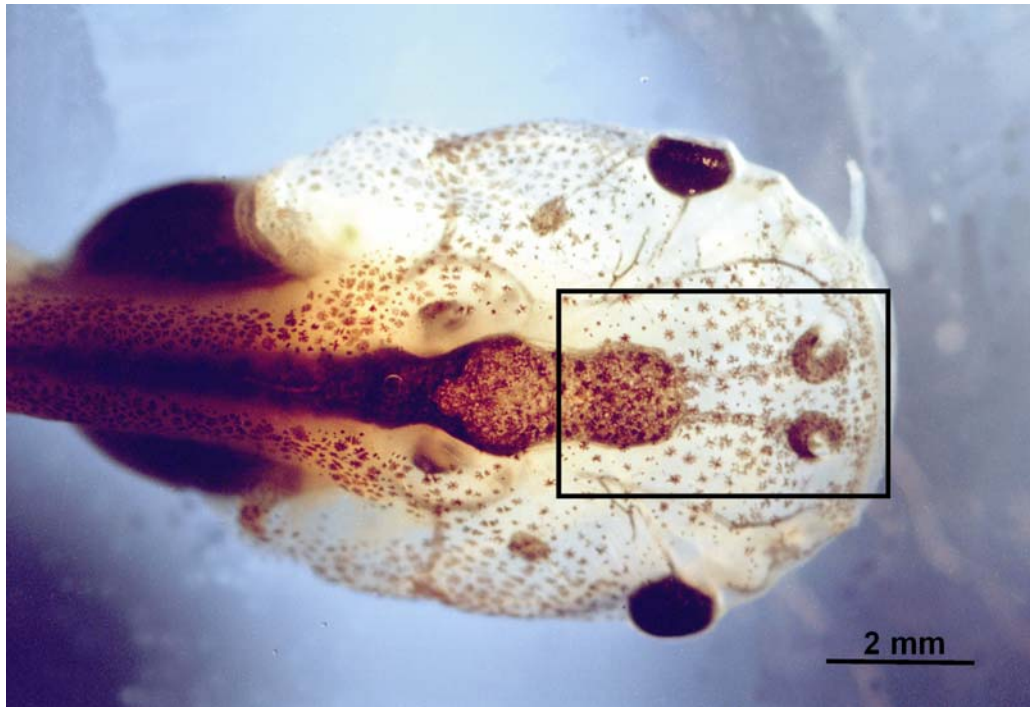
Figure 4. Tadpole of *Xenopus laevis* (stage 54)
The black rectangle indicates the block of tissue cut out for the experiments.

2.1.1 The constitution and development of the nose of *Xenopus laevis*

The nose of the adult *Xenopus laevis* is made up of three interconnected chambers that form three different epithelia for the detection of different classes of odorants. The largest chamber forms the principal cavity ("air nose"), which is permanently filled with air and can be closed underwater by a membrane. The other two chambers, the lateral olfactory cavity ("water nose") and the vomeronasal organ are permanently filled with water (Föske, 1934; Altner, 1962). The olfactory epithelium of the principal cavity serves for the detection of air-borne, the olfactory epithelium of the lateral cavity detects water-borne stimuli (Freitag *et al.* 1998). The vomeronasal organ is implicated with the detection of pheromones (Halpern, 1987).

The ORNs in the water nose and in the air nose are endowed with ORs of different classes named class I ORs and class II ORs, respectively. The class I ORs are related to ORs of fish, whereas class II ORs are related to ORs of mammals. Olfactory receptor neurons of the vomeronasal organ express neither class I nor class II ORs (Freitag *et al.* 1995).

In the following it is briefly described what is known about the development of the three

olfactory epithelia in *Xenopus laevis*. At the stage 23 the two olfactory placodes become visible (Klein and Graziadei, 1983). The development of the principal cavity and the vomeronasal organ (see Figure 5) start at the stage 40. The formation of the lateral cavity starts after about three weeks at the stages 51-52 and its differentiation goes on during metamorphosis (stages 55-66; Föske, 1934). It is not yet clear at which point the olfactory system becomes fully functional. The first synapses between axons of ORNs and dendrites of mitral cells in the OB have been detected at the stage 37-38 (Byrd and Burd, 1991), but mature ORNs could not be specifically stained prior to the stage 45 (Hansen *et al.* 1998).

The distribution of the two different classes of ORs (class I and class II) within the developing nose has been extensively studied. Class I ORs are detectable as early as at the stage 32, less than 2 days after fertilisation. Class II ORs could not be detected before the stage 49, approximately 12 days after fertilisation (Mezler *et al.* 1999). From the stage 49 to at least stage 55 (beginning of the metamorphosis) both receptor types are expressed in the principal cavity. There are still controversial opinions what exactly happens during metamorphosis (for detailed information see: Petti *et al.* 1999 and Mezler *et al.* 1999). Finally, in the principal cavity (air-nose) of the adult frog only mammalian-like receptors (class II) are detectable and in the lateral cavity (water-nose) only fish-like receptors (class I) are detectable (Freitag *et al.* 1995).

The three different olfactory epithelia (principal cavity, lateral cavity and vomeronasal organ) of *Xenopus laevis* are basically organized as already described (see section 1.2). All of the three epithelia are made up of ORNs, sustentacular cells and basal cells. As other vertebrates, *Xenopus laevis* possesses two types of ORNs, one type having cilia and the other type having microvilli (see Figure 6). The distribution of these different ORNs is stage-dependent. There are also two types of sustentacular cells in *Xenopus laevis*. Like the two types of ORNs, the two types of sustentacular cells also have short cilia or microvilli on their apical membranes (Hansen *et al.* 1998).

Not much is known about the composition of the mucus layer covering the olfactory epithelia of *Xenopus laevis*. It seems that its ionic composition is of fundamental importance for the odorant transduction mechanisms in ORNs (Schild and Restrepo, 1998). Especially the concentration of potassium and chloride seems to be crucial. There is some evidence that, because of high potassium concentration in the mucus, the reversal potential for potassium is less negative than the membrane potential (Joshi *et al.* 1987; Minor *et al.* 1992). If this is true the calcium-dependent potassium channels present in the cilia of ORNs of some species

(Schild and Restrepo, 1998) could lead to depolarisation, and not to hyperpolarisation. The same is true for chloride, whose reversal potential is reported to be near 0 mV (Frings *et al.* 2000).
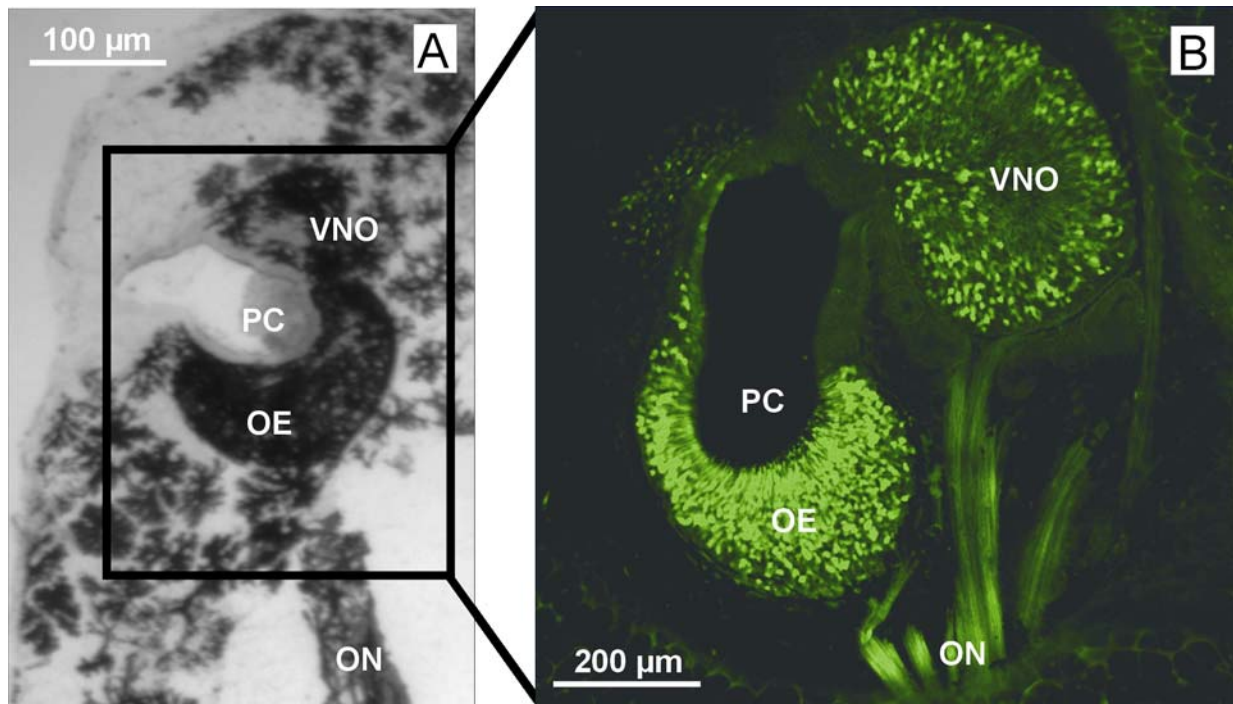
Figure 5. Nasal cavity of a tadpole *of Xenopus laevis* (stage 51)
A: block of tissue containing the left nasal cavity and the initial part of the olfactory nerve. **B**: overview over a horizontal slice of the tissue block shown in **A**. The receptor neurons of the olfactory epithelium and the vomeronasal organ were backfilled through the nerve using biocitin/avidin staining (for staining procedures see section 2.8). PC: principal cavity, VNO: vomeronasal organ, OE: olfactory epithelium and ON: olfactory nerve.
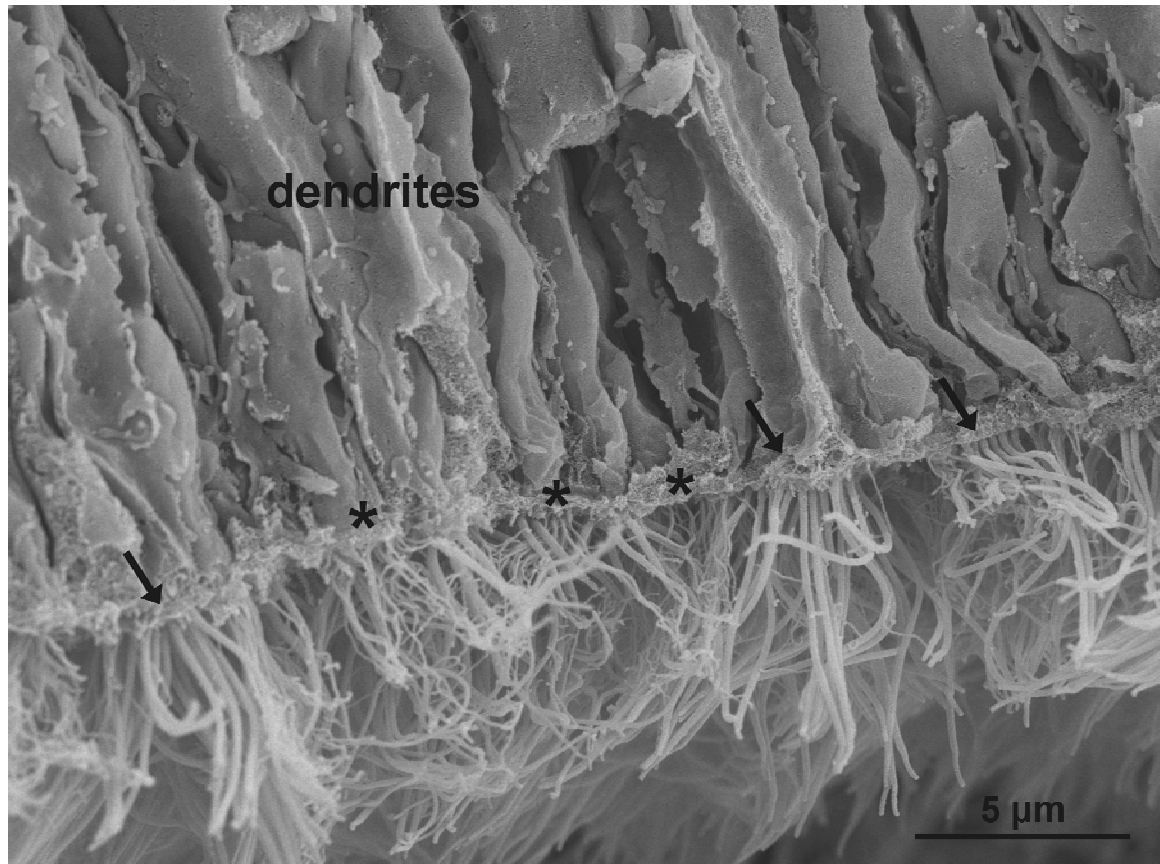
Figure 6. Scanning electron micrograph of the apical part of the olfactory epithelium of a *Xenopus laevis* tadpole (stage 54)
The micrograph shows the terminal part of dendrites of ORNs. Note the two different types of ORNs, one with cilia (arrows) and the other one with microvilli (asterisks). Note that the cilia have a larger diameter than microvilli. [micrograph kindly provided by Leonid Nezlin]

2.2 Tissue preparations

2.2.1 Tissue dissociation and preparation of isolated ORNs

Isolated ORNs were prepared from the olfactory mucosa of tadpoles (stages 48 to 54; Nieuwkoop and Faber, 1956) of *Xenopus laevis*. Tadpoles were anesthetized in a mixture of water and ice and after subsequent decapitation, the tissue above the mucosa was removed and the mucosa was extirpated and placed into cell dissociation solution (DS$_1$, see section 2.6) which contained papain (Sigma, Deisenhofen, Germany). After 3 minutes in this solution, the mucosa was transferred into a second cell dissociation solution (DS$_2$, see section 2.6) without papain and mechanically macerated using two pairs of fine forceps. The resulting pieces of mucosa were then triturated with a plastic pipette of 2 mm inner diameter. After these separating procedures bath solution (see section 2.6) was added and samples of 100 - 150 µl of the cell suspension were stored at 5 °C on glass coverslips coated with Concanavalin A (Sigma, Deisenhofen, Germany; 1mg ml^{-1}). The cells were used within 6 hours after preparation. Figure 7 shows typical dissociated ORNs of a *Xenopus laevis* tadpole viewed through a microscope equipped with Nomarski optics (Axioskop 2, Zeiss, Göttingen, Germany).

2.2.2 Slice preparation of the olfactory mucosa for patch-clamp recordings, transporter measurements and calcium imaging

For the slice preparation, tadpoles of *Xenopus laevis* (stages 49 to 54; Nieuwkoop and Faber, 1956) were anesthetized and killed as described above. Then a block of tissue containing the olfactory mucosae, the intact olfactory nerves and the anterior two thirds of the brain was cut out and kept in bath solution (see section 2.6). The tissue block was glued onto the stage of a vibroslicer (VT 1000S, Leica, Bensheim, Germany) and cut horizontally into 120 - 130 µm thick slices. Figure 8 shows a typical slice of the olfactory mucosa of a *Xenopus laevis* tadpole. Figure 9 shows a mucosa slice stained with biocytin/avidin by backfilling the receptor neurons through the nerve. The slice was counterstained with propidium iodide (see section 2.8 for a detailed description of staining procedures).

2.2.3 Nose-olfactory bulb preparation

For the nose-olfactory bulb preparation, tadpoles of *Xenopus laevis* (stages 51 to 53; Nieuwkoop and Faber, 1956) were anesthetized and killed as described above. Then a block of tissue containing the olfactory mucosae, olfactory nerves and the brain was cut out. The tissue block was glued onto the stage of a vibroslicer, and only the dorsal surface of the OB was sliced off. The olfactory mucosae and olfactory nerves were left intact. Figure 10 shows a typical nose-olfactory bulb preparation of a *Xenopus laevis* tadpole.
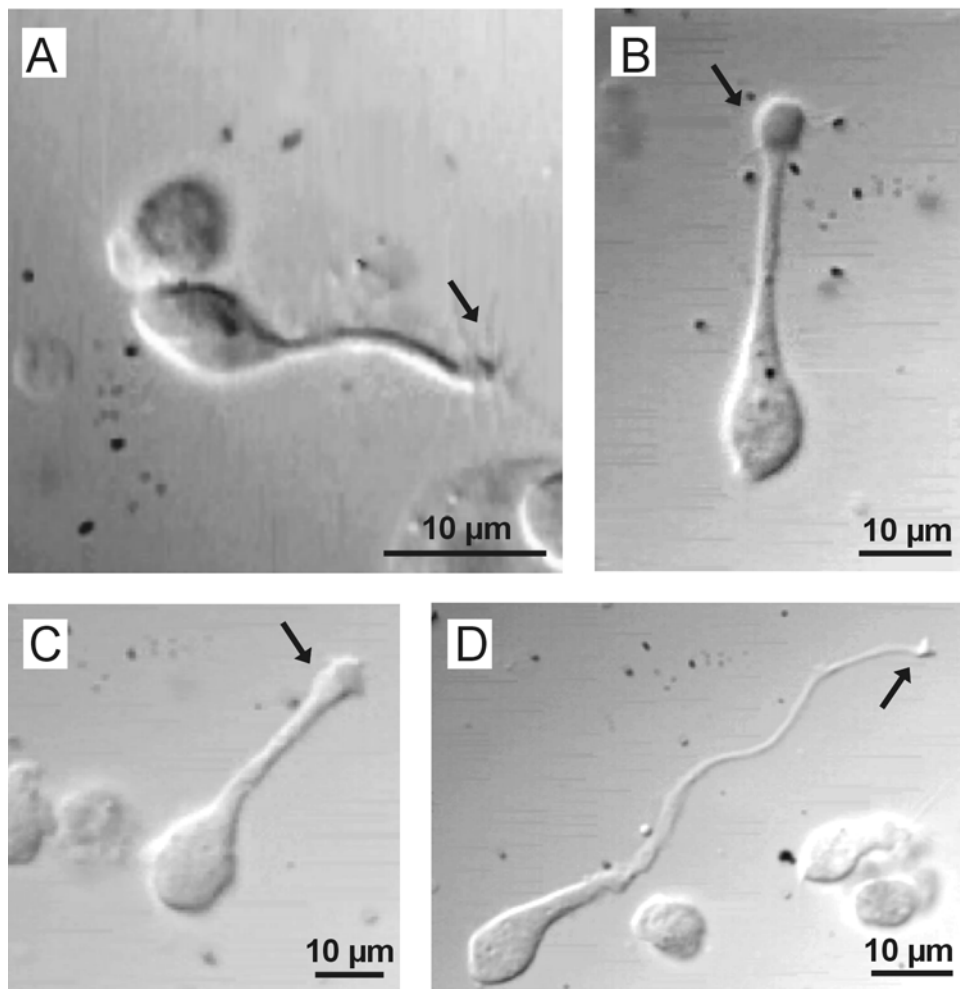
Figure 7. Isolated ORNs of a tadpole of *Xenopus laevis* (stage 52)
A: ORN with soma, dendrite and dendritic knob with cilia (arrow). Only ORNs that satisfied these morphological criteria were selected for recording. The ORNs shown in **B** and **C** have a swollen knob (arrows) with no visible cilia and the ORN shown in **D** has a very long dendrite and a small knob (arrow), but no cilia. ORNs like those shown in **B**, **C** and **D** were discarded.
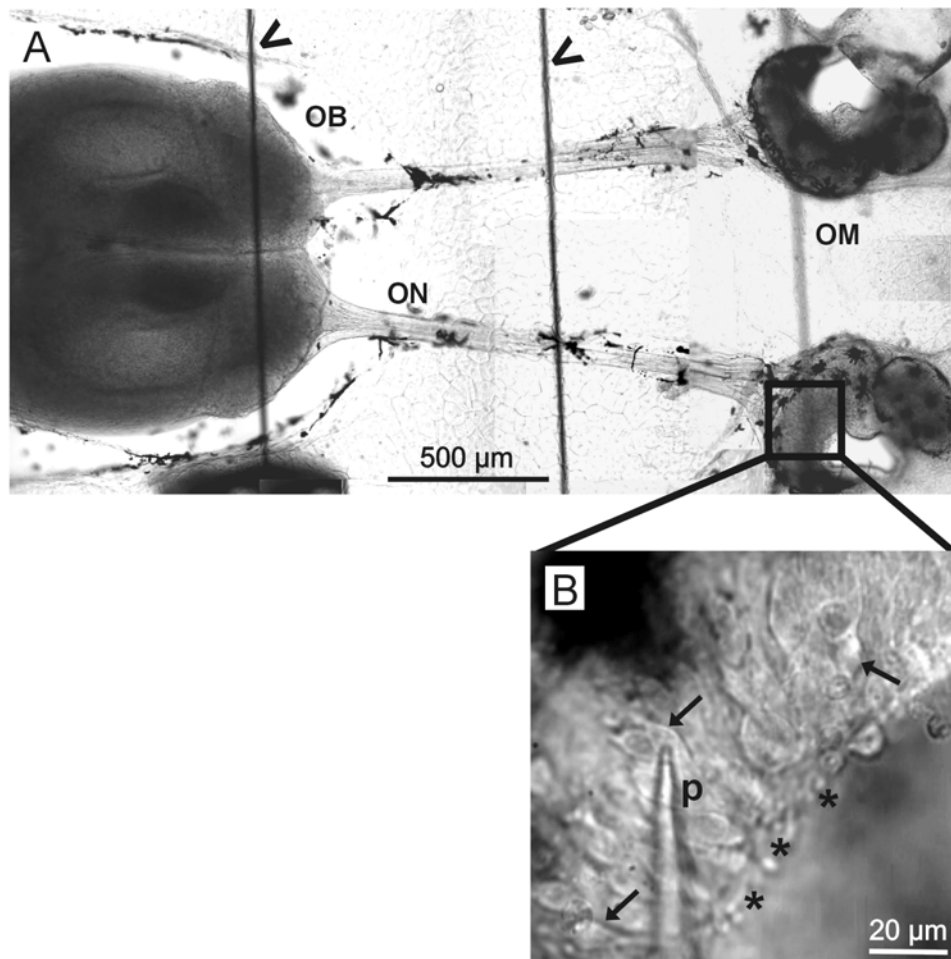
Figure 8. Slice of the olfactory epithelium (mucosa slice) of a tadpole (stage 53)
A: typical mucosa slice with left and right olfactory mucosae (OM), olfactory nerves (ON) and the anterior part of the brain including the left and the right olfactory bulb (OB). Note that both OM are sliced in order to get access to the cells of the olfactory epithelium. Two nylon filaments of the grid used for fixing the slice in the recording chamber are visible (<). **B**: higher magnification of the part of the olfactory epithelium encircled with a square in **A**. Several ORNs are recognizable (arrows) and also a few knobs are visible (asterisks). Note a patch pipette (p) on the membrane of one of the indicated ORNs.
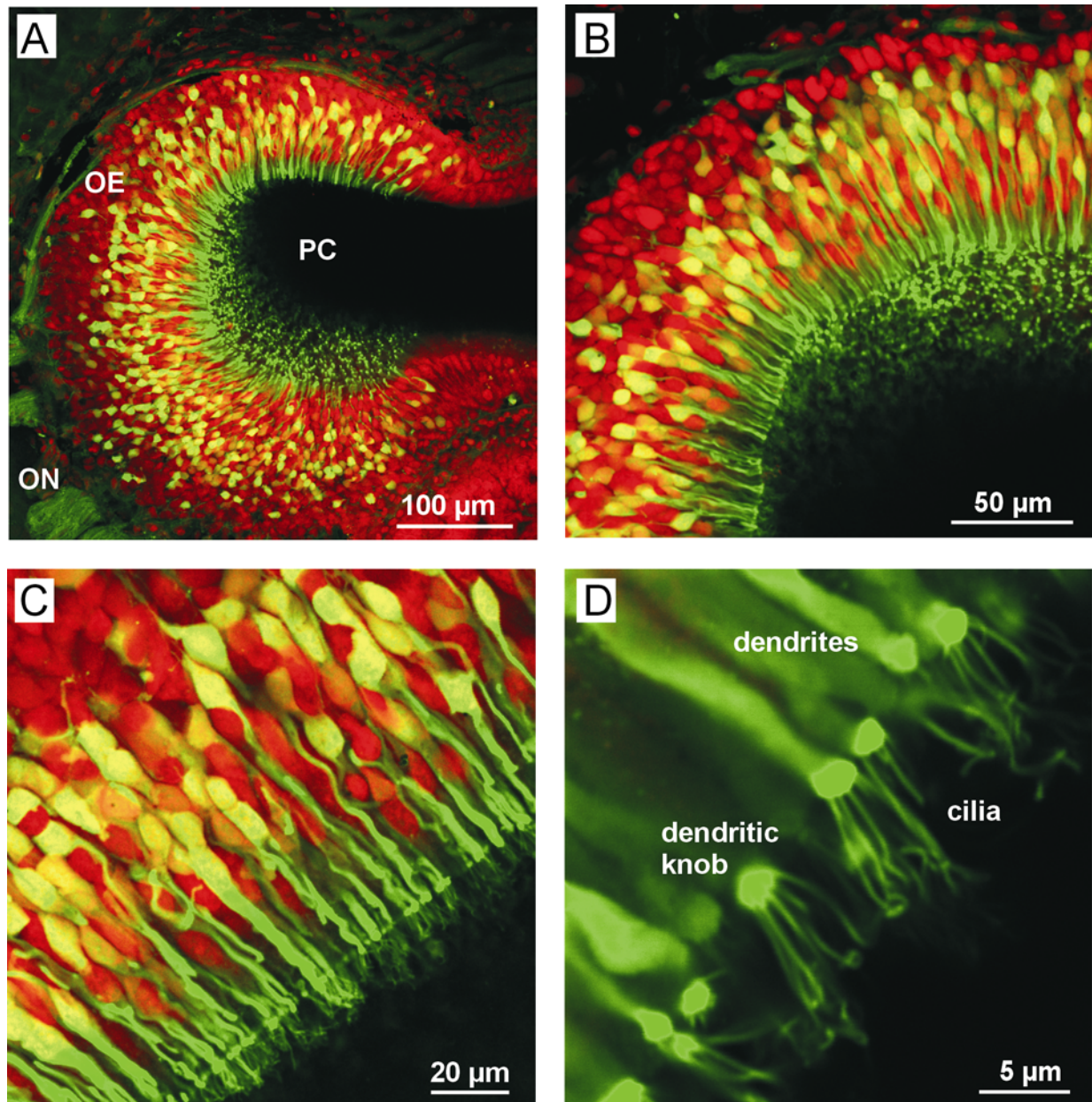
Figure 9. Slice of the olfactory epithelium of a *Xenopus laevis* tadpole (stage 54)
A: horizontal overview over the olfactory epithelium (PC, principal cavity, OE, olfactory epithelium and ON, olfactory nerve). The neurons were backfilled through the nerve using biocytin/avidin staining (green fluorescence), and then the slice was counterstained with propidium iodide (red fluorescence; for staining procedures see section 2.8). **B** and **C:** higher magnifications of **A** showing the typical shape of ORNs in a slice. **D:** higher magnification of the apical part of ORNs showing dendrites, dendritic knobs and cilia.
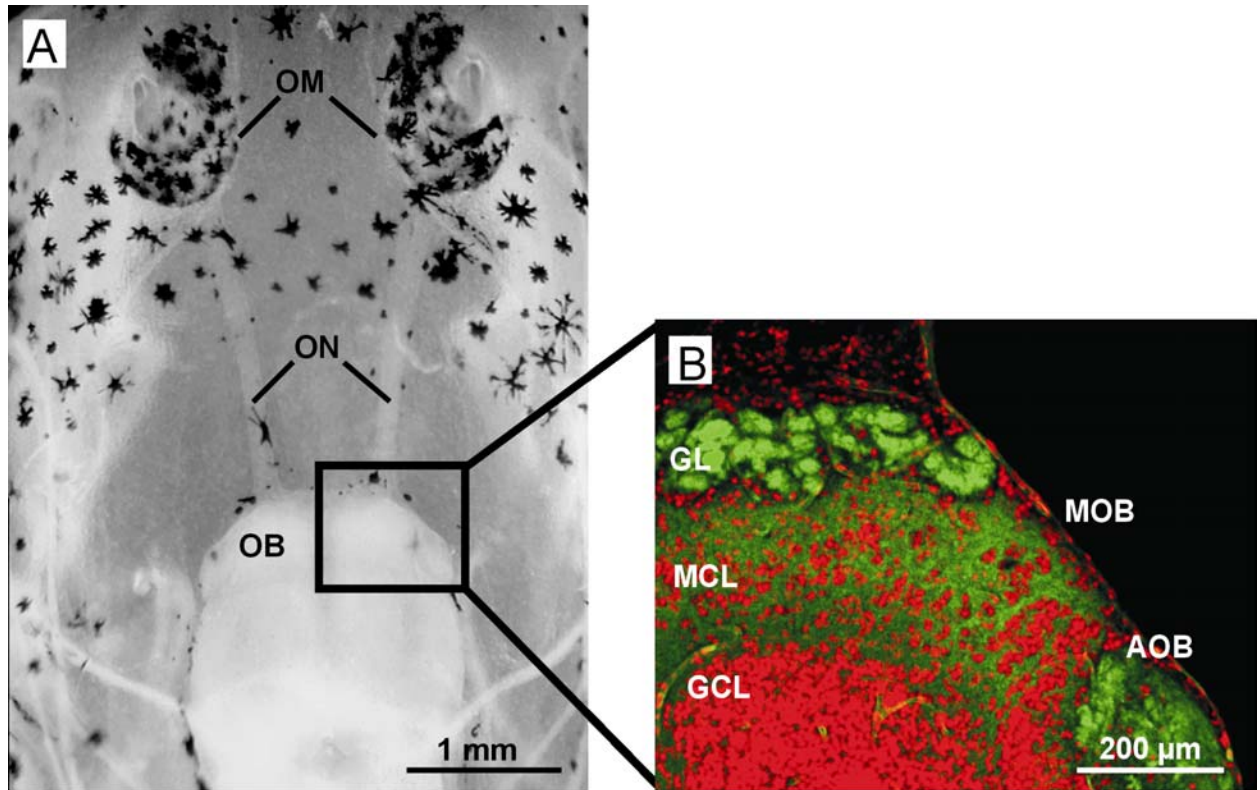
Figure 10. Nose-olfactory bulb preparation of a *Xenopus laevis* tadpole (stage 53)
A: typical nose-olfactory bulb preparation with the two olfactory mucosae (OM), the olfactory nerves (ON) and the anterior part of the brain including the olfactory bulbs (OB). **B**: olfactory bulb double labeled with an antibody against synaptophysine (green fluorescence) and propidium iodide (red fluorescence; for staining procedures see section 2.8) showing the glomerular layer (GL) and the organization of cell nuclei in the mitral- (MCL) and granule cell layer (GCL). MOB: main olfactory bulb, AOB: accessory olfactory bulb.

2.3 The patch-clamp technique

2.3.1 Basic principles

The patch-clamp technique is an electrophysiological method that allows the recording of currents flowing across biological membranes through ion channels. This technique with all its applications is well described in the original paper by Hamill and colleagues (Hamill *et al.* 1981). Briefly, a small fire polished glass pipette with a tip diameter of approximately 1 µm, containing a recording electrode, is pressed against the cell membrane. Thereby, it is important to achieve a tight seal between pipette and membrane. The resistence between cell membrane and pipette is critical for the ongoing of the experiment. The seal resistance should be in a range of several gigaohms ("gigaseal"). Once a gigaseal is obtained the so-called "on-cell" configuration is achieved. This configuration allows the recording of the current flowing through the membrane patch covered by the pipette or the recording of currents resulting from charge displacements of the membrane. Starting from this configuration it is possible to attain a number of configurations (see Figure 11). By applying a short pulse of negative pressure through the pipette the patch can be broken creating a hole in the cell membrane under the pipette and gaining a low-resistance access to the cell interior. One has to take in mind that within seconds or at most a few minutes after breaking through the membrane, the intracellular solution will be exchanged by the pipette solution (wash-out effect). The formation of the so-called "whole-cell" configuration does not compromise the gigaseal between pipette and cell membrane. This is of primary importance because it prevents leak currents flowing between the pipette and the reference electrode and flooding of the cell with bath solution. In the whole-cell configuration it is possible to clamp the cell at a certain constant voltage and record the current flowing through the ion channels of the entire cell (voltage-clamp). Another possibility is to apply a constant current to the cell and measure changes in its membrane potential (current-clamp). The parameter that has to be held constant (voltage or current) is controlled by an amplifier via a feedback system. In other words, the current-clamp makes it possible to monitor voltage-dependet events like depolarizations, hyperpolarizations, generator potentials, or action potentials; the voltage-clamp allows to observe and investigate the corresponding currents.
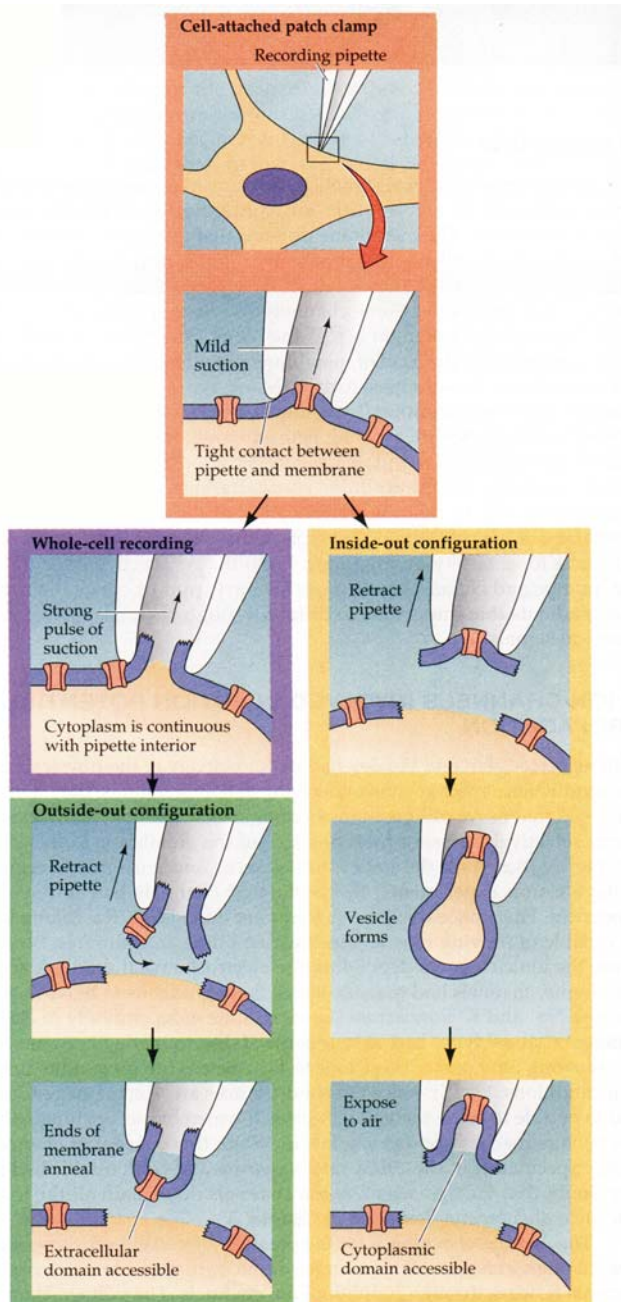
Figure 11. Schematic overview of the various possible configurations in the patch-clamp technique
For detailed explanation of each of the above shown configurations see text (pages 20 and 22). [modified from Purves D, Augustine GJ, Fitzpatrick D, Katz LC, LaMantia AS, McNamara JO (1997); In "Neuroscience", page 70; Sunderland, MA: Sinauer Associates, Inc.]

Combining the on-cell configuration and the principle of voltage-clamp makes it possible to record action potential-equivalent charge displacements of the membrane as current changes of the membrane patch under the patch pipette. This allows to monitor activity changes of the cell without affecting the composition of the intracellular solution. This is not possible when recording in the whole-cell configuration.

Investigations of ion channels isolated from the cell excised patches can be performed by erupting the patch from the surrounding cell membrane. Two different modes of excised patches are possible. The "inside-out" configuration, which is reached by pushing back the pipette from the cell attached configuration, and the "outside-out" configuration, which is performed from a whole cell patch by removing the pipette from the cell membrane. In both modes a piece of membrane remains sticked to the pipette. In the inside-out configuration the intracellular surface of the membrane faces towards the bathing solution, in the outside-out configuration it is the extracellular side.

2.3.2 Recording and data evaluation

For patch-clamp measurements recording chambers containing isolated ORNs or mucosa slices fixed with a grid (Edwards *et al.* 1989) were viewed through an Axioskop 2 equipped with Nomarski optics. Olfactory receptor neurons were easily recognized by their characteristic shape (see Figures 7, 8 and 9).

Patch electrodes with a tip diameter of 1 - 2 µm and approximately 7 - 10 MΩ resistance were fabricated from borosilicate glass with 1.8 mm outer diameter (Hilgenberg, Malsfeld, Germany) using a two-stage electrode puller (Narishige, Tokyo, Japan) and fire-polished. Pulse protocols, data acquisition and evaluation programs were written in "C". Voltage pulses were delivered from a microcontroller (Schild *et al.* 1996) to a D/A converter and then to the patch-clamp amplifier (EPC7; List, Darmstadt, Germany) in order to assess the impedance in the on-cell and whole-cell configuration. Holding voltage in the on-cell configuration was 0 mV, while in whole-cell recordings, the average voltage of − 75 mV was set by current injection in the current-clamp mode. Currents and voltages were recorded on video tape using a PCM unit (Instrutech, Elmont, N.Y., USA). The data were digitized off-line using an 8-pole Bessel filter, an A/D converter and a PC. Further data analysis was performed on a PC under the LINUX operating system.

2.4 Calcium imaging

The calcium imaging technique is very useful for visualizing the activity of excitable cells by monitoring their calcium responses (Smetters *et al.* 1999). The calcium imaging experiments in the mucosa slice were made using a laser-scanning confocal microscope (Zeiss LSM 510/Axiovert 100, Jena, Germany) and the calcium imaging experiments in the nose-olfactory bulb preparation were performed using an upright microscope (Axioskop 2) coupled to a frame-transfer, back-illuminated CCD camera (Visitron, München, Germany) and a custom-built monochromator with a Xenon light source.

2.4.1 Calcium imaging using confocal laser-scanning microscope

The optical path of confocal laser-scanning microscopy (CLSM) is shown in Figure 12. In a confocal microscope a fluorescent specimen is excited with laser light and the emitted fluorescence is then detected confocally. The goal of this optical arrangement is to detect the fluorescence light emitted by the specimen in the focal plane and to prevent the detection of out-of-focus light (Schild, 1996).

In order to produce a two-dimensional picture, the specimen is scanned pointwise by a laser beam. The resulting picture contains information of a plane through the specimen orthogonal to the optical axis. By moving the objective in z-direction it is possible to make a stack of two-dimensional pictures of the specimen along the z-direction. Putting together this stack of different pictures a three-dimensional picture can be assembled.

Most systems have more than one detector (in most cases a photomultiplier) in parallel, so that the parallel light can be split and detected in different wavelength bands. The advantage of this is the possibility of double labelling with two fluorescent dyes with different emission spectra, as well as emission ratioing techniques. For detailed information about confocal microscopy see Pawley (1995) and Schild (1996).

High spacial resolution is a great advantage of calcium imaging with the CLSM. However, most of the commonly used fluorescent calcium dyes, e.g. Fura-2, are UV excitable and are not readily utilized with the majority of confocal microscopes. Moreover, the sequential line-by-line-scanning of the object makes the system slow. Usually one line of the object is scanned in about 2 ms and the whole object in about 0.5 to 1 s depending on the size of the

selected scanning area. Thus, the signals received from two different points of the specimen are actually shifted in time. Higher temporal resolution can be achieved by skipping points or lines, or by decreasing the scanning area. However, this faster time resolution has to be paid for by loss of the 2D-resolution. Furthermore, very often a reduction of the scanning area is not possible, especially if the neurons of a whole slice are to be imaged. For this reason the CLSM is not an appropriate imaging method for monitoring fast processes. Nevertheless, CLSM perfectly fits to calcium imaging characterized by slow second-rate dynamics.
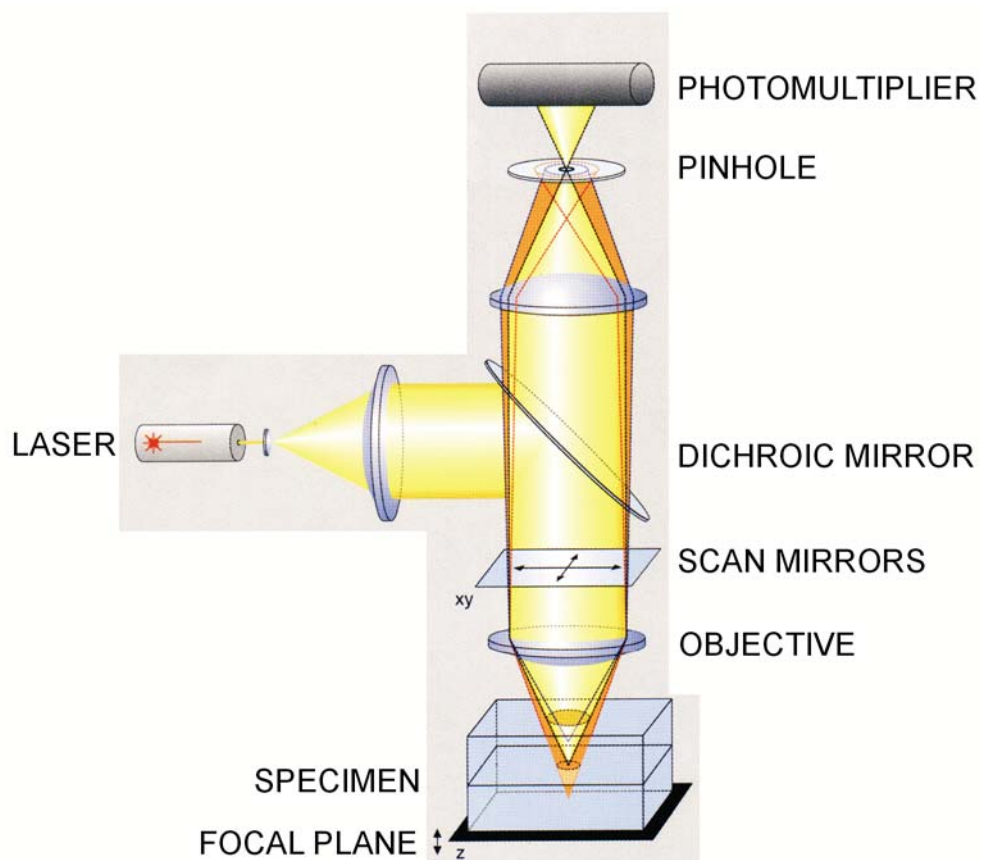
Figure 12. Schematic representation of the optical path of a confocal laser-scanning microscope

2.4.2 CCD-imaging setup

Figure 13 shows the schematic assembly of the CCD-imaging setup used for calcium imaging experiments in the nose-olfactory bulb preparation.

The main advantages of calcium imaging using charged coupled devices (CCD) as detector units, are their high quantum efficiency and high temporal resolution. These properties make CCD-imaging the method of choice for calcium imaging of fast processes. In contrast to CLSM, where the object is scanned line by line, this system records all of the pixels of the object simultaneously. Thus, signals coming from different points of the object are not shifted in time. Another advantage is the more flexible choice of the light source than in CLSM systems. An UV light source can be easily coupled into the system. This makes it possible to use calcium dyes such as Fura-2 and profit of their favorably properties, i.e. low bleaching and the ability of excitation ratioing. The disadvantage of this system is its low spatial resolution in z-direction. As the images are devoid of confocal contrast they appear blurred if compared to CLSM images. The fact that the CCD-imaging system is coupled to an upright microscope makes it possible to combine calcium imaging and patch-clamp in a slice preparation. The combination of these techniques is particularly promising for the ongoing projects in our lab.

2.4.3 Calcium-sensitive dyes

Fluorescent calcium-sensitive dyes change their fluorescence when binding a calcium ion. Some dyes show a shift in their excitation and/or emission spectrum and are therefore suitable for quantitative estimates of "calcium". If measuring at two different wavelengths and calculating the ratio of the outcoming images, many error sources can be eliminated, first of all the volume dependence of the fluorescence. Other calcium-sensitive dyes do not show a shift in their spectra and are therfore suitable only for qualitative calcium measurements. With such dyes ratioing is possible only if two different dyes are used simultaneously. For a detailed description of the principles of ratioing see Pawley (1995). Figure 14 shows the molecular structure of the calcium dyes Fura-2 and Fluo-4 used for the imaging experiments in the nose-olfactory bulb preparation and the mucosa slice, respectively.
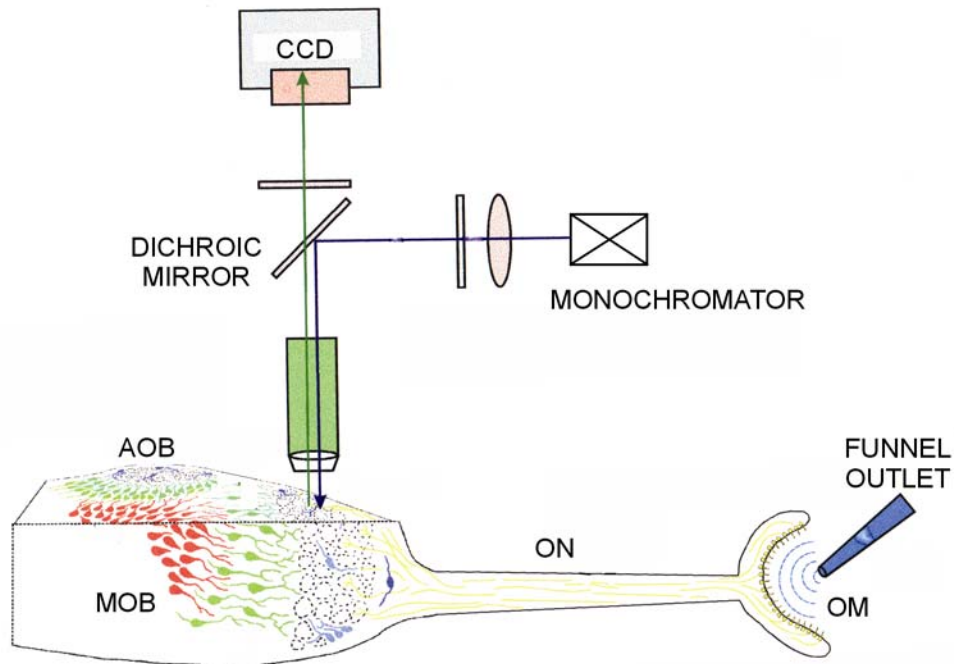
Figure 13. Schematic representation of the CCD-imaging setup used for calcium imaging in the nose-olfactory bulb preparation
Note also the schematic drawing of the nose-olfactory bulb preparation. The olfactory mucosa (OM) and the olfactory nerve (ON) are left intact, while the OB is sliced for exposing its cells to the excitation light. MOB, main olfactory bulb; AOB, accessory olfactory bulb.

Calcium-sensitive dyes are availabe as salts or as acetoxymethyl (AM) ester derivates. These derivates are uncharged molecules that permeate cell membranes. Once inside the cell, the lipophilic blocking groups are cleaved by nonspecific esterases and the dyes become charged molecules that remain trapped inside the cell. This allows the simultaneous loading of all of the cells in a tissue slice.

For a detailed description of the processes underlying fluorescence and bleaching of calcium-sensitive dyes see Pawley (1995).
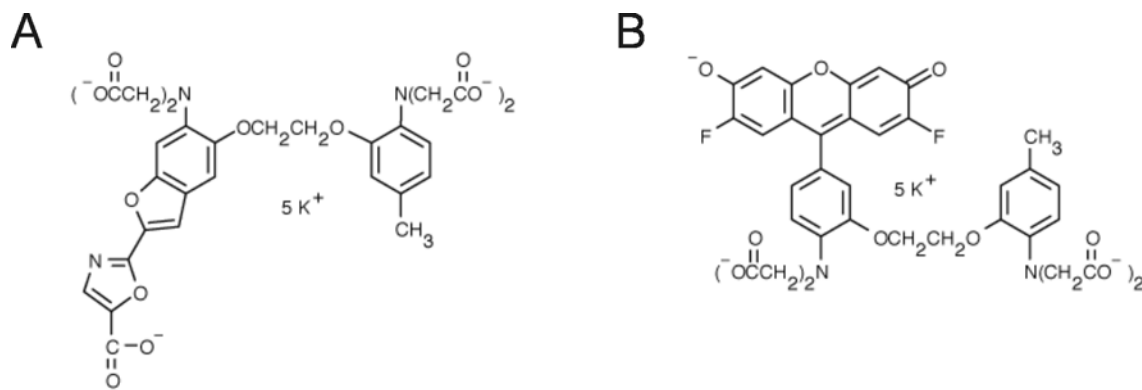
Figure 14. Molecular structures of the calcium dyes Fura-2 (A) and Fluo-4 (B)

2.4.4 Recording and data evaluation

Calcium imaging in the mucosa slice

For calcium-indicator dye loading, the mucosa slice was transferred into a recording chamber, and 200 µl of bath solution (see section 2.6) containing 50 µM Fluo-4/AM (Molecular Probes, Leiden, The Netherlands) and 50 µM MK571 (for explanation see section 2.7) were added. After incubation on a shaker at room temperature for 1 hour, the tissue slice was placed between two grids in a recording chamber to allow diffusion from both sides and placed on the microscope stage of an Axiovert 100M to which a laser-scanning unit (LSM 510) was attached. Before starting the calcium imaging experiment, the slice was rinsed with bath solution for at least 20 minutes.

Fluorescence images (excitation at 488 nm; emission > 505 nm) of the olfactory mucosa were acquired at 0.25 - 1.27 Hz and 786,4 ms exposure time per image with 3 to 5 images taken as control images before the onset of odor delivery. The fluorescence changes $\Delta F/F$ were calculated for individual ORNs as $\Delta F/F = (F_1 - F_2) / F_2$, where F_1 was the fluorescence averaged over the pixels of an ORN, while F_2 was the average fluorescence of that ORN prior to stimulus application, averaged over three images. Background intensity was zero.

Calcium imaging in the nose-olfactory bulb preparation

For calcium-indicator dye loading the nose-olfactory bulb preparation was transfered in a

recording chamber, and 200 µl of bath solution (see section 2.6) containing 50 µM Fura-2/AM (Molecular Probes, Leiden, The Netherlands) were added. After incubation for 1 hour at room temperature on a shaker, the preparation was rinsed with bath solution, glued into the recording chamber using 5% low melting point agarose (Sigma, Deisenhofen, Germany), covered with bath solution and viewed under an upright microscope (Axioskop 2) using a 10x objective. The preparation was rinsed with bath solution for at least 20 minutes before starting the experiment.

To estimate intracellular calcium concentrations ($[Ca^{2+}]_i$), fluorescence image pairs F340/F380 (alternating excitation at 340 and 380 nm; emission > 505 nm) of the OB were taken using a frame transfer, back-illuminated CCD camera and a custom built monochromator with a Xenon light source. Image pairs were acquired at 0.96 Hz and 500 ms exposure time per image. The $[Ca^{2+}]_i$-responses of mitral- and granule cells were represented as ratio images, whereby the mean values of the autofluorescence of unstained slices were taken as background values. The background-corrected ratio R of the fluorescence images excited at 340 and 380 nm (F340 and F380) was taken as an estimate of $[Ca^{2+}]_i$, and correspondingly, the changes $\Delta R(t) = R(t) - R(t=0)$ were taken as estimates for $\Delta[Ca^{2+}]_i (t)$.

2.5 Transporter measurements

2.5.1 Recording and data evaluation

For transporter measurements, the mucosa slice was placed between two grids in a recording chamber to allow diffusion from both sides. The AM-esters of the fluorescent dyes and the transport inhibitors were applied in bath solution at the concentrations indicated (see sections 2.6 and 3.8). The recording chamber was then placed on the microscope stage and recording started approximately two minutes after the beginning of incubation. To observe the time course of dye loading we used either an Axiovert 100M to which a laser-scanning unit (LSM 510) was attached, or an Axioskop 2 with a CCD camera attached. The fluorescence intensities of all dyes except Fura-2 were measured using the LSM 510 with excitation wavelength 488 nm. Fura-2 was excited at 380 nm and its loading was controlled with the CCD camera.

The progressive increase of fluorescence in the slice was measured by taking an image every three minutes (in case of Fura-red or calcium-green) or every minute (in case of calcein). The fluorescence images were evaluated by calculating intensity histograms and average intensities, leaving out all pixels not covered by the slice. Thus, the intensities shown are averages over all cells of a slice.

2.5.2 Transporter model

To describe uptake and removal of fluorescent dyes into and from cells, I started out with the model used by Jakob *et al.* (1998). The tissue under investigation is incubated in an AM-ester of a fluorescent dye with extracellular concentration c_o. The molecules diffuse through the plasma membrane (rate constant, k_D; flux, $k_D (c_o - c_{AM})$) into the cytosol, and intracellular dye/AM-molecules with concentration c_{AM} are hydrolyzed with rate k_e or extruded through P-glycoprotein across the plasma membrane (rate k_p). Assuming the hydrolysis of the AM-ester as the rate limiting step (Jakob *et al.* 1998; Goodfellow *et al.* 1996), c_{AM} approaches a quasi-stationary concentration, which follows from the condition $dc_{AM} / dt = 0$, i.e.

$$k_D (c_o - c_{AM}) - c_{AM} (k_e + k_p) = 0 \qquad \text{or}$$
$$c_{AM} = c_o k_D / (k_D + k_e + k_p) \tag{1}$$

While c_{AM} cannot be observed directly, the fluorescence of the corresponding salt is a measure of its concentration c_s, which increases with ongoing hydrolysis.

With

$$dc_s / dt = k_e c_{AM} \tag{2}$$

and eq. 1 we have

$$dc_s / dt = c_o k_e k_D / (k_D + k_e + k_p) \tag{3}$$

Thus, the concentration c_s increases linearly, and the slope of the increase is limited by the pump rate k_p. In case the pump is completely blocked or not expressed ($k_p = 0$), the increase of c_s is maximum. Otherwise the pump activity reduces the increase of c_s, and thus the increase in fluorescence, with time.

Fluorescence intensities are assumed to be proportional to c_s, so that a constant rise of c_s is reflected by a constant increase in fluorescence F, i.e. $\Delta F/\Delta t = const$.

2.6 Solutions

The composition of the dissociation-, bath- and pipette solutions are listed in Table 1. All chemicals used for the preparation of the solutions were purchased from Sigma (Deisenhofen, Germany). The solutions were prepared using double distilled water (Aqua bidestillata) with calcium concentration in the nanomolar range.

All solutions, were adjusted to pH 7.8 (Howell *et al*. 1970). The osmolarities of the bath and pipette solutions were adjusted to 230 mOsmol and 190 mOsmol, respectively.

	NaCl	KCl	CaCl$_2$	MgCl$_2$	CsCl	CsMeSO$_3$	Glucose	Na-Pyruvate	K-Gluconate	HEPES	EGTA	Na$_2$-ATP	Na$_2$-GTP	PAPAIN
DS$_1$	109	2					10			10	2			10-15 U/ml
DS$_2$	109	2					10			10				
B	98	2	1	2			5	5		10				
I	2	47		2					43	10	0.2	2	0.1	
I$_{Cs}$	2			2	40	44				10	0.2	2	0.1	

Table 1. Composition of the dissociation-, bath- and pipette solutions (concentrations are given in mM)
DS = dissociation solution; B = bath solution; I = standard pipette solution; I$_{Cs}$ = pipette solution with cesium. Where not differently indicated, the standard pipette solution (I) was used.

2.7 Odorants, dyes and pharmacological agents

Patch-clamp and calcium imaging experiments

For odorants, two mixtures of volatile stimuli (Table 2), 19 amino acids (Table 3) and the extract of amphibia food based on *Spirulina* algae (SP) were used. As pharmacological agents activating the cAMP transduction pathway in an odorant-independent way the adenylate cyclase activator forskolin, the phosphodiesterase inhibitor 3-isobutyl-1-methylxanthin (IBMX), and the membrane permeable cAMP analog 8-(4-chlorophenylthio)adenosine 3′:5′-cyclic monophosphate (pCPT-cAMP) were used.

Citralva, lilial and lyral were purchased from International Flavor & Fragrances (Hilversum, The Netherlands) and the algae were from Mikrozell (Dohse Aquaristik, Bonn, Germany). Other odorants and pharmacological agents were from Sigma (Deisenhofen, Germany).

The algae extract was made by dissolving 0.5 g of SP powder in 100 ml bath of solution, centrifuging it at 1000 g for 5 minutes and filtering it through a single use filter (0.5 µm pore size, Minisart, Sartorius AG, Göttingen, Germany).

Mixture	Compounds
V_1	citralva, eugenol, l-carvone, geraniol, citronellal
V_2	lilial, lyral, ethylvanillin

Table 2. Mixtures of volatile stimuli
Mixtures V_1 and V_2 of volatile odorants (Sklar *et al.* 1986). V_1 and V_2 contain odorants believed to stimulate the production of the second messengers cAMP and IP_3, respectively.

The amino acids as well as pCPT-cAMP were dissolved in the bath solution (10 mM stock, each), while forskolin and the IBMX were dissolved in dimethylsulphoxide (DMSO; 10 mM and 50 mM stock, respectively). The mixtures of volatile stimuli were dissolved in DMSO (0.1 M stock). Stimulus solutions were prepared immediately before use by dissolving the respective stock solution in the bath solution.

In patch-clamp experiments and calcium imaging experiments in the mucosa slice, the amino acids were applied either as a mixture of 19 amino acids (AA; 200 μM), or as submixtures (LCN, SCN, BAS, ACID or AROM; 200 μM), or as single amino acids, each at a concentration of 200 μM. In the calcium imaging experiments in the OB, critical amino acids (L-glutamate, L-aspartate, L-glutamine and L-asparagine) that could act directly on OB neurons, were not applied. Therefore, the amino acid mixture used in calcium imaging experiments in the OB contained only 15 amino acids compared to the mix of 19 amino acids used for all of the other experiments. In the calcium imaging experiments in the OB the amino acids were applied at a concentration of 100 μM.

All volatile odorants were applied at a final concentration of 100 μM, except of ethylvanillin, which was applied at 50 μM. Forskolin was used at final concentrations of $10 - 100$ μM, IBMX and pCPT-cAMP were applied at final concentrations of 500 μM and 2.5 mM, respectively. The AM forms of the calcium-indicator dyes Fura-2 and Fluo-4, used to stain the cells of the OB in the nose-olfactory bulb preparation and the ORNs in the mucosa slice, respectively, were dissolved in DMSO (Sigma, Deisenhofen, Germany) and Pluronic F-127 (Molecular Probes, Leiden, The Netherlands) and then diluted to a final concentration of 50 μM using bath solution. To avoid transporter mediated destaining of the cells in the mucosa slices, 50 μM of MK571, a specific inhibitor of the multidrug resistance-associated proteins (MRP, Gekeler *et al.* 1995; Abrahamse and Rechkemmer, 2001) was added to the Fluo-4 incubation solution (see also sections 3.8 and 4.5 for detailed information about multidrug resistance in ORNs). Tetrodotoxin (TTX, 2 μM; Molecular Probes, Leiden, The Netherlands), a blocker of voltage-gated sodium channels, was dissolved in the bath solution where indicated.

Mixture	Amino acids
LCN	proline, valine, leucine, isoleucine, methionine
SCN	glycine, alanine, serine, threonine, cysteine, asparagine, glutamine
BAS	arginine, lysine, histidine
ACID	glutamate, aspartate
AROM	tryptophane, phenylalanine
AA	LCN, SCN, BAS, ACID and AROM

Table 3. Mixtures of L-amino acids
Mixtures of L-amino acids following Caprio and Byrd (1984). LCN, long chain neutral amino acids. SCN, short chain neutral amino acids. BAS, basic amino acids. ACID, acidic amino acids. AROM, aromatic amino acids.

Transporter measurements

Fura-Red, Fura-2, calcein-green and calcein were used as fluorescent dyes and potential transporter substrates, and probenecid, sulfinpyrazone, MK571, verapamil and PSC 833 were used as transport inhibitors. Probenecid and sulfinpyrazone are inhibitors of organic anion transport (Burckhardt and Pritchard, 2000; Pritchard and Miller, 1993; Declèves *et al*. 2000; Abrahamse and Rechkemmer, 2001), which also inhibit MRP-mediated calcein efflux from cells (Feller *et al*. 1995; Versantvoort *et al*. 1995; Evers *et al*. 2000; Morrow *et al*. 2000). MK571 is a specific inhibitor of MRP (Gekeler *et al*. 1995; Abrahamse and Rechkemmer, 2001). Verapamil is an inhibitor of P-glycoprotein (Ford and Hait, 1990; Fujita *et al*. 1997; Jakob *et al*. 1998; Laupeze *et al*. 2001; Abrahamse and Rechkemmer, 2001). PSC 833 is a very specific blocker of P-glycoprotein (Declèves *et al,* 2000; Miller *et al*. 2000; Thévenod *et al*. 2000). The AM forms of the dyes were dissolved in DMSO and Pluronic and then diluted

to a final concentration of 50 µM (Fura-red, Fura-2 and calcium-green) or 250 nM (calcein) using bath solution. The inhibitors used were dissolved according to the instructions provided by the suppliers. The fluorescent dyes used were purchased from Molecular Probes (Leiden, The Netherlands). PSC 833 was a generous gift from Novartis Pharma (Basel, Switzerland) and MK571 was purchased from Alexis (Grünberg, Germany). All other chemicals were from Sigma (Deisenhofen, Germany).

2.8 The application system

In patch-clamp and calcium imaging experiments the bath solution was applied to the recording chamber by gravity feed from a storage syringe through a funnel drug applicator (Schild, 1985). The tip of the applicator was placed as close as possible to the isolated ORNs or to the olfactory mucosa. In calcium imaging experiments in the nose-olfactory bulb preparation, the tip of the applicator was placed directly above the ipsilateral mucosa. The continuous flow from the funnel into the mucosa was 250 µl/minute in patch-clamp and calcium imaging experiments in the nose-olfactory bulb preparation and 350 µl/minute in calcium imaging experiments in the mucosa slice. Odorants and pharmacological agents were pipetted directly into the funnel without stopping the bath solution flow using a 1 ml pipette. Outflow was through a syringe needle placed close to the tip of the applicator to ensure that odorant molecules were removed rapidly. The advantages of this application system are that numberless odorants can be applied and that mechanosensitive responses of ORNs can be prevented. A schematic representation of the application funnel is shown in Figure 15. The minimum interstimulus interval in patch-clamp experiments was 1 minute, in calcium imaging experiments in the mucosa slice 2 minutes, and in calcium imaging experiments in the nose-olfactory bulb preparation 5 minutes.

The dilution of the stimulus within the funnel was less than 1%. The dilution of the stimulus in the mucosa was determined by putting a confocal volume (approx. 1 fl) of the laser-scanning confocal microscope (LSM 510/Axiovert 100), firstly, in front of the funnel outlet and, secondly, in front of the epithelial surface and measuring the respective fluorescences. For this control measurement the fluorescent probe tetramethylrhodamine (Sigma, Deisenhofen, Germany; TMR, 500 nM) was used as a "dummy stimulus". The dilution factor was 0.91 ± 0.02 (mean $\pm$ SD, n = 7). The delay between TMR leaving the funnel outlet and

reaching the mucosal surface was less than 1 second, and after the end of stimulation, TMR was completely rinsed from the mucosa within 15 seconds.
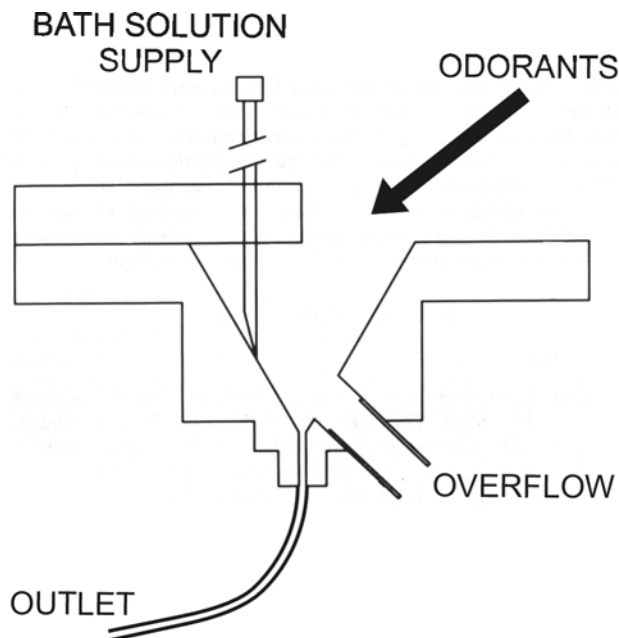
Figure 15. Schematic drawing of the funnel used for the application of bath solution, odorants, and pharmacological agents [modified from Schild, 1985]

In calcium imaging experiments in the nose-olfactory bulb preparation, an additional bath applicator with a higher flow rate of 550 µl/minute was positioned close to the OB. To exclude any direct effects of odorant stimuli on OB neurons, a series of control experiments were performed. After stimulation with odorants, the olfactory nerves were cut and the stimulation was repeated. No response to either stimuli was seen after transsection of the olfactory nerves, and no differences from control conditions were observed. However, to further exclude any direct effects on OB neurons, amino acids which could act directly on OB neurons were not included in the stimulation mixture (see also section 2.7).

2.9 Biocytin/propidium iodide staining of the olfactory mucosa and synaptophysin/propidium iodide staining of the olfactory bulb

Tadpoles were anaesthetized and sacrificed as described in section 2.2. For staining the olfactory mucosa, a block of tissue containing the olfactory mucosae, the olfactory nerves and the anterior part of the brain, including the OB, was cut out. The blocks of tissue were pinned to the bottom of a silicone-covered Petri dish, and the tissue above the OB was removed. Then, 5 µl of DMSO was dropped onto the OB and crystals of biocytin (Molecular Probes, Leiden, The Netherlands) were pinched into the glomerular layer using a fine needle. After 40 minutes of nerve backfilling the blocks were put into bath solution for 1 hour. Then the blocks were fixed in 4% paraformaldehyde (PFA) in phosphate buffer saline (PBS, pH 7.4) overnight, washed in PBS, embedded in 5% low melting point agarose, and vibrotome sectioned at 70 µm. Sections were washed in PBS containing 0.2% Triton X-100 (PBST), and the tissue was incubated in avidin, ALEXA 488 conjugated (Molecular Probes, Leiden, The Netherlands; 1:200 in PBST) for 2 hours at room temperature. After washing (3 x 15 minutes) in PBS, sections were incubated for 15 minutes in 25 µg/ml propidium iodide (Molecular Probes, Leiden, The Netherlands) in PBS to stain cell nuclei. Sections were washed in at least 5 changes of PBS and transferred into 60% glycerol/PBS for at least 1 hour and finally mounted on slides in 80% glycerol/PBS.

For immunostaining the OB, the slices of the anterior part of the brain were fixed in PFA and vibrotome sectioned at 70 µm. Then the sections were washed in PBST for 20 minutes, and nonspecific binding was blocked with 2% normal goat serum (NGS; ICN, Aurora, Ohio, USA) in PBST for 1 hour at room temperature. The tissue was then incubated overnight at 4 °C with the primary antibodies against synaptophysin (rabbit, polyclonal, G113/p38frog) diluted 1:1000 in the blocking solution. Antibodies against synaptophysin were generously supplied by Dr. Reinhard Jahn (Max Planck Institute for Biophysical Chemistry, Göttingen, Germany). Primary antibodies were washed off with PBS (3 x 15 minutes), and Alexa 488 goat anti rabbit secondary antibodies (Molecular Probes, Leiden, The Netherlands) were applied at a dilution of 1:250 in 1% NGS/PBST for 2 hours at room temperature. After washing off the secondary antibodies in PBS, the sections were incubated for 15 minutes in 25 µg/ml propidium iodide in PBS to stain cell nuclei and finally washed and mounted on slides as described above. Preparations were viewed and imaged using a laser-scanning confocal microscope (LSM 510/Axiovert 100).

2.10 Immunocytochemistry against P-glycoprotein

Tadpoles of *Xenopus laevis* (stages 52-54) were anaesthetized and sacrificed as described in section 2.2. A block of tissue containig the olfactory mucosae, the olfactory nerves and the anterior part of the brain was cut out and immediately transferred in 4% PFA in PBS, pH 7.4, overnight at 4° C. For further processing the tissue blocks were washed in PBS, embedded in 5% low melting point agarose, and vibrotome sectioned at 70 μm. Sections were then washed in PBST and nonspecific binding was blocked with 2% NGS (ICN) in PBST for 1 hour at room temperature. The tissue was then incubated overnight at 4 °C in the primary monoclonal antibody against P-glycoprotein C219 developed in mouse (Alexis, Grünberg, Germany) diluted 1:20 in 2% NGS/PBST or in natural mouse serum (NMS, 1:20; Sigma, Deisenhofen, Germany) as a negative control. Primary antibody or NMS was washed off with PBS, and Alexa 488-conjugated goat anti mouse secondary antibodies (Molecular Probes, Leiden, The Netherlands) were applied at a dilution of 1:250 in 1% NGS/PBST for 2 hours at room temperature. The secondary antibody was washed off in several changes of PBS and then the sections were incubated for 15 minutes in 25 μg/ml propidium iodide in PBS for cell nuclei staining. Sections were washed in at least 5 changes of PBS and transferred into 60% glycerol/PBS for at least 1 hour, and mounted on slides in 80% glycerol/PBS. Preparations were viewed and imaged using a laser-scanning confocal microscope (LSM 510/Axiovert 100).

3. Results

PART A

A COMPARISON BETWEEN PREPARATIONS: ISOLATED OLFACTORY RECEPTOR NEURONS VS. OLFACTORY RECEPTOR NEURONS IN THE MUCOSA SLICE

Patch-clamp recordings upon the application of odorants were made in 102 isolated ORNs and in 298 ORNs in slice preparations. The isolated ORNs and the ORNs in the slice were obtained from 37 and 117 animals, respectively.

3.1 Recording duration

The average recording time of 102 isolated ORNs recorded in the on-cell mode was 6.4 minutes and rarely longer than 15 minutes (Figure 16A). All of the isolated ORNs were lost due to seal break, which always happened before the end of the stimulus protocol. Recordings in the slice were categorized in three classes: Some ORNs (106) were lost (seal break) before the end of the experimental protocol (Figure 16B). Some of the ORNs in this group responded to odorants, but as none of them survived the stimulus protocol it was not possible to determine the complete odorant response profile of these ORNs.

Others (165) did not respond to any of the stimuli tested, and the recording was terminated prior to seal break (Figure 16C). The recording times of successful experiments, which were stopped after the end of the experimental protocol (27 ORNs), are shown in Figure 16D. The minimum recording time of successful slice experiments was equal to the maximum recording time of isolated ORNs. The recording time of on-cell recordings in the slice preparation averaged over successful and unsuccessful recordings (Figures 16B and D) was 16.4 minutes. The average recording time of the successful recordings (Figure 16D) was 44.5 minutes.
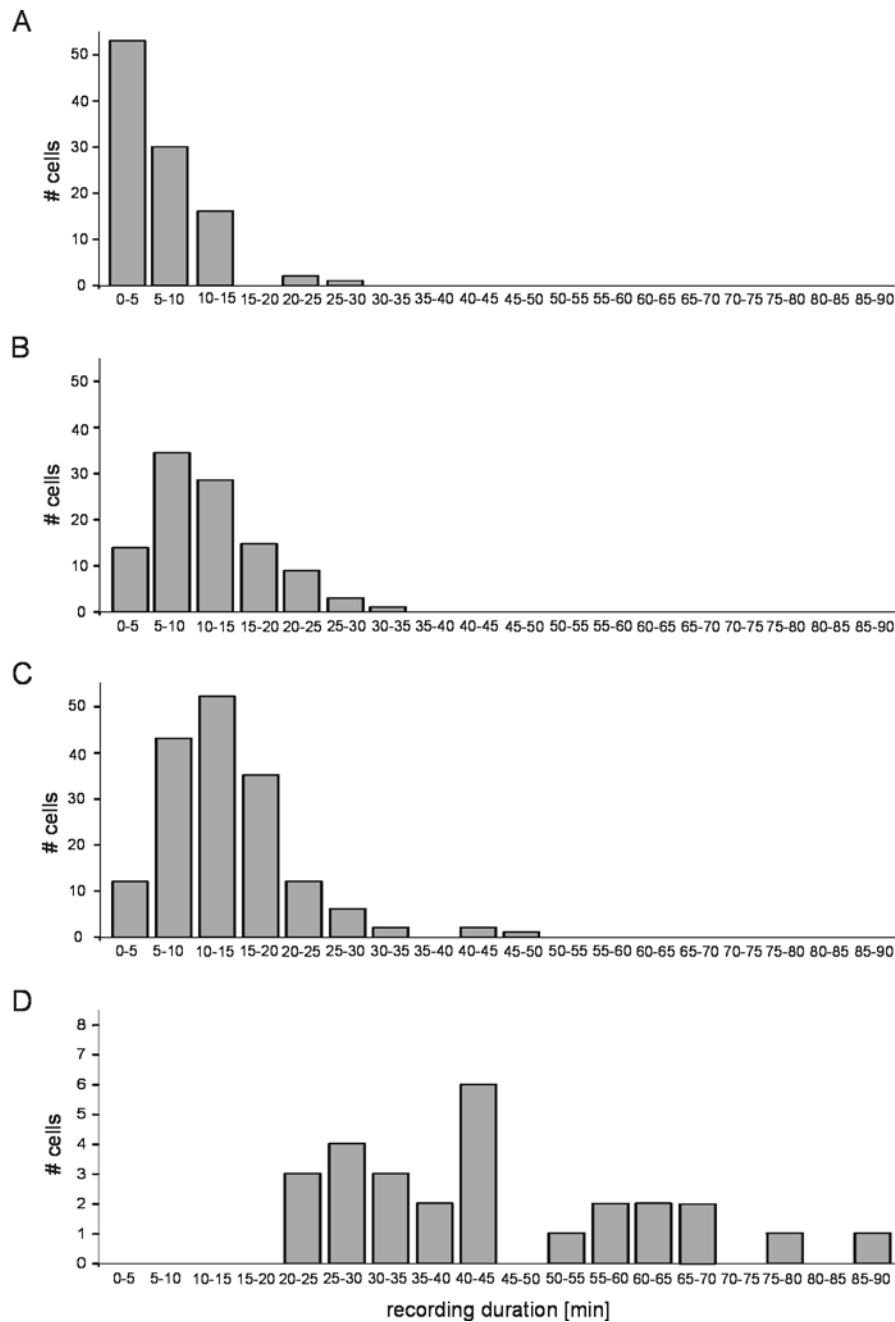
Figure 16. Histograms of the recording times of isolated ORNs and ORNs in the mucosa slice
A: recording times of 102 isolated ORNs. The recording times of ORNs in the slice are plotted in **B**, **C** and **D**. **B:** 106 ORNs lost (seal break) before the end of the experimental protocol, **C:** 165 ORNs did not respond to any of the stimuli applied, and therefore the recording was terminated, **D:** recording times of the successful experiments stopped at the end of the experimental protocol (27 cells). Recording time was measured from seal formation to the end of the recording.

3.2 On-cell mode odorant responses of isolated ORNs

In the on-cell mode of the patch-clamp technique (Hamill *et al.* 1981), individual action potentials are reflected by a biphasic, mixed capacitative/ohmic current associated with the time course of the membrane potential during an action potential (Lynch and Barry, 1989). In these experiments the pipette voltage was clamped to 0 mV. 102 isolated ORNs (stages 48 to 54) were tested for odorant responses in the on-cell mode using (i) a mixture of amino acids (36 cells), (ii) single amino acids (82 cells), or (iii) the mixtures of volatile odorants V1 and V2 (21 cells). Only ORNs that satisfied a number of morphological criteria were selected for recording. They had to have an intact soma and dendrite as well as a dendritic knob and at least 4 visible cilia. 36% of these ORNs showed a spontaneous spiking rate of 3 spikes per second on the average. The remainig ORNs had no spontaneous spiking rate. None of these cells responded to any of the stimuli.

3.3 On-cell mode odorant responses of ORNs in the slice

Recordings from 111 ORNs (stages 49 to 54) in the mucosa slice using the on-cell mode were made. All of these cells were tested for responsiveness to amino acids. Seventeen ORNs (15.3%) responded to amino acids. Figure 17 shows an example of a cell which responded to the AA mixture, to a mixture of basic amino acids (BAS), to L-arginine and to L-lysine. The cell did not respond to the third basic amino acid, L-histidine, nor to the mixtures of acidic (ACID) or aromatic (AROM) amino acids, nor to the short chain neutral (SCN) or long chain neutral (LCN) amino acids.

The overall effect of all responses on the spiking rate was excitatory though the spontaneous spiking activity was always sufficiently high (Figure 18) to observe a decrease if it should have occurred. The amino acid-sensitive ORNs had spontaneous spiking rates from 2 to 13 spikes/s. No correlation between odorant-sensitivity and spontaneous activity could be observed.

None of the cells tested for volatile odorants responded to the mixtures V1 or V2.

In most experiments, at least some stimuli were applied repeatedly to assess the reproducibility of the recording. The responses to L-arginine shown in Figure 19 are

representative for all odorant-sensitive ORNs. This and other experiments indicate that the responses to amino acids remain stable over a long period of time.
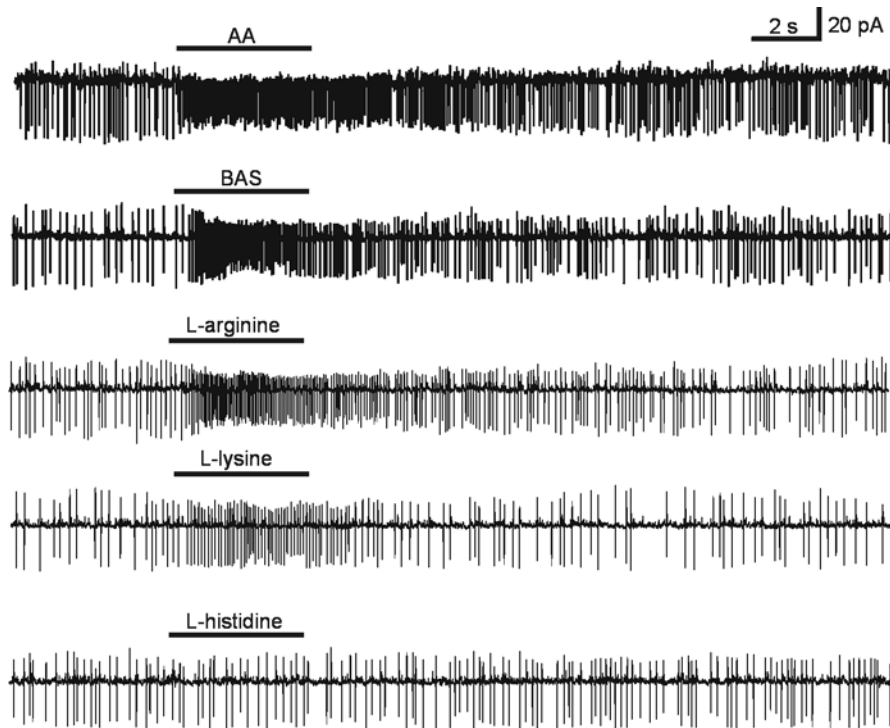
Figure 17. Odorant responses of an ORN in the mucosa slice recorded from a tadpole (stage 53) in the on-cell mode
The current traces from top to bottom show responses to the mixture of amino acids (AA), the mixture of basic amino acids (BAS), to L-arginine and L-lysine. There was no response to the third basic amino acid L-histidine. The ORN did not respond to the mixtures of long chain neutral amino acids (LCN), short chain neutral amino acids (SCN), aromatic (AROM) and acidic (ACID) amino acids (traces not shown). All amino acids were applied at a concentration of 200 µM.

3.4 Whole-cell mode odorant responses of ORNs in the slice

As odorant responses of isolated ORNs when recorded in the whole-cell mode show a fast run-down (Lucero *et al.* 1992; Dionne, 1992; Lischka and Schild, 1993), this configuration was not used with isolated ORNs. Instead I made whole-cell recordings in the mucosa slice from 187 ORNs (stages 49 to 54). Amino acids, algae extract and volatile odorants were applied as stimuli. Ten of 116 ORNs (8.6%) that were tested for responsiveness to amino acids showed a response. 86 ORNs were tested for responsiveness to both amino acids and

algae extract (SP). Five ORNs responded to both AA and SP, while 4 responded to AA but not to SP, and 26 responded to SP but not to AA. Fifty-one of the ORNs did not respond to either stimulus.

Odorant application induced receptor potentials with superimposed action potentials (Figures 20A and B). Threshold for action potentials was ca. -55 mV, which corresponded to the threshold of the voltage-dependent sodium current determined in voltage-clamp experiments (Figure 20C, observed in 15 ORNs).

Odorant responses of ORNs recorded in the whole-cell configuration in the slice showed a pronounced run down (Figure 21, seen in 9 other ORNs).

None of the cells tested for volatile odorants responded to the mixtures V1 or V2.
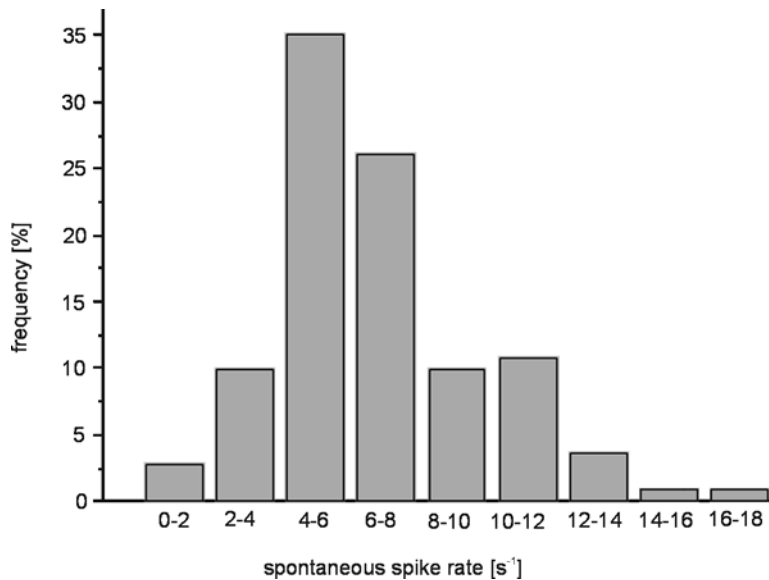
Figure 18. Frequency histogram of spontaneous spiking activities of ORNs in the mucosa slice
111 ORNs (stage 49-54) recorded in the on-cell mode were evaluated for this histogram.
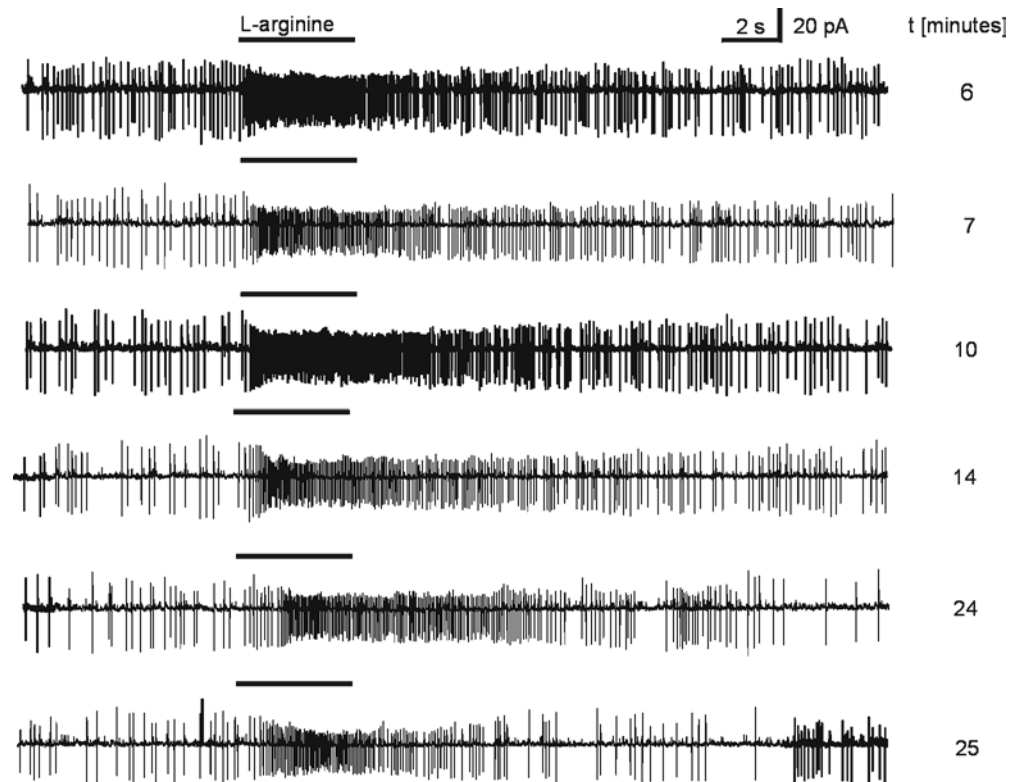
Figure 19. Reproducibility of odorant responses over the time of an experiment
The responses to L-arginine of the ORN shown in Figure 17 are given here. Responses were taken at the times indicated at the right of the respective trace.
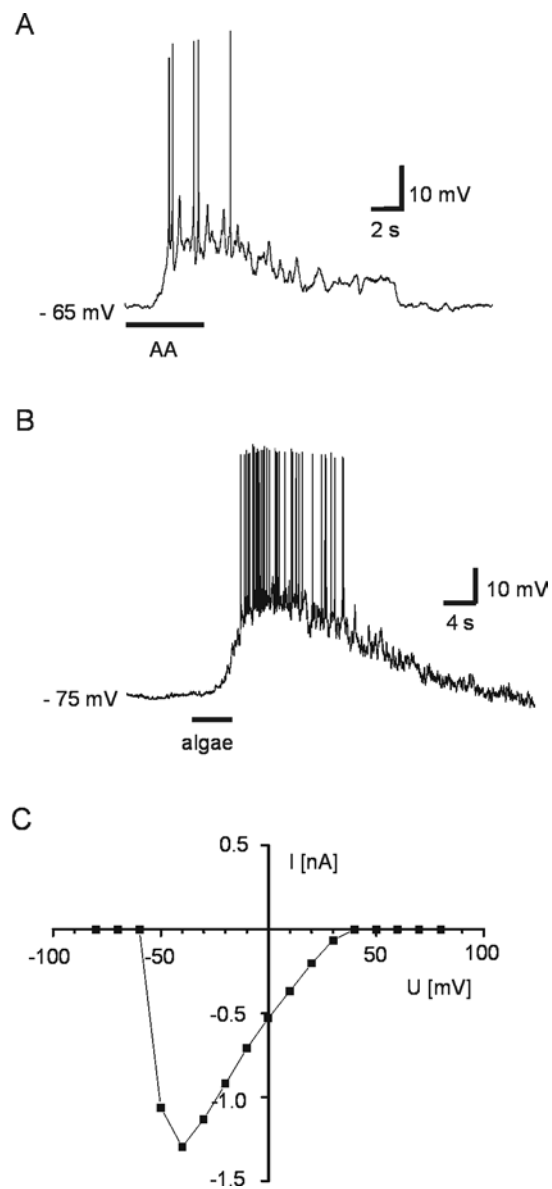
Figure 20. Odorant responses in whole-cell current-clamp mode
A: response of an ORN (stage 52) to the mixture of all amino acids (AA). **B:** response of an ORN (stage 51) to algae extract. **C:** activation curve of the voltage-dependent sodium current in ORNs.
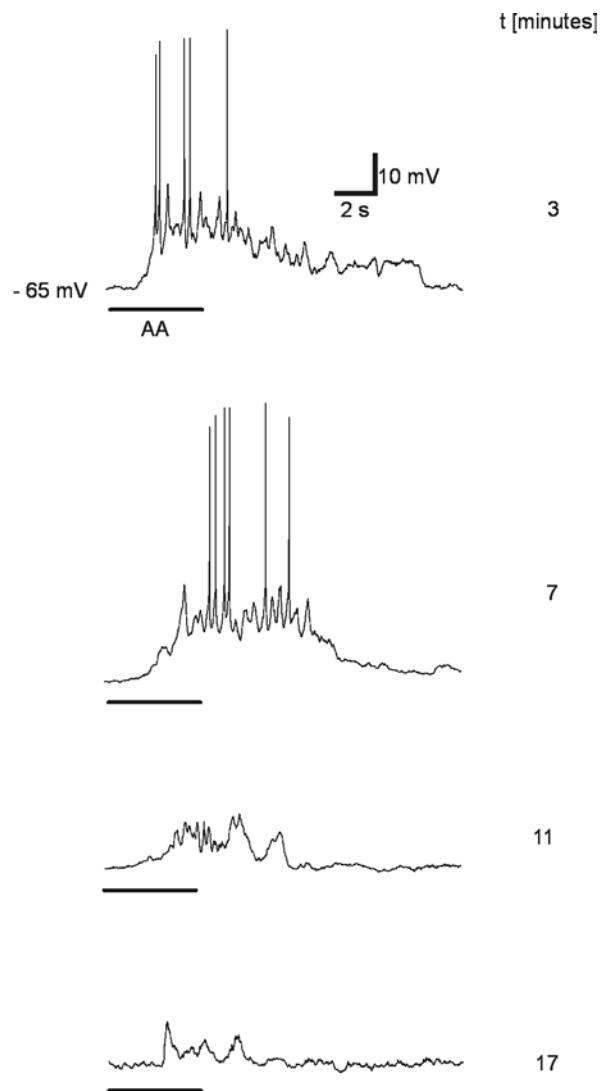
Figure 21. Run-down of odorant responses over the time of an experiment
Run-down of the responses to the mixture of all amino acids (AA) of the ORN shown in Figure 20A.
Responses were taken at the times indicated at the right of the respective trace.

PART B

AMINO ACID RESPONSES OF OLFACTORY RECEPTOR NEURONS IN THE MUCOSA SLICE PREPARATION: A PATCH-CLAMP STUDY

3.5 Responses to amino acids

The response behavior of ORNs (stages 49 to 54) upon application of 19 amino acids was recorded using the patch-clamp technique. 227 cells were tested, 111 in the on-cell configuration and 116 in the whole-cell configuration. The amino acids were applied either as a mixture of 19 amino acids (AA), each at a concentration of 200 µM, or as amino acid submixtures (Figure 22), or as single amino acids, each at 200 µM. 27 ORNs out of 227 responded to at least one amino acid. In 11 cells all 19 amino acids were tested (Table 4). In all cases the overall effect on spiking rate was excitatory, whereby the spontaneous spiking activity of the ORNs was always sufficiently high (Figure 23) to detect a decrease if it should have occurred.

Figure 24 shows an example of a cell (Table 4, cell #3) which responded to the amino acid mixture, to the mixtures of the long chain neutral amino acids (LCN), the short chain neutral amino acids (SCN), the basic amino acids (BAS), as well as to L-methionine, L-glutamine and L-histidine. It responded neither to the mixtures of aromatic amino acids (AROM) or acidic amino acids (ACID) nor to other long chain neutral, short chain neutral or basic amino acids. Stimulus responses came back to spontaneous activity within a variable time that depended on the specific stimulus and never exceeded 60 seconds.

3.6 Lack of correlation between responses to amino acids and to activators of the cAMP-mediated transduction pathway

Ninety ORNs were tested with forskolin (10 to 100 µM) and amino acids (200 µM) using the patch-clamp technique, 51 in the on-cell configuration and 39 in the whole-cell-configuration. 21 out of these ORNs exhibited a response. Nine of these 21 ORNs responded to forskolin, but not to amino acids (Figure 25B and D). The remaining 12 ORNs responded to amino

acids but, interestingly, only 5 of these 12 ORNs also responded to forskolin (Figure 25A, D), while 7 responded to amino acids only (Figure 25C, D). This result, though based on small numbers, clearly indicates that some amino acids are transduced in a cAMP-independent way.
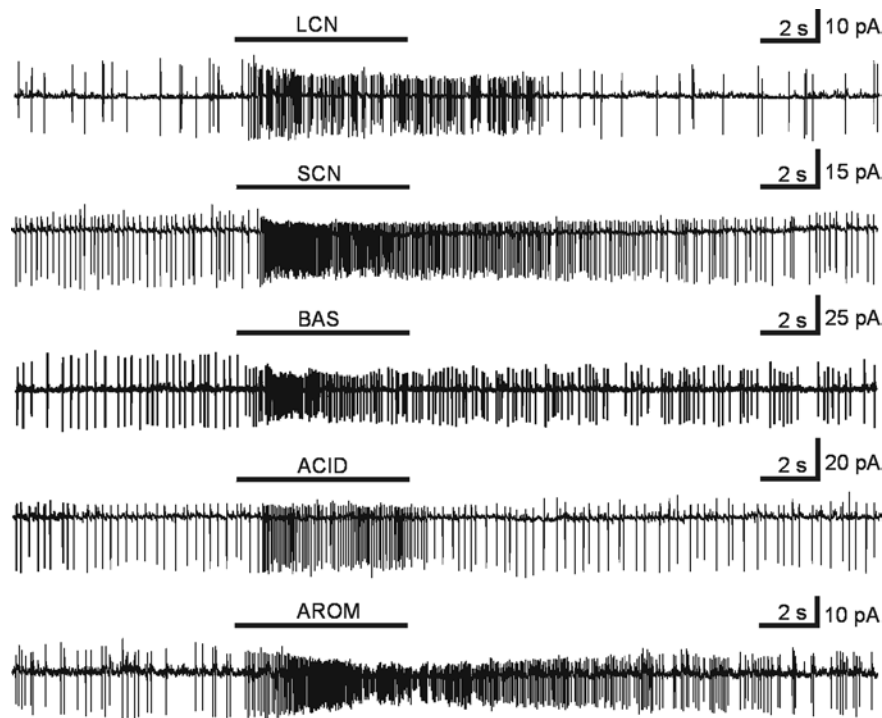
Figure 22. Odorant responses of different ORNs (stages 53 and 54) in the mucosa slice recorded in the on-cell configuration
The current traces from top to bottom show excitatory responses to the mixtures of long chain neutral (LCN), short chain neutral (SCN), basic (BAS), acidic (ACID) and aromatic (AROM) amino acids. In all of the submixtures the concentration of the individual amino acids was 200 µM.

Cell #		1	2	3	4	5	6	7	8	9	10	11
SCN	Gly											
	Ala											●
	Ser											
	Thr											
	Cys											
	Asn											
	Gln			●							●	
LCN	Val	●							●			
	Leu								●	●		
	Ile								●			
	Met	●		●	●		●			●		
	Pro											
ACID	Asp		●									
	Glu											
BAS	Arg					●		●		●		
	Lys					●		●				
	His			●								
AROM	Phe							●				
	Trp							●				

Table 4. Specificity profiles of tadpole ORNs in response to amino acids
Of the 27 ORNs that responded to amino acids 11 were tested with all 19 amino acids. The dot size in the table represents the relative increase of spiking rate with respect to spontaneous activity:

● : > 350% , ● : 250% to 350% , ● : 130% to 250% , no dot: no significant change from spontaneous activity
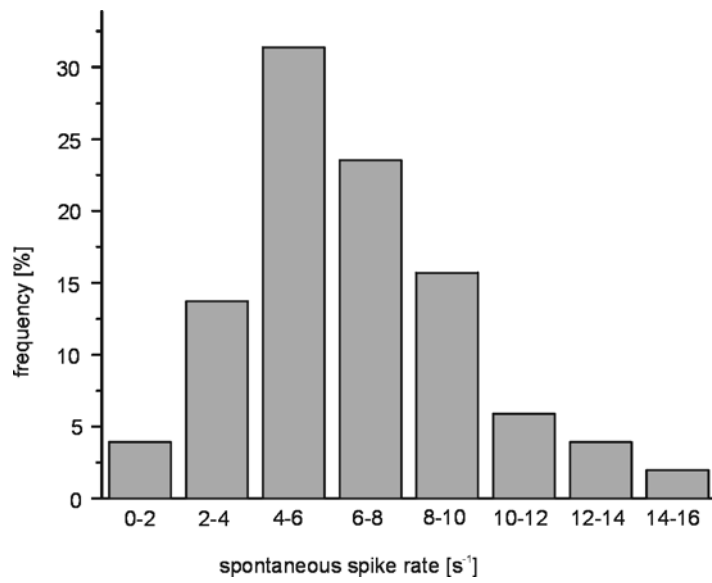
Figure 23. Frequency histogram of spontaneous spiking activities of ORNs in the mucosa slice
51 ORNs (stage 49-54) recorded in the on-cell mode and tested for both forskolin and amino acids were evaluated for this histogram.
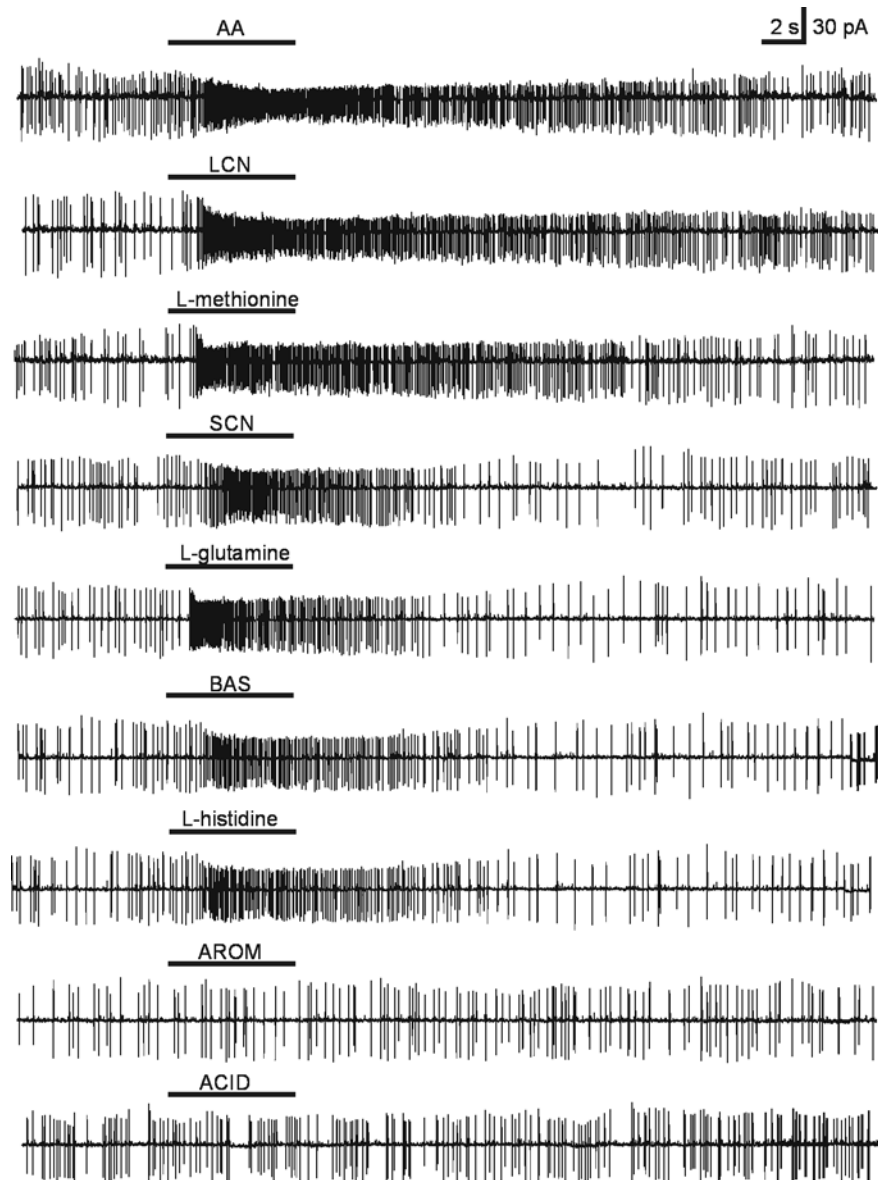
Figure 24. Odorant responses of a single ORN in the mucosa slice from a tadpole (stage 53) recorded in on-cell configuration
The current traces from top to bottom show responses to the mixture of amino acids (AA), the mixture of long chain neutral amino acids (LCN), to L-methionine, the mixture of short chain neutral amino acids, to L-glutamine , the mixture of basic amino acids (BAS) and to L-histidine. There was no response to the mixtures of aromatic (AROM) and acidic (ACID) amino acids. All amino acids were applied at a concentration of 200 µM. The traces were arranged according to the intensities of the responses to the different stimuli.
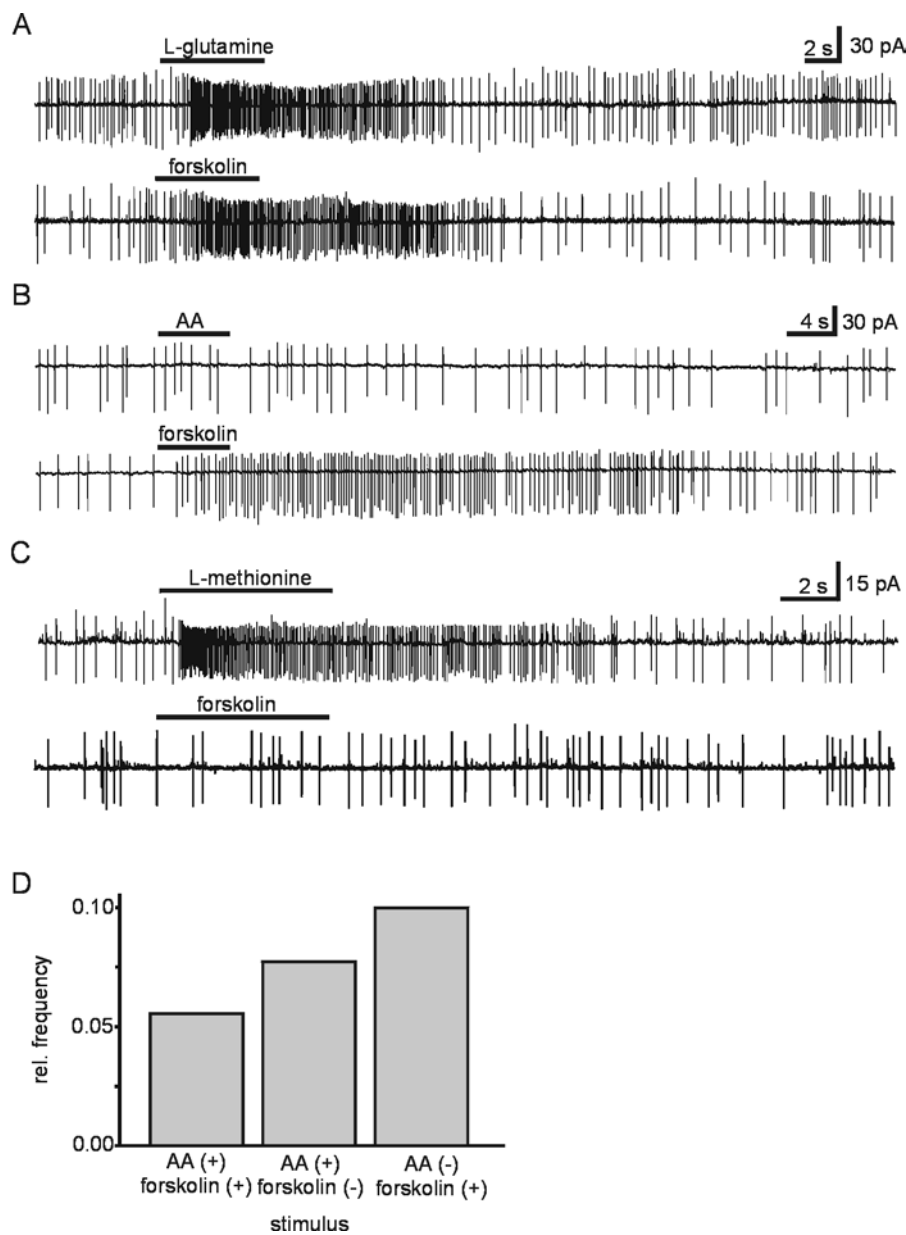
Figure 25. Correlation of odorant and forskolin responses
A: ORN (stage 53) excited by both L-glutamine (200 µM) and forskolin (50 µM). **B:** ORN (stage 51) excited by forskolin (50 µM) but not by the mixture of amino acids (AA, 200 µM). **C:** ORN (stage 54) excited by an amino acid (L-methionine, 200 µM) but not by forskolin (50µM). **D:** occurrences of correlated and uncorrelated responses to forskolin and amino acids. 69 out of the 90 ORNs tested responded neither to amino acids nor to forskolin.

PART C

PROJECTION OF cAMP-INDEPENDENT AND cAMP-DEPENDENT RESPONSES OF OLFACTORY RECEPTOR NEURONS ONTO THE OLFACTORY BULB: A CALCIUM IMAGING STUDY

3.7 Calcium imaging of olfactory bulb neurons after mucosal application of amino acids and pharmacological agents activating the cAMP transduction pathway

Considering the general view that different odorant-receptor specificities are mapped onto different areas of the OB (Ressler *et al.* 1994; Mombaerts *et al.* 1996; Nikonov and Caprio, 2001; Fuss and Korsching, 2001), it should be expected that the projection area of amino acid-sensitive ORNs is not congruent with the projection area of forskolin-sensitive ORNs. This hypothesis was tested using calcium imaging of the postsynaptic population of OB neurons, while applying forskolin (100 µM) or amino acids (100 µM) to the olfactory mucosa. Using this method it was possible to monitor changes in the intracellular calcium concentration $[Ca^{2+}]_i$ in OB neurons. A mix of 15 amino acids (see section 2.7) was used. Figures 26A to F show a representative example of calcium responses in mitral- and granule cells in response to stimulation with amino acids (shown in red) and forskolin (shown in green). The spatial distributions of OB neurons that responded to amino acids and forskolin were clearly different and showed very little overlap (Figures 26C to E). The majority of OB neurons responding to stimulation of the olfactory mucosa with the mixture of amino acids always was located in the lateral half of the OB (n = 33 slices), whereas the population of neurons responding to forskolin was located in the medial half of the OB (n = 8 slices). In cases where both stimuli were used in the same preparation, less than 5% of the neurons responded to both stimuli (n = 8 slices). These neurons were located at an intermediate position (Figures 26F). The time courses of calcium responses to amino acids and forskolin were very similar with a steep increase in intracellular calcium after stimulus onset followed by a plateau and a slow decrease outlasting the stimulus application. Figures 26G and H show three representative time courses of $[Ca^{2+}]_i$ in neurons within the mitral cell layer upon stimulation with amino acids and forskolin.
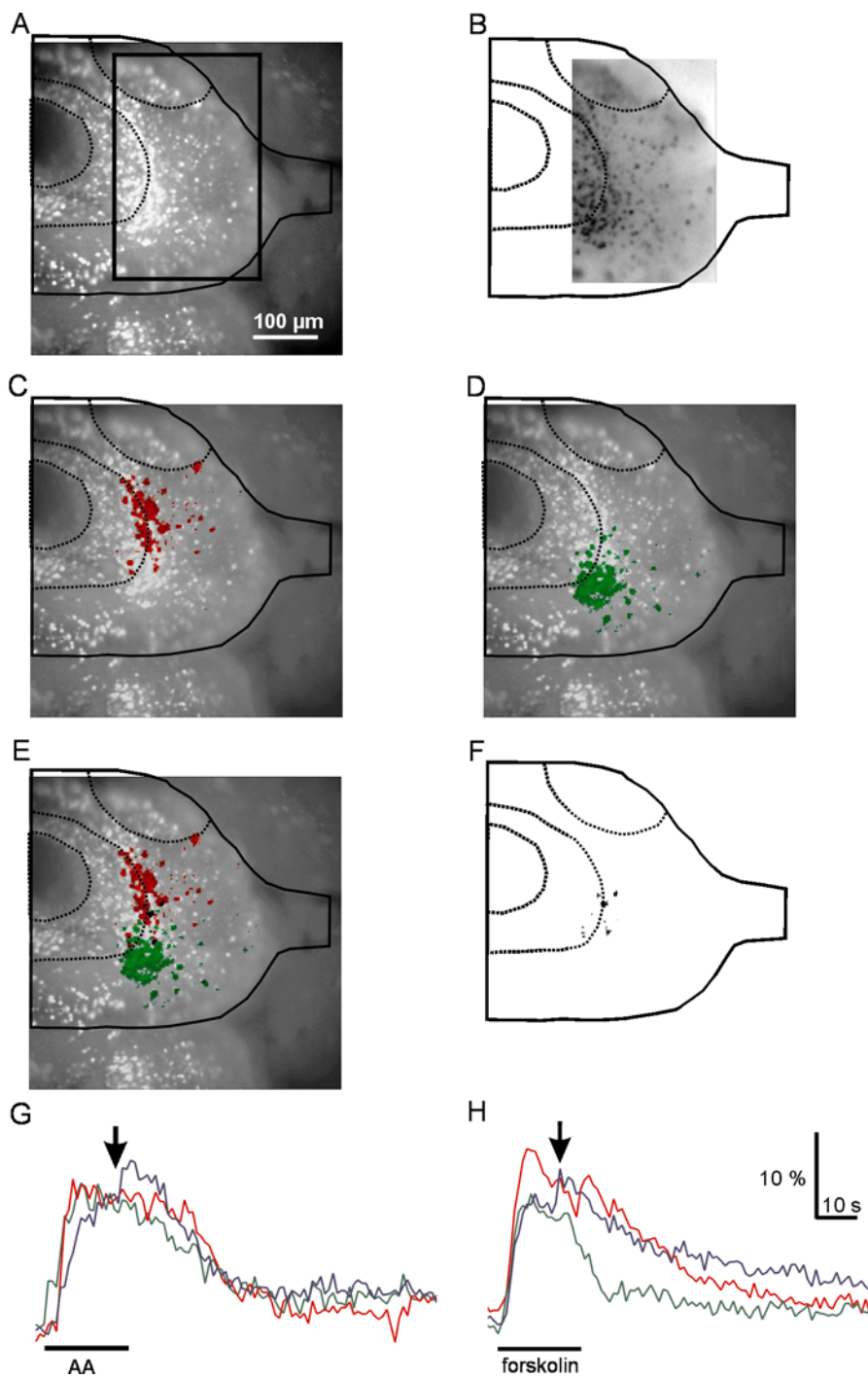
Figure 26. Comparison of changes of [Ca^{2+}]$_i$ in olfactory bulb neurons in response to stimulation of the olfactory mucosa with amino acids and forskolin
A: fluorescence image (excitation at 380 nm) of the olfactory bulb of a tadpole (stage 51) with outlines indicating the borders of the olfactory bulb, olfactory nerve, ventricle and the approximate borderlines between the mitral- and granule cell layers and of the accessory olfactory bulb. Cell bodies of mitral- and granule cells exhibit bright fluorescence. The box indicates the region of interest used for calcium imaging. **B:** ratio image at the time t = 0 s. **C** and **D:** spatial response patterns to stimulation with amino acids (100 µM, **C**, in red) and forskolin (100 µM, **D**, in green) expressed as stimulus-induced ratio changes. For identification of the location of olfactory bulb neurons, the ratio changes were

superimposed to the fluorescence image shown in **A**. **E:** superimposed images of the responses to amino acids and forkolin. **F:** areas of overlap between the responses to stimulation with amino acids and forskolin. Note that only a small subset of neurons responded to both stimuli. **G** and **H:** time courses of calcium responses (expressed as ratio changes) in olfactory bulb neurons in the mitral cell layer to stimulation with amino acids (**G**) and forskolin (**H**). Three representative examples are shown in each case. The arrows indicate the time chosen for the spatial response patterns shown in the images in Figures **C** to **F**.

Though it was clear at this point of the study that the map of amino acid-sensitive ORNs upon the OB differed from that of forskolin-sensitive ORNs, there was still an uncertainty as to whether forskolin, particularly at the high concentrations used, acted by activating the adenylate cyclase. In addition to or instead of its effect upon the adenylate cyclase, forskolin might have acted as an odorant. To remove this ambiguity I tested, in addition to forskolin (50 or 100 μM), the effects of IBMX (500 μM), and pCPT-cAMP (2.5 mM). The neurons activated by forskolin were also activated by IBMX and pCPT-cAMP (Figure 27). The overlap with the neuron ensemble activated by amino acids was as small as described above, though slightly higher for pCPT-cAMP. In the 12 slices tested the overlap was less than 5% for forskolin or IBMX and less than 9% for pCPT-cAMP.
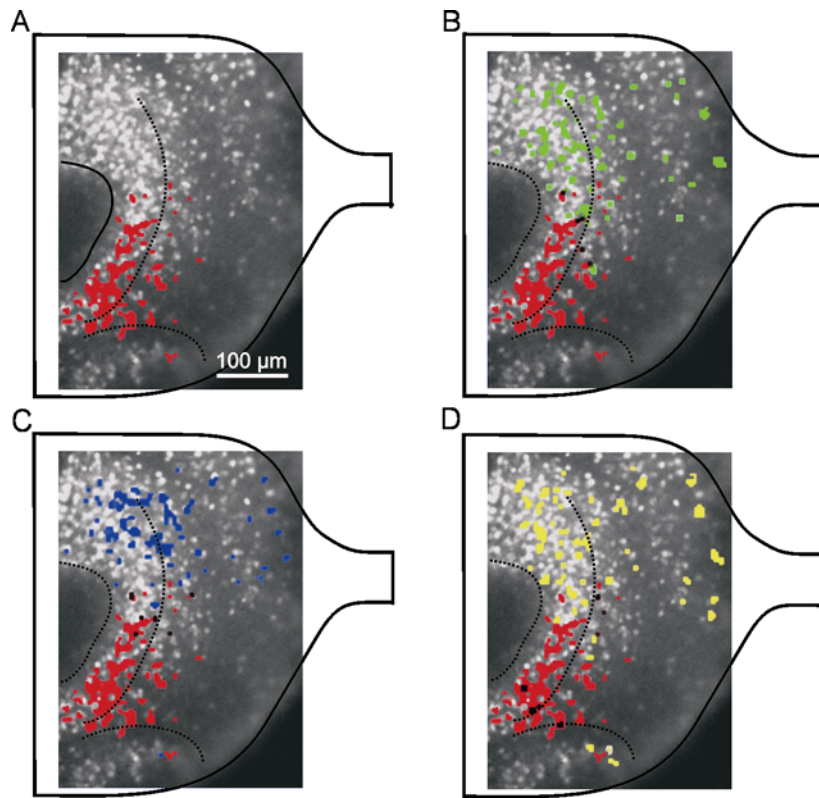
Figure 27. Comparison of [Ca^{2+}]$_i$-responses in olfactory bulb neurons upon stimulation of the olfactory mucosa with amino acids, forskolin, IBMX and pCPT-cAMP
Background (**A** through **D**) of a tadpole olfactory bulb (stage 52) imaged and shown as in the preceding figure. **A:** [Ca^{2+}]$_i$-activation pattern in response to the mixture of amino acids (100 µM, shown in red) superimposed to the background image. **B** to **D:** [Ca^{2+}]$_i$-activation patterns in response to forskolin (50 µM, **B**, green), IBMX (500 µM, **C**, blue) and pCPT-cAMP (2.5 mM, **D**, yellow) were superimposed to the image shown in **A**. The areas of overlap are shown in black.

PART D

MULTIDRUG RESISTANCE TRANSPORTERS IN OLFACTORY RECEPTOR NEURONS

The impossibility to ssuccessfully load mucosa slices with AM-ester derivates of calcium-indicator dyes eliminates an opportunity of simultaneous calcium imaging of many ORNs. Knowing the enormous potential of such imaging, I found it necessary to lay special emphasis on the causes of these loading difficulties. The goal of this study was to find a way to load mucosa slices with AM-dyes in order to be able to make calcium imaging experiments with the simultaneous registration of many ORNs and to take full advantage of this powerful technique.

3.8 Pharmacological and immunohistochemical evidence for the presence of multidrug resistance in ORNs

The starting point for this study was the surprising observation shown in Figure 28. When a tissue slice containing the olfactory mucosa and the OB (Figure 28A) was incubated for 60 minutes in Fura-red/AM, the cells of the OB were clearly loaded with Fura-red (Figure 28B), while the olfactory mucosa showed almost no staining (Figure 28C).

Assuming transporter-mediated destaining during incubation, the dye loading experiment was repeated with probenecid (2.5 mM) added to the incubation solution (all other parameters kept constant). Probenecid is a known inhibitor of organic anion transport (Burckhardt and Pritchard, 2000; Pritchard and Miller, 1993), which also inhibits MRP-mediated calcein efflux from cells (Feller *et al.* 1995; Versantvoort *et al.* 1995). With probenecid added to the incubation solution the dye uptake by the olfactory mucosa was markedly increased (Figure 28E) and became similar to the uptake by the OB (Figure 28D). The OB itself, especially the neuropil, was stained more intensely, too (Figure 28D).

Poor staining of the olfactory mucosa occurred not only with Fura-red/AM incubation (observed in 10 slices), but likewise with calcium-green/AM (3 slices), Fura-2/AM (8 slices) and calcein/AM (4 slices) incubation. Adding probenecid (2.5 mM) to the bath solution
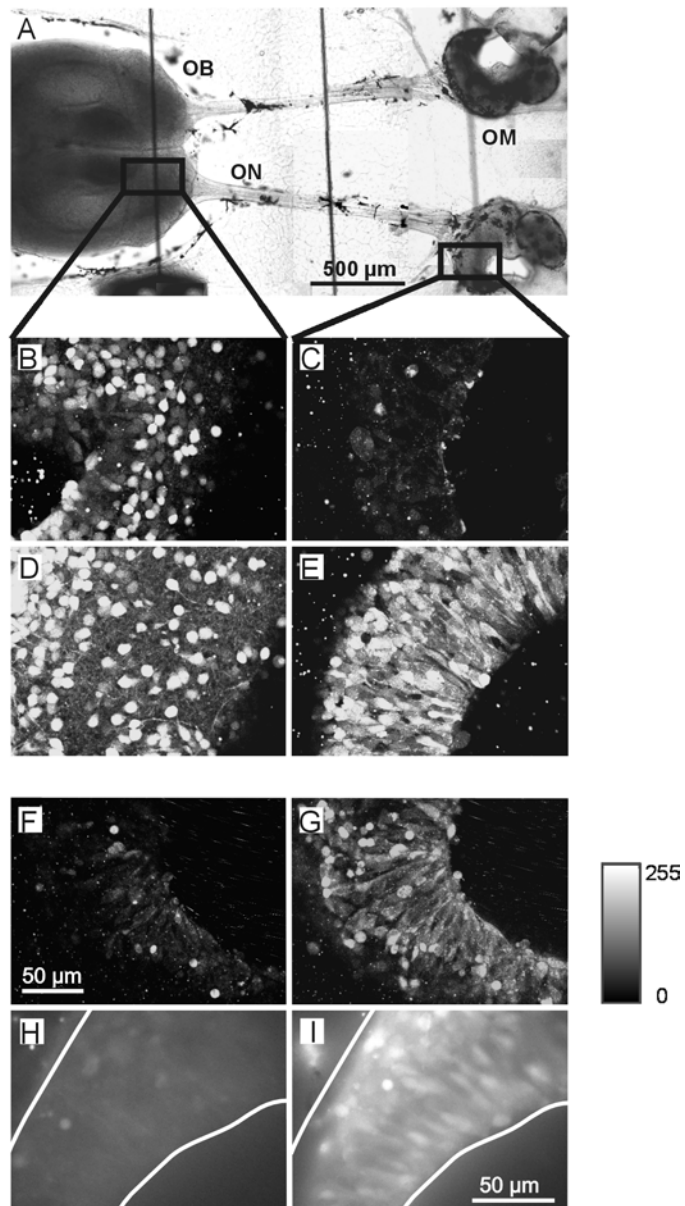
Figure 28. Effect of probenecid on the net uptake of calcium-indicator dyes in the olfactory mucosa (OM) and the olfactory bulb (OB)
A: overview over the OM, the olfactory nerve (ON) and the OB. **B** and **C:** laser scanning images of the OB (**B**) and the OM (**C**) of a slice incubated for 60 minutes in bath solution containing 50 μM Fura-red/AM. **D** and **E:** OB (**D**) and OM (**E**) of a slice incubated for 60 minutes in bath solution containing 50 μM Fura-red/AM and probenecid 2.5 mM. **F** and **G:** slice of an OM exposed to 50 μM Fura-red/AM for 30 minutes without probenecid (**F**), and then for 30 minutes following addition of 2.5 mM probenecid to the bath (**G**). **H** and **I:** CCD-images of a slice of an OM incubated for 30 minutes in 50 μM Fura-2/AM without probenecid (**H**) and with probenecid (2.5 mM) (**I**). For clarity, the borders of the epithelium are drawn in **H** and **I**. Bar scales from low (black) to high (white) fluorescence intensities (12 bit, pictures **B** to **G**).

increased the staining with Fura-red, calcium-green, Fura-2 and calcein (n = 6, 3, 5 and 4 slices, respectively). To see the probenecid-induced increase of staining in one slice at a time, 6 slices were incubated for 30 minutes in Fura-red/AM without probenecid (Figure 28F) and then, for another 30 minutes, with probenecid added (Figure 28G). Clearly, the staining during the second 30 minutes was more effective. The intensity histograms (see section 2.5.1) underwent a marked right-shift during incubation (Figure 29).
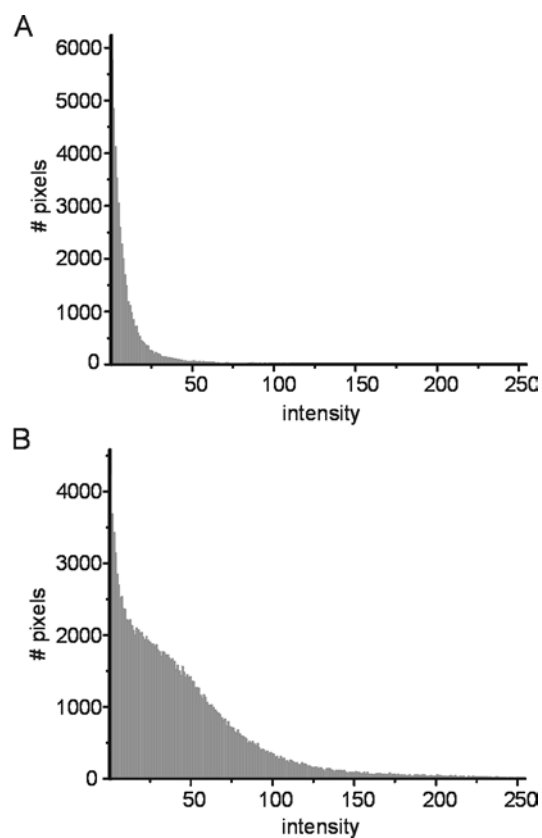
Figure 29. Intensity histograms of confocal images of the olfactory epithelium
A: intensity histogram of the image shown in Figure 28F (control). **B:** intensity histogram corresponding to Figure 28G (probenecid in the incubation solution). Pixels that were not covered by the slice were not considered for calculating the histograms.

The above experiments were carried out using a laser scanning microscope. To measure the net uptake of Fura-2/AM CCD-imaging was used. The resulting images, though blurred and devoid of confocal contrast, show very little fluorescence after 30 minutes incubation in Fura-2/AM in the absence of probenecid (Figure 28H) but marked Fura-2 fluorescence after

another 30 minutes incubation in Fura-2/AM and probenecid (2.5 mM) (Figure 28I). Similar results were observed in 7 slices.

The time course of staining was investigated by taking images at constant time intervals while incubating the slice and representing the intensities I averaged over the slice as a function of time (t; I(t)).

The average intensities I(t) of Fura-red increased very slowly if no transport-inhibitor was present (Figure 30A, from t = 0 to t = 40 min). In the example shown the fluorescence increase was 0.12 min^{-1} without probenecid and 0.69 min^{-1} with probenecid (2.5 mM) added. The net uptake ratio was thus 5.8. In 11 identically performed Fura-red/AM incubation experiments an average net uptake ratio of 5.78 ± 1.41 was found.

MK571, a specific inhibitor of MRP (Gekeler *et al.* 1995; Abrahamse and Rechkemmer, 2001), affected the staining with Fura-red/AM in a way comparable to probenecid (Figure 30B). The average net uptake ratio in 9 identically performed experiments, with MK571 added at a concentration of 50 μM, was 6.73 ± 1.41. In individual ORNs randomly selected from a slice of the olfactory mucosa, MK571 (50 μM) had the same effect on the uptake of Fura-red showing net uptake ratios in the range between 5.91 and 11.32 (n = 6 ORNs, Figure 30C).

One of the MRP isoforms, MRP-5, is known to transport cyclic nucleotides such as cAMP (Jedlitschky *et al.* 2000). As cAMP is the second messenger in many ORNs (Schild and Restrepo, 1998), it was intriguing to see whether or not cAMP increased the net uptake of Fura-red, i.e. whether cAMP would be extruded across the plasma membrane. In 6 out of 6 slices this was not the case (Figure 30D).

Fluorophore bleaching did not affect the experiments. Even a 60-fold increased laser power exposure did not lead to a noticable amount of bleaching. In this test experiment slices were loaded with calcein/AM in presence of MK571 (50 μM) for 1 hour. After the loading phase a bath solution containing MK571 (50 μM) but no dye was applied. Then the fluorescence at a laser power P_0 as used in all experiments was measured. Even at a high frame acquisition rate of 1 frame per second, i.e. 60 times or 180 times faster than in the experiments with calcein or calcium dyes, respectively, no bleaching was observed (Figure 31). However, when taking pairs of images, one pair per 2 seconds, the first at ten times the laser power used before ($10P_0$) and the second at P_0, a fast bleaching of fluorescence occured (Figure 31). As the average exposure in the experiments was at least 60 times less than in the first part of Figure 31, it can be concluded that bleaching did not affect the measurements.
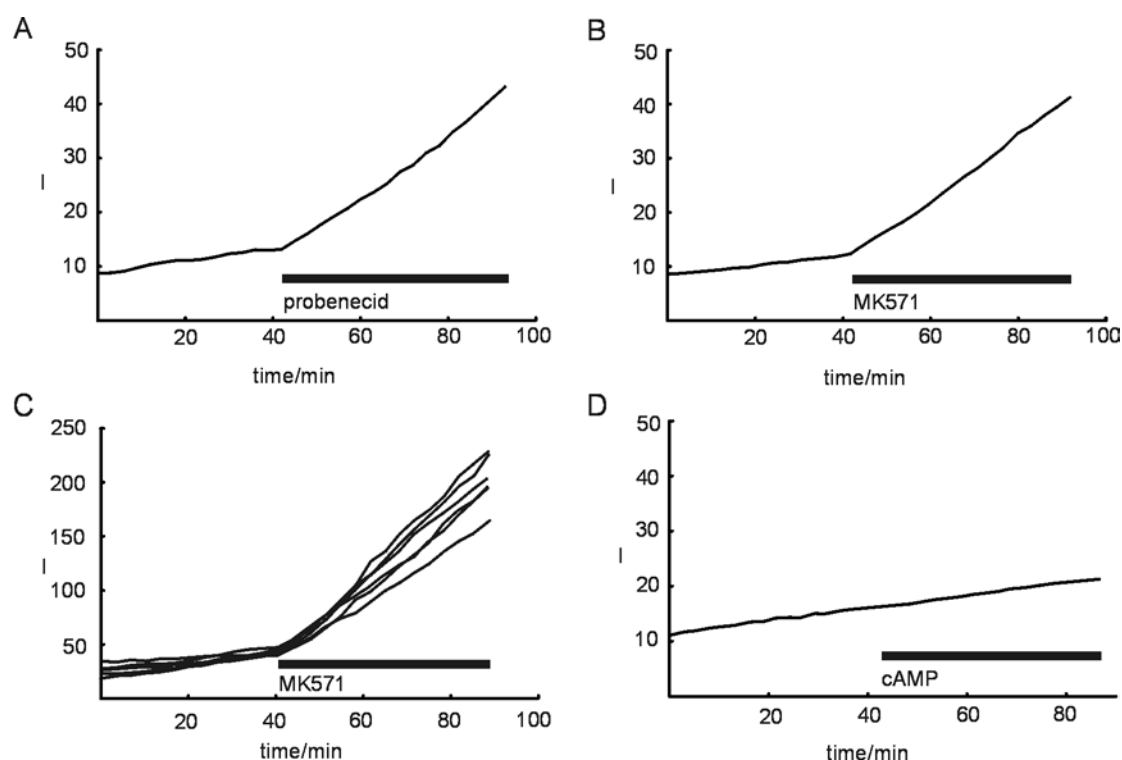
Figure 30. Time courses of Fura-red accumulation in mucosal slices in the absence and presence of probenecid, MK571 and of cAMP
Mucosal slices were incubated in 50 µM Fura red/AM (in bath solution). The bars under the traces show the time over which the indicated drug was added to the incubation solution. The concentration of Fura red/AM was kept constant over the whole incubation. Effects of 2.5 mM probenecid (**A**) and 50 µM MK571 (**B**). **C:** Fura-red accumulation in 6 individual ORNs before and after application of 50 µM MK571. **D:** no effect of 5 mM cAMP upon the uptake of Fura-red.

Interestingly, verapamil, a known inhibitor of P-glycoprotein (Ford and Hait, 1990; Fujita *et al*. 1997; Jakob *et al*. 1998; Laupeze *et al*. 2001; Abrahamse and Rechkemmer, 2001) improved the net uptake of Fura-red, too, though with a lower net uptake ratio (Figure 32A). The inhibitory effects on the extrusion system(s) of verapamil and MK571 were clearly saturated at 125 µM and 50 µM, respectively (Figures 32A and B). Still, verapamil together with MK571, both at saturating concentrations, were more efficient in blocking the extrusion of Fura-red than MK571 alone (Figure 32C). This suggests that Fura-red was extruded by both, MRP and P-glycoprotein.
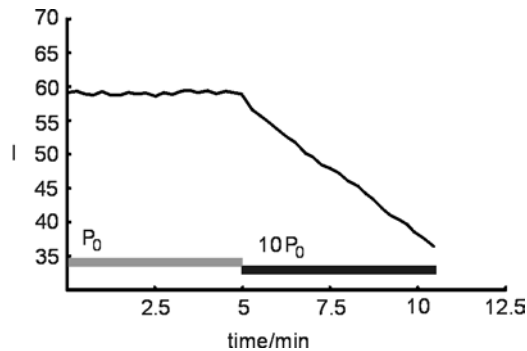
Figure 31. Fluorophore bleaching does not interfere with dye accumulation measurements
A mucosal slice loaded with calcein and placed in a bath solution containing MK571 (50 µM) was exposed, once every second, to a laser beam power P_0. In all experiments reported in this manuscript (except for this figure), the power P_0 was applied either once every minute (calcein) or once every three minutes (calcium dyes). For the experiments shown in this figure frames were taken once every second. The exposure to P_0, even at a frame rate of one per second, did not induce fluorophore bleaching (grey bar, laser power P_0). In a second phase of this experiment (black bar, laser power $10P_0$), once every two seconds, twin pulses were applied, the first being ten times stronger ($10 P_0$) as the second (P_0). This resulted in a substantial fluorophore bleaching.

The presence of P-glycoprotein in *Xenopus laevis* tadpole ORNs was confirmed by incubation and staining with a monoclonal antibody (see section 2.10), showing a spotty antibody staining predominantly in the basolateral compartments of cells in the epithelium (Figure 33). The linear time course of the net uptake curves of Fura-red is consistent with the salt of Fura-red not being removed from the cells (see section 4.5, eq. 4, $k_{M,s} = 0$). However, if calcium-green/AM was used as calcium-indicator dye and probenecid (2.5 mM) as transport inhibitor, the intensity time course, $I(t)$, deviated markedly from linearity (Figure 34A). $I(t)$ instead saturated and appeared to be proportional to $(1-e^{-t/\tau})$ suggesting a concentration-dependent extrusion of the salt of calcium-green (see section 4.5, eq. 4).

Calcein, the fluorescence of which is calcium-independent and which is structurally related to calcium-green rather than to Fura-red, had net uptake kinetics similar to that of calcium-green Figure 34B). Virtually identical results were obtained when using sulfinpyrazone (1mM), another known inhibitor of organic anion transport (Decleves *et al*. 2000; Abrahamse and Rechkemmer, 2001; Figure 34C) or MK571 (50 µM, Figure 34D) as transport blockers.

While Figure 34 shows that calcein is extruded by MDR, its extrusion was also reduced by verapamil (250 µM, Figure 35A) and PSC 833 (10 µM, Figure 35B), two specific blockers of P-glycoprotein (Declèves *et al.,* 2000; Miller *et al.,* 2000; Thévenod *et al.,* 2000). Thus, both MDR and P-glycoprotein are expressed in *Xenopus laevis* tadpole ORNs.
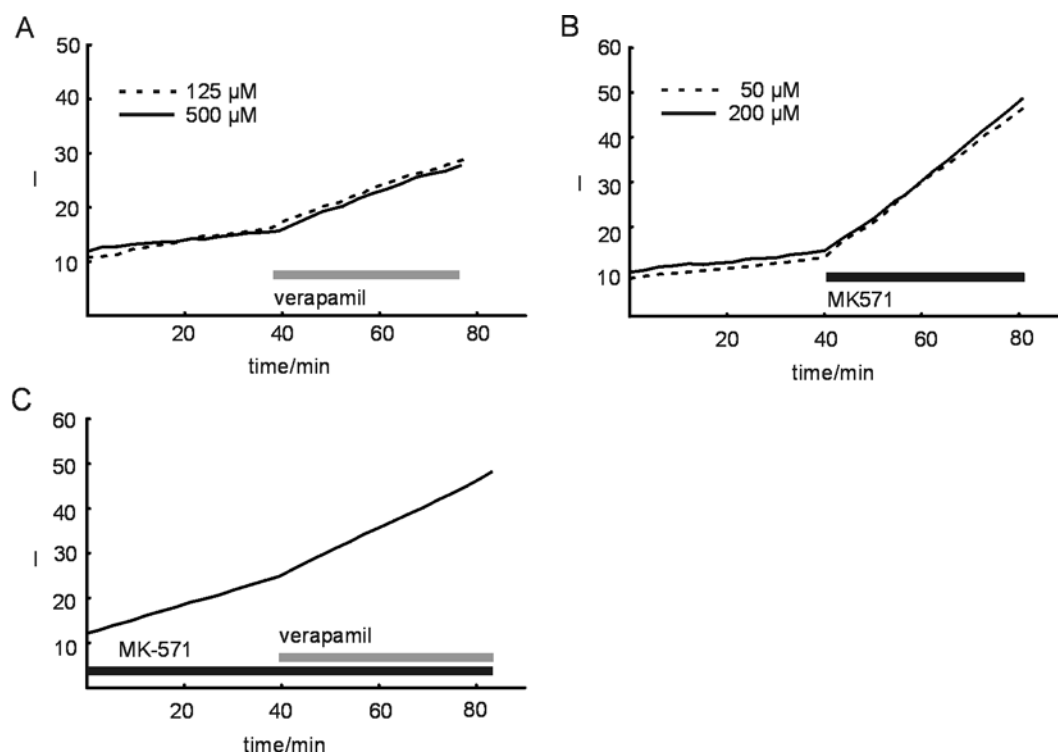
Figure 32. Time courses of Fura-red accumulation in mucosal slices in the absence and presence of inhibitors of multidrug resistance P-glycoprotein (MDR1) and of multidrug resistance-associated proteins (MRP)
Mucosal slices were incubated in bath solution containing 50 µM Fura-red/AM. **A:** effects of 125 µM (dashed line) and 500 µM verapamil (solid line) upon dye uptake are similar. **B:** MK571 at 50 µM (dashed line) had virtually the same effect as the same drug at 200 µM (solid line). The average net uptake ratios in **A** for verapamil concentrations 125 µM and 500 µM were 2.73 ± 0.78 (n = 4) and 2.55 ± 0.52 (n = 5), respectively. With MK571 50 µM and 200 µM the average net uptake ratios were 6.73 ± 1.41 (n = 9) and 6.36 ± 0.66 (n = 6), respectively. **C:** a mucosal slice incubated in bath solution with 50 µM Fura-red/AM was exposed, first, for 40 minutes to MK571 (50 µM) and then for another 40 minutes to both MK571 (50 µM) and verapamil (125 µM). The accumulation effects are clearly additive. The average net uptake ratio was 1.69 ± 0.12 (6 slices). Laser power in **C** was half the power used in **A** and **B**.
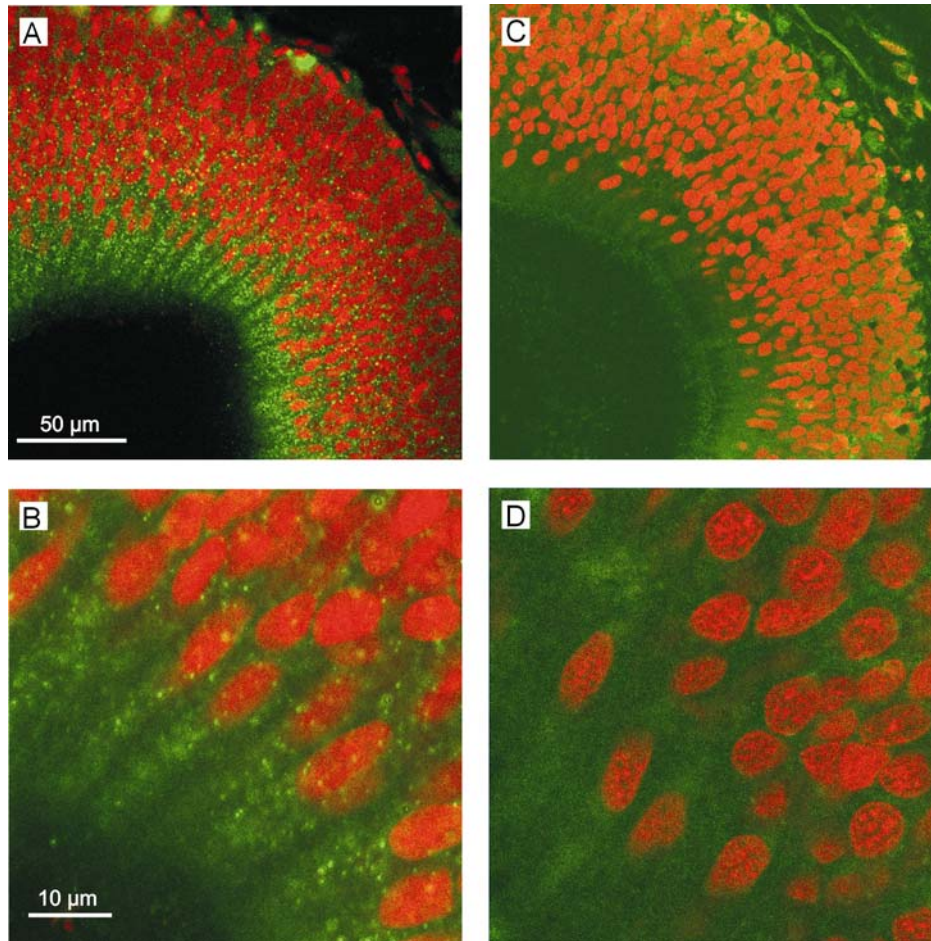
Figure 33. Immunostaining of the olfactory epithelium with the MDR1-specific monoclonal antibody C219

A: immunostaining of a mucosal slice of a *Xenopus laevis* tadpole by C219 antibody (1:20, green fluorescence). **B:** higher magnification of **A**. The slice was counterstained with propidium iodide to show cell nuclei (red fluorescence). Note that the antibody stains the basolateral part (cell bodies and dendrites) of the cells. No detectable staining in knobs and cilia. **C** and **D:** mucosal slice incubated in natural mouse serum (NMS, 1:20) instead of primary antibody (= negative control).
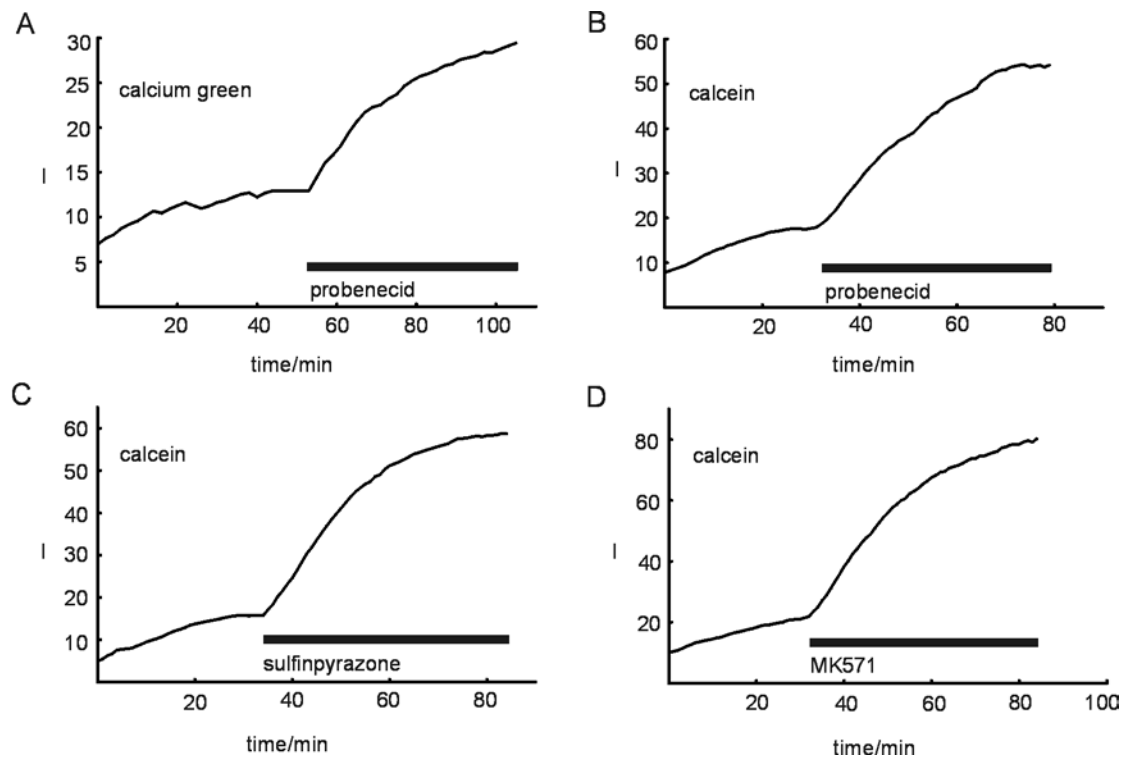
Figure 34. Nonlinear time course of calcium-green accumulation in mucosal slices without and with probenecid and of calcein accumulation without and with probenecid, sulfinpyrazone and MK571

Mucosal slices were incubated in bath solution containing 50 µM calcium-green/AM (**A**) or 250 nM calcein/AM (**B**, **C** and **D**). Effects of the addition of 2.5 mM probenecid (**A** and **B**), 1 mM sulfinpyrazone (**C**) and 50 µM MK571 (**D**). Virtually identical results were obtained from 5, 12, 6 and 5 slices treated the same way as shown in **A**, **B**, **C** and **D**, respectively.
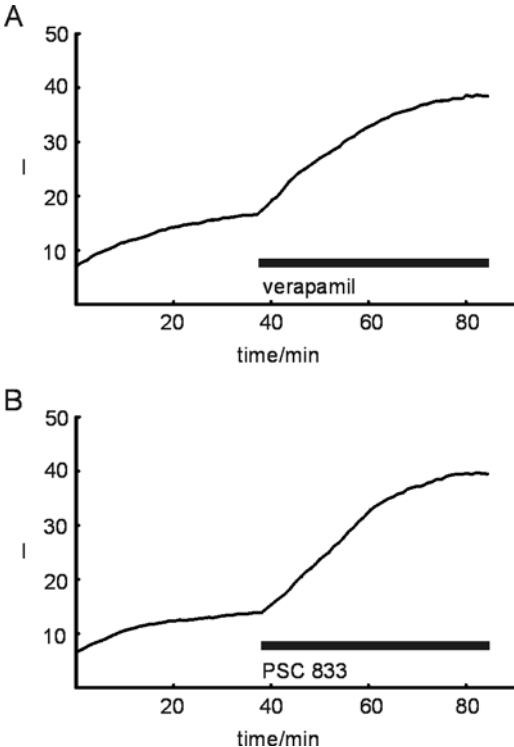
Figure 35. Verapamil and PSC 833 increase calcein accumulation
Mucosal slices were incubated in a bath solution containing 250 nM calcein/AM. Effects of the addition of 250 µM verapamil (**A**) and 10 µM PSC 833 (**B**). Virtually identical results were obtained from 5 and 6 slices treated the same way as shown in **A** and **B**, respectively.

In the above the increased efficiency of dye uptake by blocking MDR and P-glycoprotein was shown while the slices were incubated in a solution containing AM-esters of fluorescent dyes. As a last part of this study the effect of MK571 after the dye had been taken up and was washed out of the bath was analyzed. Figure 36 shows an example of blocked calcein extrusion. After removal of calcein/AM from the bath, the fluorescence decreased slowly as long as MK571 (50 µM) was applied, while, without MK571 in the bath, the decrease of fluorescence was markedly faster (Figure 36A). On the other hand, in standard bath solution, i.e. without calcein/AM and whithout MK571, the fast extrusion of calcein was almost completely stopped by adding MK571 (50 µM) to the bath (Figure 36B).
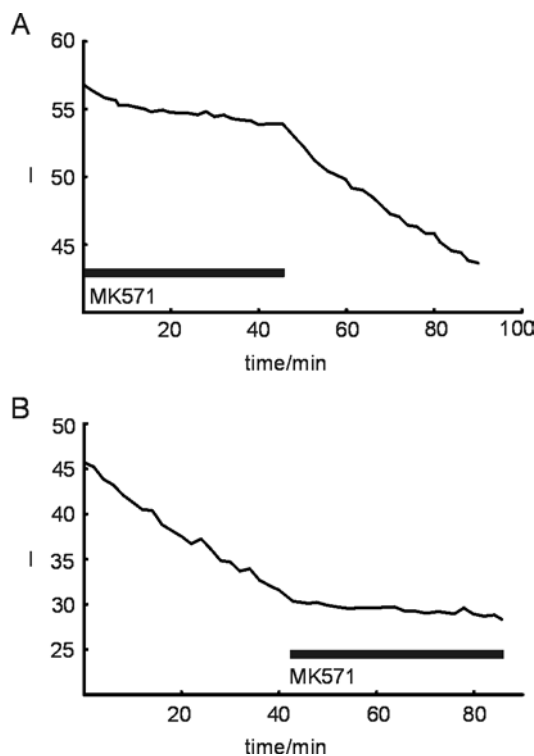
Figure 36. MK571 blocks calcein extrusion
A: fluorescence of a mucosal slice loaded with calcein and placed in a bath solution containing MK571 (50 µM). After 40 minutes MK571 was removed leading to a fast decay of fluorescence. **B** shows the complementary case where a mucosal slice loaded with calcein was first placed in standard bath solution without blocker leading to a fast decay of fluorescence. After 40 minutes addition of MK571 (50 µM) virtually stopped the fluorescence decay. Identical results were obtained from 3 and 4 slices treated the same way as shown in **A** and **B**, respectively.

PART E

AMINO ACID RESPONSES OF OLFACTORY RECEPTOR NEURONS IN THE MUCOSA SLICE PREPARATION: A CALCIUM IMAGING STUDY

The finding that ORNs possess multidrug resistance transporters was crucial for the success of the calcium imaging experiments in mucosa slices (see sections 3.8 and 4.5). It is necessary to add a blocker for multidrug resistance transporters to the AM-dye loading solution to succeed in loading mucosa slices with calcium-indicator dyes.

3.9 Responses to amino acids

Calcium imaging experiments were performed on 52 slices of the *Xenopus laevis* tadpole olfactory mucosae. In 4 of the above mentioned slices, one of which shown in Figure 37, all of the 19 amino acids were tested. Figure 37A shows cells of the olfactory epithelium stained with the calcium-indicator dye Fluo-4. Some of the cells had a high fluorescence from the beginning (asterisks) presumably because they did not survive the tissue slicing. Such cells were discarded from further evaluation. The encircled cells were responsive to a mixture of 19 amino acids (AA) as seen from the increase in intracellular calcium concentration $[Ca^{2+}]_i$ in Figures 37B to D. After an interstimulus interval of 2 minutes the five submixtures of amino acids (LCN, SCN, BAS, ACID and AROM) and subsequently the 19 single amino acids were applied, one after another. All amino acids were applied at a concentration of 200 μM.

Figure 38 shows the selectivities of the three ORNs marked with an arrow in Figure 37A. ORN #1 (Figure 38A) responded only to L-glycine and the corresponding submixture of short chain neutral amino acids. ORN #2 (Figure 38B) responded to L-methionine and, though slightly weaker, to L-isoleucine, as well as to the corresponding long chain neutral submixture. It also responded to L-alanine and to L-arginine, as well as to the corresponding short chain neutral and basic submixtures. The third ORN (Figure 38C) responded to the eight amino acids L-leucine, L-methionine, L-cysteine, L-alanine, L-threonine, L-arginine, L-histidine and L-tryptophane, whereby the response to L-histidine was small but clearly correlated to the stimulus onset. The $[Ca^{2+}]_i$ came back to a resting level within a variable

time after the application of the stimulus. It depended on the specific stimulus and never exceeded 60 seconds.
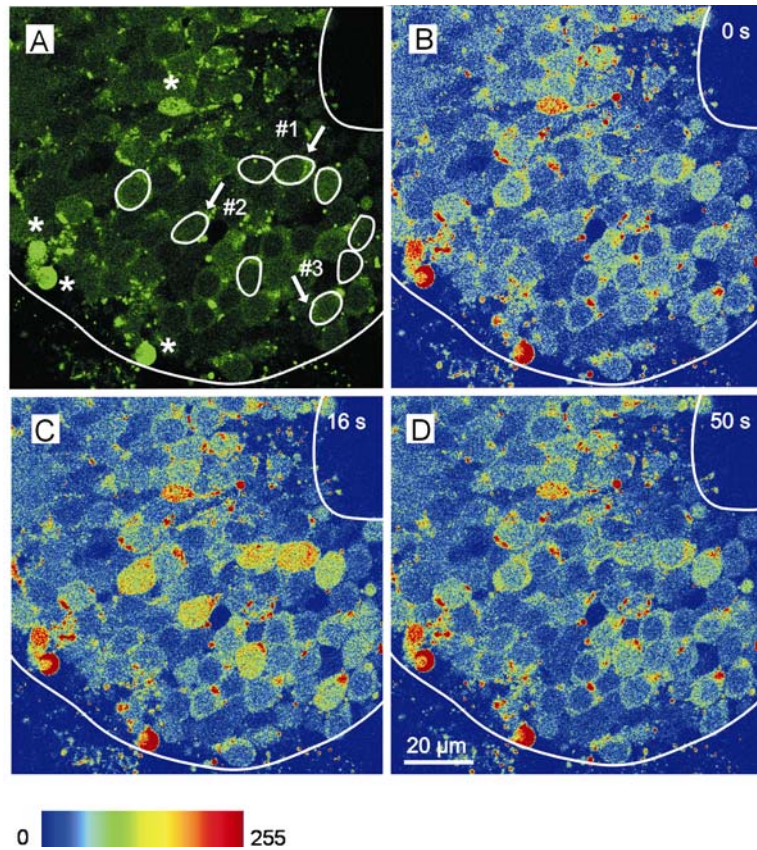
Figure 37. Slice of the olfactory epithelium of a *Xenopus laevis* tadpole and amino acid-induced [Ca^{2+}]$_i$-increases in individual ORNs in a mucosa slice
A: fluorescence image of a mucosa slice (stage 52, image acquired at rest) stained with Fluo-4. Amino acid-sensitive ORNs are encircled. The asterisks indicate ORNs showing high basal fluorescence levels at rest. The responses to amino acids of the ORNs indicated by arrows are shown in Figure 38. **B to D:** sequence of three pseudocolored images of the slice showing that stimulation with a mixture of amino acids (200 μM, each) transiently increases calcium-dependent fluorescence in the ORNs encircled in **A**. **B:** before the application of the amino acid mixture (t= 0 s). **C:** at the peak of the response (t= 16 s). **D:** after return to the basal fluorescence level (t= 50 s).
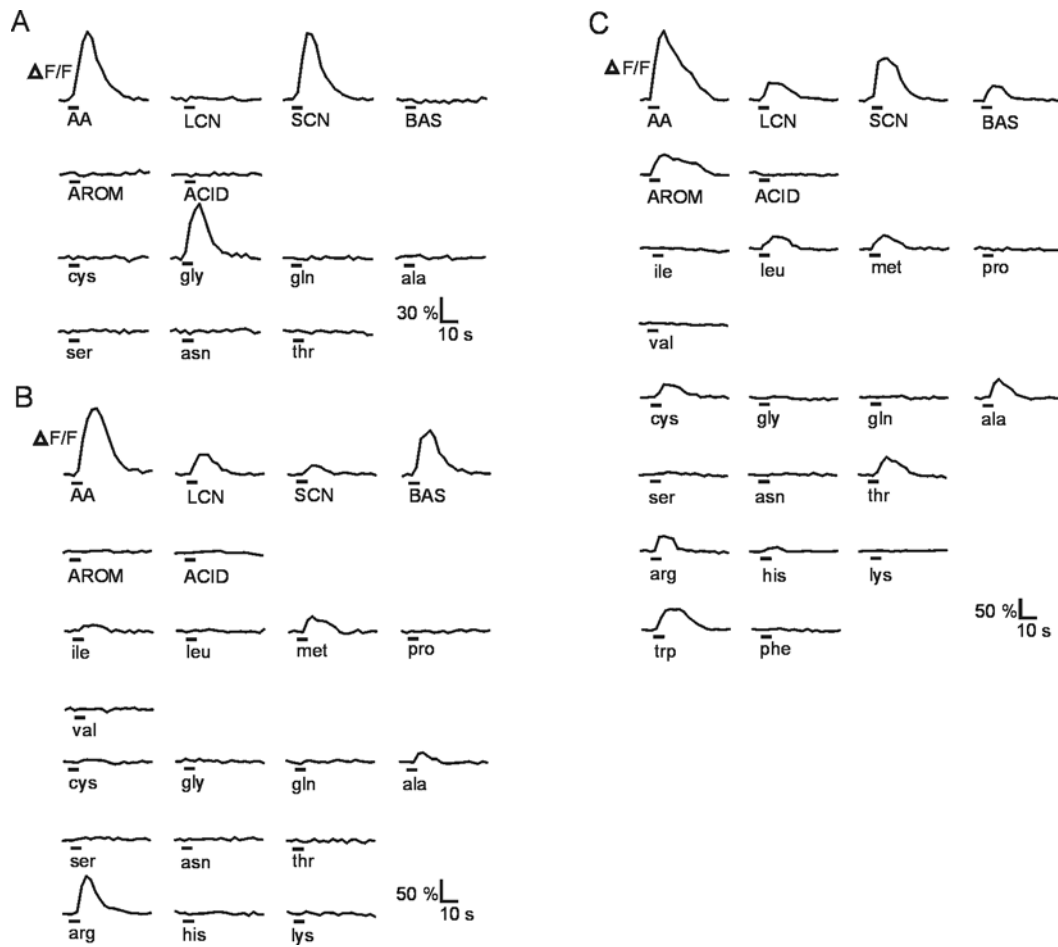
Figure 38. Amino acid-induced changes in calcium-dependent fluorescence of three individual ORNs in a mucosa slice
A: time course of $[Ca^{2+}]_i$ transients of ORN #1 (see Figure 37A), evoked by the application of amino acids. The traces show responses to the mixture of 19 amino acids (AA), to the mixture of short chain neutral amino acids (SCN) and to L-glycine. No response to the mixtures of the long chain neutral (LCN), the basic (BAS), the aromatic (AROM) and the acidic (ACID) amino acids. No response to the remaining single amino acids of the SCN mixture. **B:** ORN #2 (see Figure 37A) responded to the mixture of AA, the mixture of LCN, to L-methionine and, though slightly weaker, to L-isoleucine, the mixture of SCN, to L-alanine, the mixture of BAS and to L-arginine. No response to the mixtures AROM or ACID, nor to the remaining single amino acids of the responsive groups. **C:** ORN #3 (see Figure 37A) responded to the mixtures of AA, LCN, to L-leucine and L-methionine, the mixture of SCN, to L-cysteine, L-alanine and L-threonine, the mixture of BAS, to L-arginine and, though slightly weaker, to L-histidine, the mixture of AROM and to L-tryptophane. No response to the ACID mixture, nor to the remaining single amino acids of the responsive mixtures. All amino acids were applied at a concentration of 200 µM.

The attempt to perform a thorough classification of the response patterns of ORNs to amino acids failed using the patch-clamp technique. The exact response pattern of only 11 out of 227 patched ORNs (see Table 4; section 3.5) could be determined. The major difficulties encountered using the patch-clamp technique were to find amino acid responsive ORNs (only 27 out of the 227 patched ORNs responded to amino acids) and to maintain the seal for an appropriate time to test all of the 19 amino acids if an ORN responded to amino acids (this was possible in only 11 out of the 27 amino acid responsive ORNs).

Using the calcium imaging technique this undertaking seems to be much easier. Though as yet only 4 mucosa slices were tested for the responsiveness to all 19 amino acids, the complete response pattern of 21 ORNs was defined (Tabel 5). In one of the 4 slices the specificity profiles of as many as 13 ORNs could be determined. Figures 38 A to C show the amino acid-induced changes in calcium-dependent fluorescence of the ORNs #5, #2 and #13 (Table 5), respectively.

CELL #	SCN							LCN					ACID		BAS			AROM	
	Gly	Ala	Ser	Thr	Cys	Asn	Gln	Val	Leu	Ile	Met	Pro	Asp	Glu	Arg	Lys	His	Phe	Trp
1	x	x			x	x	x		x							x	x	x	
2		x								x	x				x				
3		x			x						x					x			
4		x		x	x		x		x	x					x				
5	x																		
6		x			x	x	x		x	x	x				x	x		x	x
7																	x		
8	x	x	x				x				x					x	x	x	x
9															x				
10		x			x	x	x	x	x	x	x				x	x			
11															x				
12		x	x	x	x		x		x	x	x				x		x	x	x
13		x		x	x				x		x				x		x		x
14																	x		
15															x				
16	x	x					x		x		x						x	x	x
17		x				x	x				x			x					
18							x		x		x								
19					x		x												
20						x													
21						x													

Table 5. Specificity profiles of ORNs in response to amino acids
Four mucosa slices of tadpoles (stages 51 to 53) were imaged. The specificity profiles of 21 ORNs could be determined. The amino acids that elicited an increase in $[Ca^{2+}]_i$ in each ORN are marked with an x. For clarity the responses of amino acids of the 5 different submixtures are given in different colors.

3.10 What gives rise to calcium-increase in ORNs after application of odorants?

The odorant-induced $[Ca^{2+}]_i$-increase could be brought about either by the spiking activity of the ORN and concomitant activation of high-voltage activated (HVA) calcium channels (Schild and Restrepo, 1998), or by calcium influx through calcium-permeable ion channels, directly or indirectly activated by the odorants, but independent from spiking. Obviously, both effects could overlap.

Figures 39A to C show that the odorant-induced $[Ca^{2+}]_i$-increase in an ORN upon stimulation with an amino acid is reduced but not completely blocked by 2 µM TTX. This evidence was confirmed in 59 ORNs (Figure 39D). The reduction of odorant-induced $[Ca^{2+}]_i$-increase under TTX varied between approx. 18.6% and 93.8% (mean = 59.7%). On the other hand, the same concentration of TTX completely blocked spike-associated currents measured in the on-cell configuration of the patch clamp technique (Figure 39E) and the voltage-gated sodium current recorded in the whole-cell configuration of the patch-clamp technique (Figures 39F and G). The evidence shown in Figure 39E and in Figures 39F and G was confirmed in 6 and 7 ORNs, respectively. Taken together, these experiments indicate that odorant-induced spiking on the one hand and transduction channels on the other contribute in a varying manner to the overall $[Ca^{2+}]_i$-increase of the ORNs after stimulation with amino acids.
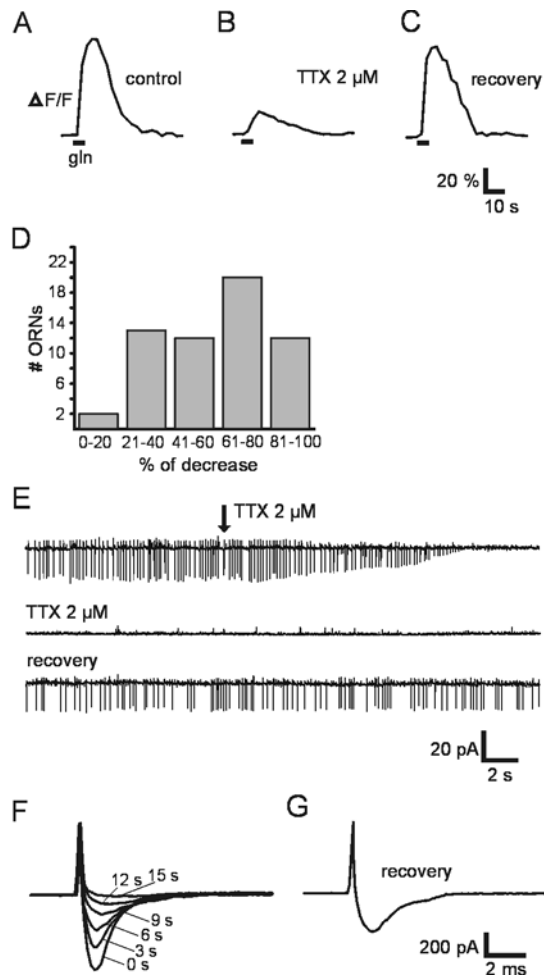
Figure 39. Influence of TTX on odorant-induced [Ca^{2+}]$_i$ transients, spike-associated currents and sodium currents of *Xenopus laevis* tadpole ORNs
A: L-glutamine (200 µM) -induced [Ca^{2+}]$_i$ transient of an individual ORN (stage 53) of a mucosa slice.
B: 5 minutes after the addition of 2 µM TTX to the bath solution the L-glutamine-induced [Ca^{2+}]$_i$ transient was clearly smaller but still present. With TTX the slope of the transient was smaller. **C:** after a wash-out time of 12 minutes the L-glutamine-induced [Ca^{2+}]$_i$ transient recovered completely. **D:** relative decrease of odorant-induced [Ca^{2+}]$_i$ transients after addition of TTX (2µM) to the bath solution plotted as a histogram (n = 59 ORNs).
E: current traces showing spike-associated currents of an ORN (stage 54) of a mucosa slice recorded in the on-cell configuration of the patch-clamp technique. Less than 15 seconds after the addition of TTX (2 µM) to the bath solution (see arrow in the upper trace) the spike-associated currents are completely blocked. As long as TTX was present in the bath solution the spike-associated currents did not recover (middle trace). Thirteen minutes after the beginning of wash-out the spike-associated currents are almost completely recovered (bottom trace). **F:** voltage-activated sodium currents of an ORN in the slice preparation recorded in the voltage clamp configuration of the patch-clamp technique. To block potassium currents, a pipette solution containing cesium instead of potassium was used (I$_{Cs}$; see section 2.6). The holding potential was - 80 mV. The current responses were evoked by depolarizing voltage steps to -30 mV given every 3 seconds. After the first depolarizing step TTX (2 µM) was added to the bath solution. 15 seconds after the beginning of TTX application the current was completely blocked. **G:** recovery of the current after 9 minutes of wash-out.

3.11 Lack of correlation between responses to amino acids and to activators of the cAMP-mediated transduction pathway

To confirm the evidence of a cAMP-independent transduction of amino acids obtained using the patch-clamp technique, calcium imaging experiments in the mucosa slice were performed. In order to stimulate all ORNs in a slice that would, under appropriate natural conditions, respond to a cAMP-mediated odor, forskolin (50 µM) was applied as a pseudostimulus to the olfactory mucosa. Imaging of the mucosa revealed the ORNs that responded with an increase in $[Ca^{2+}]_i$ (sequence of images shown in Figures 40 A to C). Responsive ORNs are encircled in Figure 40B. In order to stimulate all ORNs in the same slice that responded to one or more amino acids, the mixture of 19 amino acids (200 µM) was applied (sequence of images shown in Figures 40 D to F). Responsive ORNs are encircled in Figure 40E. Figure 41 summarizes these results by giving the forskolin-sensitive cells in green and the amino acid-sensitive cells in red. In this slice, there was just one ORN that responded to both stimuli (shown in yellow). The sequential application of amino acids and forskolin was repeated in 44 slices. The two kinds of stimuli always activated different sets of ORNs, with little overlap. In all of the slices tested, 1001 ORNs responded either to amino acids or to forskolin. 503 ORNs responded to the mixture of amino acids and 498 to forskolin. 54 ORNs (less than 6%) responded to both stimuli.

To confirm this result, and to rule out the possibility of forskolin acting through some other cAMP-independent mechanism, I applied the membrane-permeable cAMP analogue pCPT-cAMP (2.5 mM) in addition to forskolin and amino acids (n = 5 slices, one of them being the slice shown in Figure 40). The set of ORNs responding to pCPT-cAMP was virtually identical to that responding to forskolin and different from the set of ORNs responsive to amino acids. All of the 56 ORNs responsive to forskolin also responded to pCPT-cAMP. Seven additional ORNs were responsive only to pCPT-cAMP.

The two classes of stimuli used, i.e. amino acids on the one hand and forskolin or pCPT-cAMP on the other, also differed in the time course of the respective responses. ORNs responding to the amino acid mixture always had a fast time course (e.g. ORN #1 marked with an arrow in Figure 41) and responded neither to forskolin nor to pCPT-cAMP (Figure 42A). ORNs responding to forskolin and/or pCPT-cAMP (e.g. ORN #2 marked with an arrow in Figure 41) typically showed a much slower time course (Figure 42B), but no response to

amino acids. Only in few cases could an increase in $[Ca^{2+}]_i$ be observed upon stimulation with all three kinds of stimuli (e.g. ORN #3 marked with an arrow in Figure 41; Figure 42C).
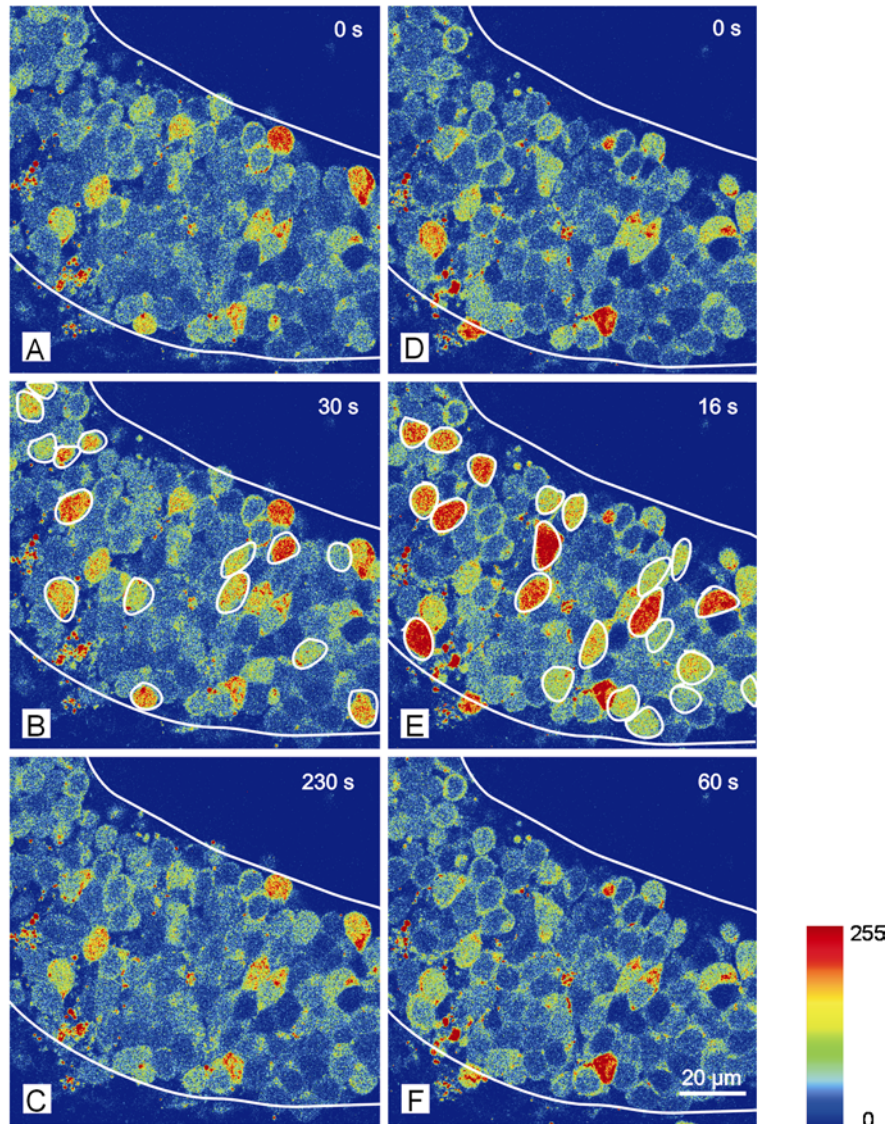
Figure 40. Comparison of changes of calcium-dependent fluorescence in ORNs of a mucosa slice in response to stimulation with amino acids and forskolin
Sequences of pseudocolored images of a mucosa slice (stage 53) showing that stimulation with forskolin (50 µM, **A** to **C**) and the mixture of amino acids (200 µM, each, **D** to **F**) transiently elevates calcium-dependent fluorescence in two different ensembles of ORNs (encircled in **B** and **E**). The upper images show the fluorescence images before application (t= 0 s), the images in the middle at the peak of the response (t= 30 s in **B** and t= 16 s in **E**) and the bottom images after return to the basal fluorescence levels (t= 230 s and t= 60 s after the beginning of the experiment in **C** and **F**, respectively).
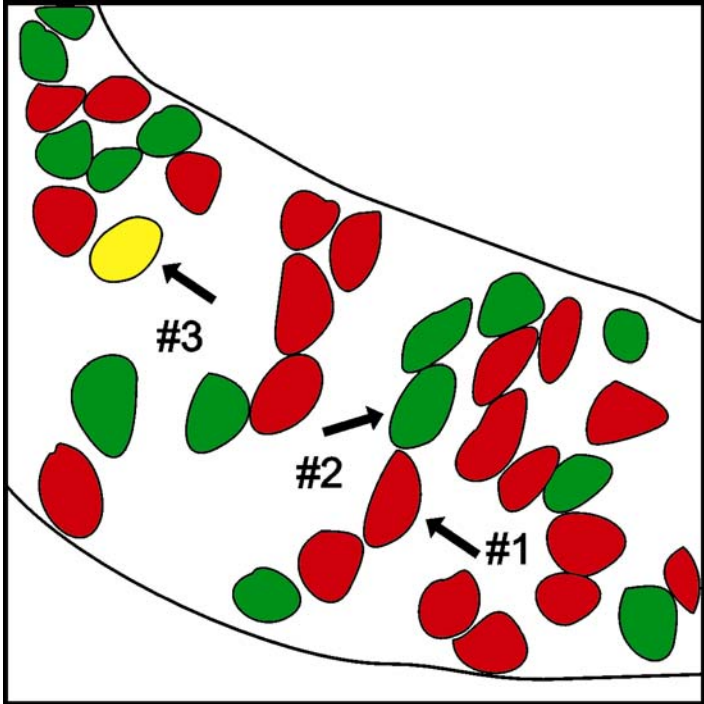
Figure 41. Schematic superposition of the forskolin- and amino acid-sensitive ORNs encircled in Figure 40B and E
ORNs sensitive to forskolin (green), to amino acids (red) and both (yellow). Only one ORN showed a response to both stimuli. The responses of the ORNs indicated with arrows are shown in Figure 42.
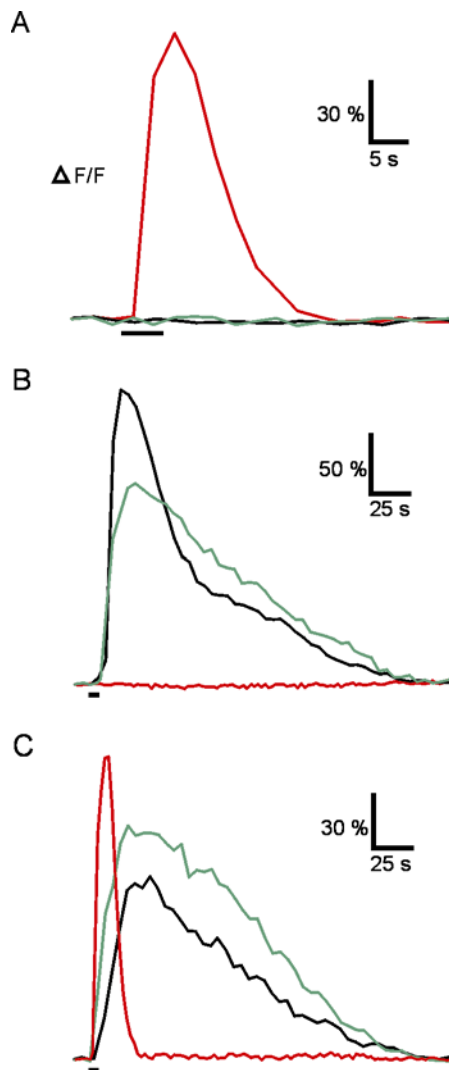
Figure 42. Time courses of calcium-dependent fluorescence changes in ORNs upon stimulation with amino acids, forskolin and pCPT-cAMP
A: ORN #1 (see Figure 41) was responsive to L-asparagine (red trace) but insensitive to forskolin (green trace) and pCPT-cAMP (black trace). **B:** ORN #2 (see Figure 41) was responsive to forskolin and pCPT-cAMP (green and black trace, respectively) but insensitive to the mixture of amino acids (red trace). **C:** ORN #3 (see Figure 41) responded to all of the three stimuli applied (L-alanine, red trace; forskolin, green trace and pCPT-cAMP, black trace).
Amino acids, forskolin and pCPT-cAMP were applied at a concentration of 200 μM, 50 μM and 2.5 mM, respectively.

4. Discussion

4.1. Comparison between isolated ORNs and ORNs in the mucosa slice

Recordings in the mucosa slice differed from those in isolated ORNs in both the recording duration and quality of odorant responses. Furthermore, all of the ORNs recorded in the mucosa slice had a substantially higher spontaneous spiking rate than isolated ORNs. Taken together, these data clearly show that the slice of the olfactory epithelium is the preparation of choice to study the response behaviour of ORNs. Most of the limitations of isolated ORNs are not present in the slice preparation.

<u>Recording duration</u>

Recording times were markedly longer in the mucosa slice than in isolated ORNs. The average recording time of the successful recordings in the slice (Figure 16D) was 44.5 minutes, whereas the average recording time for isolated ORNs was just 6.4 minutes and the maximum rarely exceeded 15 minutes. In perforated-patch recordings of isolated ORNs of a previous study (Vogler and Schild, 1999) the average recording duration was equal to or even shorter than the average recording duration in the on-cell configuration in the slice. Isolated ORN recordings are thus not the method of choice for testing many odorants on an individual cell.

<u>Odorant responses</u>

In the slice preparation 15.3% of the ORNs recorded in the on-cell configuration and 8.6% of the ORNs recorded in the whole-cell configuration showed responses to amino acids, i.e. on the average approx. 12%, which is less than the previously reported 28% recorded in isolated ORNs (Vogler and Schild, 1999). The lower frequency of odorant responses in the slice preparation compared to that previously obtained (Vogler and Schild, 1999) is possibly due to the fact that the ORNs in the present study were from earlier stages of tadpole development. ORNs were recorded at stages 49 to 54, while in the preceding study ORNs were recorded at stages 52 to 55.

All of the amino acid responses of ORNs recorded in the whole-cell configuration showed a typical run-down (see Figure 21), similar to that previously reported for different species including *Xenopus laevis* (Lucero *et al.* 1992; Dionne, 1992; Lischka and Schild, 1993)

recorded in isolated ORNs in the whole-cell configuration. On the other hand, responses recorded in the on-cell configuration and in the slice remained stable until the end of the stimulus protocol (Figure 19).

These findings, together with the fact that the recording times of ORNs in the slice are longer than in isolated ORNs clearly indicate that the slice preparation combined with the on-cell configuration of the patch-clamp technique is the method of choice for testing many odorants on an individual ORN. Futhermore, on-cell recording of ORNs in the slice have the advantage, that their spontaneous activity is always sufficiently high (see Figure 18) to allow the detection of both excitatory and inhibitory responses.

The finding that 26 out of 35 ORNs recorded in the slice preparation responded to SP, but not to AA suggests that amino acids are not the only stimuli of ORNs in the tadpole mucosa and indicates little overlap between the receptors for amino acids and those of at least some of the active components in the SP.

Disturbingly, 102 isolated ORNs tested in the on-cell recording mode did not respond to odorants at all. However, isolated ORNs recorded in the perforated-patch mode in a previous study responded to amino acids (Vogler and Schild, 1999). The lack of responsivity of isolated ORNs in the on-cell mode might have been caused by depolarized membrane potentials and partly inactivated sodium channels. ORNs, in the perforated-patch or whole-cell configuration held at a more negative potential would presumably not show this lack of responsivity. This interpretation is further supported by the fact that isolated ORNs recorded in the on-cell mode rarely showed spontaneous activity, whereas ORNs recorded in the on-cell mode in the slice were always spontaneously active. Taken together, isolated ORNs may have a less negative membrane potential than ORNs in the mucosa slice, and this would explain the lacking responsivity in on-cell recordings from isolated ORNs.

Volatile odorants, such as those contained in the mixtures V1 or V2, are reported to induce odorant responses in a large number of species including amphibia (Schild and Restrepo, 1998), in particular adult *Xenopus laevis* (air mucosa: Lischka and Schild, 1993; Zhainazarov and Ache, 1995; water mucosa: Iida and Kashiwayanagi, 1999). In the tadpole mucosa slice preparation, however, responses to volatile stimuli were never observed (0 out of 58 ORNs, mixtures V1 or V2). It is possible that a stage-dependent expression of the corresponding receptor proteins might be responsible for this discrepancy (Mezler *et al.* 1999).

In the previous perforated-patch recordings (stages 52 to 55), approximately half of the responses to single amino acids were inhibitory (Vogler and Schild, 1999), while in the present slice preparation, inhibitory responses to amino acids were never observed. This does

not necessarily imply that ORNs of *Xenopus laevis* tadpoles do not exhibit inhibitory responses, because (1) an over-all excitation in response to a stimulus mixture does not exclude an inhibitory stimulus component and (2) only 12% of the ORNs tested responded to amino acids; the responses of these cells as well as the responses of the remaining 88% of ORNs to other stimuli are unknown. In comparison, inhibitory responses of single ORNs recorded *in-vivo* are well established in catfish (Kang and Caprio, 1995), and the interaction of excitatory and inhibitory responses in the same receptor neuron has clearly been shown in lobster (Michel and Ache, 1994).

The possibility of inhibitory ORN responses in *Xenopus laevis* tadpoles cannot be excluded; however, the occurrence of inhibitions in about 50% of the responsive isolated ORNs tested in the previous study (Vogler and Schild, 1999) deviates markedly from the present results of a complete absence of inhibitory responses. This striking difference could be the result of the presence of mucus on the mucosal surface of the slice and the intact compartmentalization of the ORNs. Also the presence of sustentacular cells in the slice could be an important difference between the two preparations. Immunocytochemistry experiments in the slice preparation revealed that there is a mucus layer of about 10 μm (see also Hansen *et al.* 1998) into which cilia and microvilli protrude. The ionic composition of this mucus, in particular under our experimental conditions, is unknown. Furthermore, the exact localization of channel proteins and transporters in ORNs as well as the precise ion and protein composition of the mucus appear to be crucial in this context. If the K^+ concentration in the mucus was markedly higher than in the extracellular space (reviewed in Schild and Restrepo, 1998), the activation of K^+ channels as described by Bacigalupo and collaborators (Morales *et al.* 1994; Morales *et al.* 1995) would lead to depolarizing receptor potentials in the slice, while in isolated ORNs the receptor potentials would be hyperpolarizing and thus inhibitory.

Finally, the isolated ORNs were dissociated by enzymatic treatment. If and how this affects odorant responses has never been studied in detail. In the slice preparation this problem does not exist.

4.2 Classification of the response patterns of ORNs to amino acids

In aquatic species, amino acids are potent olfactory stimuli (Caprio and Byrd, 1984; Vogler and Schild 1999; Restrepo *et al.* 1990; Freitag *et al.* 1995; Kang and Caprio, 1995, 1997; Iida

and Kashiwayanagi, 1999). The results of this thesis confirm that amino acids are efficient olfactory stimuli in *Xenopus laevis* tadpoles.

In the first part of the work the responses to amino acid were investigated using the patch-clamp technique. It turned out that using this technique it is a drudgingly undertaking to obtain enough data to thoroughly classify the response patterns of ORNs (see Table 4). Using the patch-clamp technique the specificity profiles of only 11 out of 227 investigated ORNs could be determined. The major problem was to find amino acid responsive ORNs. The large majority of the patched ORNs were insensitive to amino acids. After a while it became clear that extending Table 4 to a complete set of response patterns would presumably require thousands of experiments using the patch-clamp technique. Despite the obvious difficulties encountered it could be shown that ORNs possess differential specificity profiles. Also the number of effective amino acids seemed to vary in different ORNs. Some ORNs (5 out of 11) responded to one amino acid, while others responded to amino acids of one or more submixture. This nicely confirms the classification of ORNs in fish (Caprio and Byrd, 1984), which was set up by cross-adaptation experiments. In this study, responses to L-histidine were correlated with responses to the LCN submixture of amino acids (Caprio and Byrd, 1984), a correlation also seen in Table 4 (cell #3).

The calcium imaging technique where the response behaviour of many ORNs of a slice can be monitored simultaneously is more promising in this respect. After an initial problem of calcium-indicator dye loading of the slices due to the multidrug resistance of ORNs (see sections 3.8 and 4.5) I have started a classification of ORN responses to amino acids using the calcium imaging technique. Using this technique, the collection of response patterns of ORNs seems to be much easier and more successful (see Table 5). In the 4 mucosa slices as yet tested for the responsiveness of all of the 19 amino acids I was able to determine the specificity profiles of 21 ORNs. Eight of the 21 ORNs responded to one amino acid (for an example see Figure 38A). The remaining 13 ORNs responded to a larger number of amino acids of one or different submixtures (for an example see Figures 38B and C). Therefore, it seems that ORNs can be split up in 2 major classes: "specialists", responsive to only one amino acid, and "generalists", responsive to a larger number of amino acids. In one of these 4 slices the specificity profiles of as much as 13 ORNs could be determined, that is more than in all of the 227 ORNs tested using the patch-clamp technique. Although so far I have just started with the determination of response spectra of ORNs using the calcium imaging technique, it is clear that this is the method of choice for getting the specificity profiles of a

large number of ORNs. Using the calcium imaging technique extending Table 5 to a few hundred ORNs is a feasible undertaking.

It has been shown that adult *Xenopus laevis* express class I ORs responsive to complex mixtures of water-soluble substances including amino acids. Oocytes expressing one of these class I receptors responded to a mixture of 22 amino acids as well as to the mixture of long chain neutral amino acids, but other mixtures, such as the mixture of basic amino acids, had no effect (Mezler *et al.* 2001). Therefore, some of the class I ORs of *Xenopus laevis* could be amino acid receptors. However, in goldfish, an OR with sequence similarities to calcium-sensing receptors (CaSR) and metabotropic glutamate receptors (mGluR) acts as a receptor for amino acids. Structure-activity analysis indicated that this receptor is preferentially tuned to recognize basic amino acids (Speca *et al.* 1999). It is, therefore, conceivable that vertebrates possess different types of receptors for amino acids.

It is a tempting idea to check whether tadpoles of *Xenopus laevis* express the above mentioned ORs. To answer this question, molecular biology, in addition to the so far used electrophysiological techniques and the calcium imaging will be necessary. Whether or not the expression of ORs in *Xenopus laevis* tadpoles is stage-dependent is another intriguing question.

4.3 Lack of correlation between responses to amino acids and to pharmacological agents activating the cAMP transduction pathway

One of the first papers on olfactory transduction (in frog and rat, Sklar *et al.* 1986) classified odorants in two classes, some of them increasing the concentration of cAMP and others that of IP_3. This was the beginning of a long-standing and still ongoing controversy on whether olfactory transduction is mediated by one second messenger, cAMP, or by more than one. Over the last decade many investigators have reported pieces of evidence indicating an involvement of second messengers other than cAMP in olfactory transduction, yet there is no species in which all elements of a non-cAMP transduction cascade have been found. Taken together, the cAMP pathway in ORNs is very well documented, while the evidence for alternative pathways is still heterogeneous and not definitive. The interpretation of the currently available data ranges from an exclusive role for cAMP in olfactory transduction to a mediatory role for cAMP and a modulatory role for other second messengers, to a multiple

mediation of olfactory transduction by different second messengers even within the same ORN (see reviews by Schild and Restrepo, 1998; Zufall and Munger, 2001, and references therein).

In this study I did not attempt to characterize any cAMP-independent transduction mechanism. I rather answered the simpler question whether or not a particular ORN sensitive to a certain known odorant is also sensitive to pharmacological agents activating the cAMP-mediated tranduction pathway.

The cAMP-mediated olfactory pathway can be activated in various odorant-independent ways, e.g. by dialysis of cAMP through a patch pipette into the cytosol (e.g. Iida and Kashiwayanagi, 2000), or by application of forskolin (e.g. Frings and Lindemann, 1991), IBMX (e.g. Kashiwayanagi and Kurihara, 1995; Zufall *et al.* 2000) or pCPT-cAMP (e.g. Kashiwayanagi and Kurihara, 1995; Reisert and Matthews, 2001) to the bath solution.

In the patch-clamp experiments about 40% of the ORNs that responded to amino acids were also excited by forskolin, which is consistent with cAMP-mediated olfactory transduction. Further, it was not unexpected that forskolin excited some ORNs that were not excited by amino acids. In these cases amino acids were not the appropriate stimuli. Interestingly, however, 7 out of 12 ORNs (about 60%) that responded to amino acids were not sensitive to forskolin (Fig. 25C). In these cases, the odorants activated a cAMP-independent olfactory pathway. These data clearly indicate that amino acid transduction is probably not a subset of cAMP-dependent transduction.

After the initial problems with calcium-indicator dye loading due to the multidrug resistance of ORNs (see section 3.8 and 4.5) it was possible to perform calcium imaging experiments in the mucosa slice. To confirm the patch-clamp data I imaged odorant responses in a slice of the olfactory epithelium using the calcium-indicator dye Fluo-4. In this way it could easily be established which ORNs of a slice responded to a particular stimulus. I then applied forskolin, an activator of the cAMP-dependent pathway. To rule out the possibility that, in addition to or instead of its effect upon the adenylate cyclase, forskolin might act as an odorant or via some other mechanism, in some slices I also applied pCPT-cAMP in addition to forskolin. In the mucosa slices tested for both drugs the ORNs activated by forskolin were also activated by pCPT-cAMP. Thus, both drugs activated the cAMP-dependent transduction pathway equally well. Moreover, pCPT-cAMP activated a few ORNs that were not activated by forskolin. In these cases pCPT-cAMP might have acted, in addition to its effect as a second messenger, as an odorant. This is in line with a previous report showing that

nucleotides are important olfactory stimuli in fish (Kang and Caprio, 1995). Here this possible explanation was not further analyzed.

Amino acids, in most cases, failed to activate forskolin- or pCPT-cAMP-sensitive ORNs (see Figures 40, 41 and 42).

The results obtained using calcium imaging confirmed the patch-clamp results on a huge number of ORNs. The overall conclusion, therefore, is that most amino acids are not transduced via a cAMP-dependent pathway in ORNs of *Xenopus laevis* tadpoles.

4.4 Projection of cAMP-independent and cAMP-dependent responses of ORNs onto the olfactory bulb

Given the two almost disjunctive sets of cAMP- and non-cAMP-dependent ORNs it was an interesting question how the respective sets of ORNs project to the OB. One would expect an activation of two different areas of the OB. To verify this assumption I analyzed the $[Ca^{2+}]_i$-response patterns in mitral- and granule cells upon stimulation of the olfactory epithelium with amino acids, on the one hand, and with forskolin, IBMX or pCPT-cAMP, on the other. Olfactory bulb neurons responding to amino acids preferentially were located in the lateral half of the OB (see Figures 26 and 27) indicating that glomeruli in the lateral OB process information about amino acids. Interestingly, a projection of amino acid-sensitive ORNs to a cluster of glomeruli in the lateral OB also was observed in imaging studies in the zebra fish OB (Friedrich and Korsching, 1997).

Only few OB neurons in *Xenopus laevis* showed a response to stimulation with both amino acids and pharmacological agents that activate the cAMP-mediated transduction pathway. On the other hand, the relatively large number of neurons responding to stimulation with forskolin, IBMX or pCPT-cAMP suggests that there is a significant number of ORNs responding to as yet unknown odorants mediated by the cAMP transduction pathway. Forskolin activated virtually the same ensemble of OB neurons as IBMX and pCPT-cAMP did (see Figure 27). Forskolin did, therefore, not appear to act as an odorant. It could be rather established that axons of ORNs responsive to cAMP-mediated stimuli project to glomeruli in the medial region of the OB (see Figures 26 and 27).

The pCPT-cAMP-sensitive neuron ensemble and the amino acid-sensitive ensemble showed a larger overlap than the forskolin- or IBMX-sensitive ensemble with the amino acid-

sensitive ensemble. As already discussed in section 4.3, in the calcium imaging experiments in the mucosa slice pCPT-cAMP activated a few more ORNs than forskolin. As nucleotides are known to be important olfactory stimuli in fish (Kang and Caprio, 1995), most probably pCPT-cAMP acts not only as a second messenger, but also as an odorant in *Xenopus laevis* tadpoles. Therefore, the larger overlap of the pCPT-cAMP-sensitive neuron ensemble and the amino acid-sensitive ensemble was not surprising, but rather a confirmation of what was seen in the experiments in the mucosa slice.

In summary, forskolin, IBMX and pCPT-cAMP, on the one hand, and amino acids, on the other, induce very distinct and almost exclusive spatial patterns of neuronal activities in the OB. This clearly shows that cAMP-mediated responses and responses to amino acids are transduced, processed and mapped differently.

4.5 Multidrug resistance transporters in ORNs

Membrane transport systems for neutral compounds as well as for organic cations and organic anions have been studied primarily in liver, gut and kidney (Barnes, 2001; Burckhardt and Wolff, 2000; Burckhardt and Pritchard, 2000; Borst *et al.* 2000; Renes *et al.* 2000; Leslie *et al.* 2001, Koepsell, 1998; Szakacs *et al.* 1998), and calcium-indicator dyes are known substrates of several of these transport systems (Neyfakh, 1988; Di Virgilio *et al.* 1989; Homolya *et al.* 1993). Taste sensory cells, which are in direct contact with the environment, have recently been shown to express the multidrug resistance P-glycoprotein (Jakob *et al.* 1998).

The fact that *Xenopus laevis* tadpole ORNs could not be loaded with calcium/AM-dyes was surprising because calcium was successfully imaged in ORNs in a number of species (Lischka and Schild, 1993; Jung *et al.* 1994; Leinders-Zufall *et al.* 2000; Ma and Shepherd, 2000). Calcium-indicator dye removal mechanisms thus appear to differ in different species and even in different stages or sets of neurons of one species (e.g. *Xenopus laevis*). When calcium-indicator dyes are dialyzed into the cytosol through a patch pipette, removal is of minor importance, since removal is compensated by dye molecules entering the cell through the pipette. On the other hand, in cases of loading with AM-esters of dyes, it has to be borne in mind that some dye removal can easily be overlooked. In many studies where fluorescence intensities are sufficiently high for imaging purposes, one usually does not consider the

possibility of indicator dye removal. Figures 28B and D exemplify such a case.

Loading calcium dyes or calcein into tadpole ORNs could be modulated by probenecid, sulfinpyrazone, MK571, verapamil and PSC 833 (see Figures 28, 30, 32, 34 and 35). The dynamics of fluorescent-increase was linear if ORNs were incubated in Fura-red/AM and nonlinear in the case of incubation with the AM-esters of calcein or calcium-green. In other species and other cell systems the AM-esters of calcium dyes and of calcein are reported to be transported by P-glycoprotein (Homolya *et al*. 1993; Brezden *et al*. 1994; Essodaigui *et al*. 1998) and MRP (Essodaigui *et al*. 1998; Olson *et al*. 2001). In addition, MRP has been reported to transport the salts of calcein, Fluo-3, 2'-7'bis(2-carboxyethyl)-5(6)-carboxyfluorescein (BCECF) and fluorescein (Feller *et al*. 1995; Essodaigui *et al*. 1998; Vernhet *et al*. 2000; Abrahamse and Rechkemmer, 2001; Nies *et al*. 1998; Draper *et al*. 1997a; Draper *et al*. 1997b; Sun *et al*. 2001). Verapamil is known to block the P-glycoprotein (Ford and Hait, 1990; Homolya *et al*. 1993), while it is believed to have no specific effect on MRP. PSC 833 is a specific inhibitor of P-glycoprotein with no effect on MRP (Declèves *et al.,* 2000; Miller *et al.,* 2000; Thévenod *et al.,* 2000). On the other hand, probenecid, which is a known blocker of many anion transport systems (Pritchard and Miller, 1993; Burckhardt and Pritchard, 2000), also blocks MRP but not P-glycoprotein (Feller *et al*. 1995; Versantvoort *et al*. 1995; Evers *et al*. 1996; Gollapudi *et al*. 1997; Jakob *et al*. 1998). MK571 and sulfinpyrazone are believed to specifically block MRP, with no effect upon P-glycoprotein (Gekeler *et al*. 1995; Evers *et al*. 1996). Taking into account these properties, the data of this study are consistent with the model diagrammatically shown in Figure 43. In this model, the AM-esters of all dyes used are extruded through both MRP and P-glycoprotein. In addition the salts of calcium-green and calcein, but not of Fura-red are extruded through MRP. Let the extrusion rates of MRP for the AM and the salt species be $k_{M, AM}$ and $k_{M, s}$, respectively, then eq. 3 (see section 2.5.2) takes the form

$$dc_s / dt = k_e \, k_D / (\, k_D + k_e + k_p + k_{M, AM} \,) \, c_o \; - \; k_{M, s} \, c_s \qquad\qquad (4)$$

The solution of this first order differential equation is an exponential function, proportional to $1 - e^{-t/\tau}$. Thus, the fluorescence increases in a nonlinear saturating way if the salt of a calcium-indicator dye is extruded from the cell, and in a linear way if this is not the case.

This description is a simplification in that possible interactions between AM-dye and salt transport as well as the ATP-dependence of MRP are neglected. However, the model appears

to be adequate in that it reflects the linear fluorescence-increase of Fura-red (for which $k_{M,s} = 0$) and the saturating behavior for calcein and calcium-green (for which $k_{M,s} \neq 0$). There are, however, too many free and unknown parameters to fit, in an unambiguous way, the model to the obtained data.
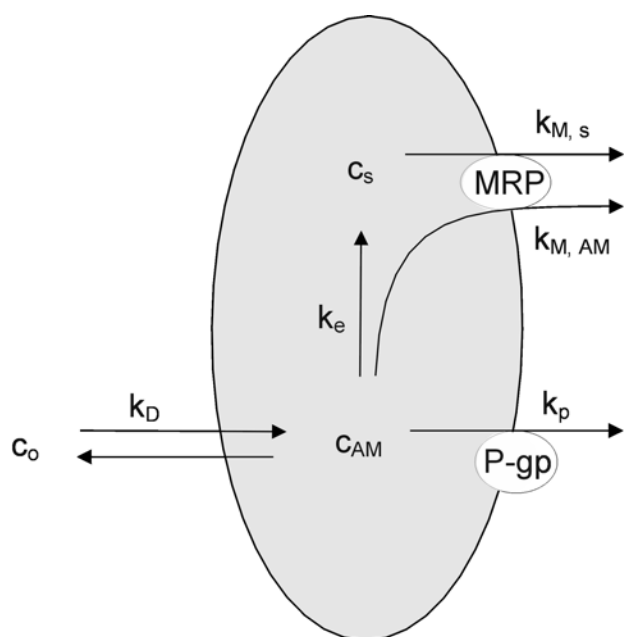
Figure 43. Model of fluorescent dye accumulation in olfactory receptor neurons
c_o and c_{AM} , concentrations of AM-ester of fluorescent dyes outside and inside the cell; c_s, concentration of the hydrolized dye inside the cell. AM-dye molecules enter the cytosol of the cell by diffusion through the plasma membrane (rate constant k_D). The AM-dye molecules can be extruded from the cytosol of the cell either by the P-glycoprotein (P-gp, rate constant k_p) or by a multidrug resistance-associated protein (MRP, rate constant $k_{M,AM}$). In addition, it is converted to the corresponding salt of the dye by cellular esterases (rate constant k_e). The multidrug resistance-associated protein (MRP) transports also the salt form of some fluorescent dyes (rate constant $k_{M,s}$).

The results regarding the drug modulation and the time-course of fluorescent dye net uptake differ in two respects from the removal mechanism found in taste sensory cells. First, dye removal can be blocked not only by P-glycoprotein inhibitors (verapamil and PSC 833), as in taste cells, indicating removal through P-glycoprotein, but also by probenecid, MK751, and sulfinpyrazone, strongly indicating an additional removal route through MRP. The presence of two different transporter systems is futher supported by the facts that MK571 had a larger inhibitory effect upon dye removal than verapamil or PSC 833 and that the effect of verapamil added to that of MK571. Second, the kinetics of removal is linear (as in taste cells)

for Fura-red, but nonlinear for calcium-green and calcein, indicating concentration-dependent removal of the salts of the latter two. MRP-mediated removal of the calcein salt was confirmed by the fact that destaining of slices loaded with calcein was blocked by MK571. As the calcein salt is known to be extruded by MRP (Essodaigui *et al.* 1998; Vernhet *et al.* 2000), this confirms the involvement of MRP.

Antibodies against P-glycoprotein stained the non-apical parts of ORNs and sustentacular cells. Though this qualitative evidence does not rule out a minor expression of P-glycoprotein on cilia, the major transport route appears to be across the basolateral membranes. The attempts to stain MRP of the *Xenopus laevis* tadpole mucosa using antibodies against rat, mice or human MRP were unsucccessful. Considering that dye extrusion was observed not only in ORNs but also in sustentacular cells, it may thus be hypothesized that sustentacular cells are involved in degrading xenobiotics.

4.6 Perspective

The most important result of this work is to have shown in a clear and unambiguous way that a number of amino acids are transduced through a cAMP-independent pathway in the main olfactory epithelium of *Xenopus laevis* tadpoles. I am not aware of any other study that clearly shows cAMP-independent transduction in ORNs in the main olfactory epithelium of a vertebrate. Of course, the question which second messenger pathways are responsible for the transduction of amino acids is inevitable. This question was beyond the scope of this thesis and I have as yet no answer to it. Combining patch-clamp and imaging experiments will most presumably give some insight here.

The discovery that ORNs possess multidrug resistance transporters is another intriguing result of this thesis. It is the first study that shows that ORNs possess transporter systems that expel xenobiotics across their plasma membrane. The finding that calcium-indicator dyes are among their substrates was of crucial importance for the calcium imaging project in the mucosa slice. Of course, the extrusion of calcium dyes is not the physiological function of these transporters. To investigate the physiological relevance of this transport systems is a tempting idea but it was beyond the scope of this thesis. I will certainly try to answer this important question in future studies.

Regarding the responses of particular ORNs to amino acids it will be most interesting to associate some response spectra to the ORs so far characterized in *Xenopus laevis*.

5. References

-Abrahamse SL, Rechkemmer G (2001) Identification of an organic anion transport system in the human colon carcinoma cell line HT29 clone 19A. Pflügers Arch 441: 529-537

-Ache BW (1994) Towards a common strategy for transducing olfactory information. Semin Cell Biol 5: 55-63

-Altner H (1962) Untersuchungen über Leistungen und Bau des Südafrikanischen Krallenfrosches *Xenopus Laevis*. Z Vgl Physiol 45: 272-306

-Avila VL, Frye PG (1978) Feeding behavior of the African Clawed frog (*Xenopus laevis* Daudin): effect of prey type. J Herpetol 12: 391-396

-Barnes DM (2001) Expression of P-glycoprotein in the chicken. Comp Biochem Phys A 130: 301-310

-Belluscio L, Gold GH, Nemes A, Axel R (1998) Mice deficient in G(olf) are anosmic. Neuron 20: 69-81

-Boekhoff I, Schleicher S, Strotmann J, Breer H (1992) Odor-induced phosphorylation of olfactory cilia proteins. Proc Natl Acad Sci USA 89: 11983-11987

-Boekhoff I, Breer H (1992) Termination of second messenger signaling in olfaction. Proc Natl Acad Sci USA 89: 471-474

-Borst P, Evers R, Kool M, Wijnholds J (2000) A family of drug transporters: the multidrug resistance-associated proteins. J Natl Cancer I 92: 1295-1302

-Bredzden CB, Hedley DW, Rauth AM (1994) Constitutive expression of P-glycoprotein as a determinant of loading with fluorescent calcium probes. Cytometry 17: 343-348

-Broillet MC, Firestein S (1996) Gaseous second messengers in vertebrate olfaction. J Neurobiol 30: 49-57

-Buck LB (1996) Information coding in the vertebrate olfactory system. Annu Rev Neurosci 19: 517-544

-Buck L, Axel R (1991) A novel multigene family may encode odorant receptors: a molecular basis for odor recognition. Cell 65: 175-187

-Burckhardt G, Pritchard JB (2000) Organic anion and cation antiporters. The Kidney: Physiology and Pathophysiology (Seldin DW, Giebisch G, eds), pp 194-222. Philadelphia: Lippincott-Raven

-Burckhardt G, Wolff NA (2000) Structure of renal organic anion and cation transporters. Am J Physiol-Renal 278: 853-866

-Byrd CA, Burd GD (1991) Development of the olfactory bulb in the clawed frog, *Xenopus laevis*: amorphological and quantitative analysis. J Comp Neurol 314: 79-90

-Caprio J, Byrd RP (1984) Electrophysiological evidence for acidic, basic, and neutral amino acid olfactory sites in the catfish. J Gen Physiol 84:403-422

-Dawson TM, Snyder SH (1994) Gases as biological messengers: nitric oxide and carbon monoxide in the brain. J Neurosci 14: 5147-5159

-Declèves X, Regina A, Laplanche JL, Roux F, Boval B, Launay JM, Scherrmann, JM (2000) Functional expression of P-glycoprotein and multidrug resistance-associated protein (Mrp1) in primary cultures of rat astrocytes. J Neurosci Res 60: 594-601

-Dionne VE (1992) Chemosensory responses in isolated olfactory receptor neurons from *Necturus maculosus*. J Gen Physiol 99: 415-433

-Di Virgilio F, Steinberg TH, Silverstein SC (1989) Organic-anion transport inhibitors to facilitate measurement of cytosolic free Ca2+ with fura-2. Method Cell Biol 31: 453-462

-Draper MP, Martell RL, Levy SB (1997a) Indomethacin-mediated reversal of multidrug resistance and drug efflux in human and murine cell lines overexpressing MRP, but not P-glycoprotein. Brit J Cancer 75: 810-815

-Draper MP, Martell RL, Levy SB (1997b) Active efflux of the free acid form of the fluorescent dye 2',7'-bis(2-carboxyethyl)-5(6)-carboxyfluorescein in multidrug-resistance-protein-overexpressing murine and human leukemia cells. Eur J Biochem 243: 219-224

-Edwards FA, Konnerth A, Sakmann B, Takahashi T (1989) A thin slice preparation for patch-clamp recordings from neurones of the mammalian central nervous system. Pflügers Arch 414: 600-612

-Essodaigui M, Broxterman HJ, Garnier-Suilerot A (1998) Kinetic analysis of calcein and calcein-acetoxymethylester efflux mediated by the multidrug resistance protein and P-glycoprotein. Biochemistry 37: 2243-2250

-Evers R, Zaman GJ, Van Deemter L, Jansen H, Calafat J, Oomen LC, Elferink RP, Borst P, Schinkel AH (1996) Basolateral localization and export activity of the human multidrug resistance-associated protein in polarized pig kidney cells. J Clin Invest 97: 1211-1218

-Evers R, de Haas M, Sparidans R, Beijnen J, Wielinga PR, Lankelma J, Borst P (2000) Vinblastine and sulfinpyrazone export by the multidrug resistance protein MRP2 is associated with glutathione export. Br J Cancer 2000 83: 375-383

-Feller N, Broxterman HJ, Wahrer DC, Pinedo HM (1995) ATP-dependent efflux of calcein by the multidrug resistance protein (MRP): no inhibition by intracellular glutathione depletion. FEBS Lett 368: 385-388

-Ford JM, Hait WN (1990) Pharmacology of drugs that alter multidrug resistance in cancer. Pharmacol Rev 42: 155-199

-Föske H (1934) Das Geruchsorgan von *Xenopus laevis*. Z Anat Entwicklungsgesch 103: 519-550

-Freitag J, Krieger J, Strotmann J, Breer H (1995) Two classes of olfactory receptors in *Xenopus laevis*. Neuron 15: 1383-1392

-Freitag J, Ludwig G, Andreini I, Rössler P, Breer H (1998) Olfactory receptors in aquatic and terrestrial vertebrates. J Comp Physiol A 183: 635-650

-Friedrich RW, Korsching SI (1997) Combinatorial and chemotopic odorant coding in the zebrafish olfactory bulb visualized by optical imaging. Neuron 18:737-752

-Frings S, Lindemann B (1991) Current recording from sensory cilia of olfactory receptor cells in situ. I. The Neuronal response to cyclic nucleotides. J Gen Physiol 97: 1-16

-Frings S, Reuter D, Kleene SJ (2000) Neuronal Ca2+ -activated Cl- channels--homing in on an elusive channel species. Prog Neurobiol 60: 247-289

-Fujita T, Yamada H, Fukuzumi M, Nishimaki A, Yamamoto A, Muranishi S (1997) Calcein is excreted from the intestinal mucosal cell membrane by the active transport system. *Life Sci* 60: 307-313

-Fuss SH, Korsching SI (2001) Odorant feature detection: activity mapping of structure response relationships in the zebrafish olfactory bulb. J Neurosci 21: 8396-8407

-Gekeler V, Ise W, Sanders KH, Ulrich WR, Beck J (1995) The leukotriene LTD4 antagonist MK571 specifically modulates MRP associated multidrug resistance. Biochem Bioph Res Co 208: 345-352

-Getchell TV, Margolis FL, Getchell ML (1984) Perireceptor and receptor events in vertebrate olfaction. Prog Neurobiol 23: 317-345

-Getchell TV (1986) Functional properties of vertebrate olfactory receptor neurons. Physiol Rev 66: 772-807

-Gollapudi S, Kim CH, Tran BN, Sangha S, Gupta S (1997) Probenecid reverses multidrug resistance in multidrug resistance-associated protein-overexpressing HL60/AR and H69/AR cells but not in P-glycoprotein-overexpressing HL60/Tax and P388/ADR cells. Cancer Chemoth Pharm 40: 150-158

-Goodfellow HR, Sardini A, Ruetz S, Callaghan R, Gros P, McNaughton PA, Higgins CF (1996) Protein kinase C-mediated phosphorylation does not regulate drug transport by the human multidrug resistance P-glycoprotein. J Biol Chem 271: 13668-13674

-Gold GH (1999) Controversial issues in vertebrate olfactory transduction. Annu Rev Physiol 61: 857-871

-Halpern M (1987) The organization and function of the vomeronasal system. Annu Rev Neurosci 10:325-362.

-Hamill OP, Marty A, Neher E, Sakmann B, Sigworth FJ (1981) Improved patch-clamp techniques for high-resolution current recording from cells and cell-free membrane patches. Pflügers Arch 391: 85-100

-Hansen A, Reiss JO, Gentry CL, Burd GD (1998) Ultrastructure of the olfactory organ in the clawed frog, *Xenopus laevis*, during larval development and metamorphosis. J Comp Neurol 398: 273-288

-Holy TE, Dulac C, Meister M (2000) Responses of vomeronasal neurons to natural stimuli. Science 289:1569-1572

-Homolya L, Hollo Z, Germann UA, Pastan I, Gottesman MM, Sarkadi B (1993) Fluorescent cellular indicators are extruded by the multidrug resistance protein. J Biol Chem 268: 21493-21496

-Howell BJ, Baumgardner FW, Bondi K, Rahn H (1970) Acid-base balance in cold-blooded vertebrates as a function of body temperature. Am J Physiol 218: 600-606

-Iida A, Kashiwayanagi M (1999) Responses of *Xenopus laevis* water nose to water-soluble and volatile odorants. J Gen Physiol 114: 85-92

-Iida A, Kashiwayanagi M (2000) Responses to putative second messengers and odorants in water nose olfactory neurons of *Xenopus laevis*. Chem Senses 25: 55-59

-Inamura K, Kashiwayanagi M, Kurihara K (1997) Blockage of urinary responses by inhibitors for IP_3-mediated pathway in rat vomeronasal neurons. Neurosci Lett 233:129-132

-Jakob I, Hauser IA, Thévenod F, Lindemann B (1998) MDR1 in taste buds of rat vallate papilla: functional, immunohistochemical, and biochemical evidence. Am J Physiol-Cell Ph 274: 182-191

-Jedlitschky G, Burchell B, Keppler D (2000) The multidrug resistance protein 5 functions as an ATP-dependent export pump for cyclic nucleotides. J Biol Chem 275: 30069-30074

-Joshi H, Getchell ML, Zielinski B, Getchell TV (1987) Spectrophotometric determination of cation concentrations in olfactory mucus. Neurosci Lett 82:321-326

-Jung A, Lischka FW, Engel J, Schild D (1994) Sodium/calcium exchanger in olfactory receptor neurones of *Xenopus laevis*. Neuroreport 5: 1741-1744

-Kang J, Caprio J (1995)In vivo responses of single olfactory receptor neurons in the channel catfish, *Ictalurus punctatus*. J Neurophysiol 73: 172-177

-Kang J, Caprio J (1997) In vivo responses of single olfactory receptor neurons of channel catfish to binary mixtures of amino acids. J Neurophysiol **77:** 1-8

-Kashiwayanagy M, Kurihara K (1995) Odor responses after complete desensitation of the cAMP-dependent pathway in turtle olfactory cells. Neurosci Lett 193: 61-64

-Kashiwayanagi M, Kurihara K (1996) Specific receptor- and non-receptor-mediated odor responses and their multiple transduction pathways. Prim Sens Neuron 1: 311-325

-Kashiwayanagi M, Shimano K, Kurihara K (1996) Existence of multiple receptors in single neurons: responses of single bullfrog olfactory neurons to many cAMP-dependent and independent odorants. Brain Res 738: 222-228

-Klein SL, Graziadei PP (1993) The differentiation of the olfactory- placode in *Xenopus laevis*: a light and electron microscope study. J Comp Neurol 217: 17-30

-Koepsell H (1998) Organic cation transporters in intestine, kidney, liver, and brain. Annu Rev Physiol 60: 243-266

-Labarca P, Simon SA, Anholt RR (1988) Activation by odorants of a multistate cation channel from olfactory cilia. Proc Natl Acad Sci USA 85: 944-947

-Laupeze B, Amiot L, Payen L, Drenou B, Grosset JM, Lehne G, Fauchet R, Fardel O (2001) Multidrug resistance protein (MRP) activity in normal mature leukocytes and CD34-positive hematopoietic cells from peripheral blood. Life Sci 68: 1323-1331

-Lazard D, Zupko K, Poria Y, Nef P, Lazarovits J, Horn S, Khen M, Lancet D (1991) Odorant signal termination by olfactory UDP glucuronosyl transferase. Nature 349: 790-793

-Leidners-Zufall T, Lane AP, Puche AC, Ma W, Novotny MV, Shipley MT, Zufall F (2000) Ultrasensitive pheromone detection by mammalian vomeronasal neurons. *Nature* 405: 792-796

-Leslie EM, Deeley RG, Cole SP (2001) Toxicological relevance of the multidrug resistance protein 1, MRP1 (ABCC1) and related transporters. Toxicology 167: 3-23

-Lischka FW, Schild D (1993) Effects of nitric oxide upon olfactory receptor neurones in *Xenopus laevis*. Neuroreport 4: 582-584

-Lischka FW, Schild D (1993) Standing calcium gradients in olfactory receptor neurons can be abolished by amiloride or ruthenium red. J Gen Physiol 102: 817-831

-Lowe G, Gold GH (1993) Nonlinear amplification by calcium-dependent chloride channels in olfactory receptor cells. Nature 366: 283-286

-Lucero MT, Horrigan FT, Gilly WF (1992) Electrical responses to chemical stimulation of squid olfactory receptor cells. J Exp Biol 162: 231-249

-Lynch JW, Barry PH (1989) Action potential initiated by single channels opening in a small neuron (rat olfactory receptor). Biophys J 55: 755-768

-Ma M, Shepherd GM (2000) Functional mosaic organization of mouse olfactory receptor neurons. Proc Natl Acad Sci USA 97: 12869-12874

-Malnic B, Hirono J, Sato T, Buck LB (1999) Combinatorial receptor codes for odors. Cell 96: 713-723

-Menini A, Picco C, Firestein S (1995) Quantal-like current fluctuations induced by odorants in olfactory receptorcells. Nature 373:435-437

-Mezler M, Konzelmann S, Freitag J, Rössler P, Breer H (1999) Expression of olfactory receptors during development in *Xenopus Laevis*. J Exp Biol 202: 365-376

-Mezler M, Fleischer J, Breer H (2001) Characteristic features and ligand specificity of the two olfactory receptor classes from *Xenopus laevis*. J Exp Biol 204: 2987-2997

-Michel WC, Ache BW (1994) Odor-evoked inhibition in primary olfactory receptor neurons. Chem Senses 19: 11-24

-Miller DS, Nobmann SN, Gutmann H, Toeroek M, Drewe J, Fricker G (2000) Xenobiotic transport across isolated brain microvessels studied by confocal microscopy. Mol Pharmacol 58: 1357-1367

-Minor AV, Bykov KA, Dmiriev AV, Skachkov SN (1992) Extracellular ion concentration in the olfactory epithelium: Steady state and changes during excitation. Chem Senses 17: 864

-Mombaerts P, Wang F, Dulac C, Chao SK, Nemes A, Mendelsohn M, Edmondson J, Axel R (1996) Visualizing an olfactory sensory map. Cell 87: 675-86

-Mombaerts P (1999) Seven-transmembrane proteins as odorant and chemosensory receptors. Science 286: 707-711

-Morales B, Ugarte G, Labarca P, Bacigalupo J (1994) Inhibitory K^+ current activated by odorant in toad olfactory neurons. Proc R Soc Lond B 257: 235-242

-Morales B, Labarca P, Bacigalupo J (1995) A ciliary K^+ conductance sensitive to charibdotoxin underlies inhibitory responses in toad olfactory receptor neurons. FEBS Lett 359: 41-44

-Morales B, Bacigalupo J (1996) Chemical reception in vertebrate olfaction: evidence for multiple transduction pathways. Biol Res 29: 333-341

-Morrow CS, Smitherman PK, Townsend AJ (2000) Role of multidrug-resistance protein 2 in glutathione S-transferaseP1-1-mediated resistance to 4-nitroquinoline 1-oxide toxicities in HepG2 cells. Mol Carcinog 29: 170-178

-Neyfakh AA (1988) Use of fluorescent dyes as molecular probes for the study of multidrug resistance. Exp Cell Res 174: 168-176

-Nezlin LP, Schild D (2000) Structure of the olfactory bulb in tadpoles of *Xenopus laevis*. Cell Tissue Res 302: 21-29

-Nies AT, Cantz T, Brom M, Leier I, Keppler D (1998) Expression of the apical conjugate export pump, Mrp2, in the polarized hepatoma cell line, WIF-B. Hepatology 28: 1332-1340

-Nieuwkoop PD, Faber J (1956) Normal table of *Xenopus laevis* (Daudin). Amsterdam: North Holland Company

-Nikonov AA, Caprio J (2001) Electrophysiological evidence for a chemotopy of biologically relevant odors in the olfactory bulb of the channel catfish. J Neurophysiol 86: 1869-1876

-Noé J, Breer H (1998) Functional and molecular characterization of individual olfactory neurons. J Neurochem 71 : 2286-2293

-Okano M, Takagi SF (1974) Secretion and electrogenesis of the supporting cell in the olfactory epithelium. J Physiol (Lond) 242: 353-370

-Olson DP, Taylor BJ, Ivy SP (2001) Detection of MRP functional activity: calcein AM but not BCECF AM as a Multidrug Resistance-related Protein (MRP1) substrate. Cytometry 46: 105-113

-Pace U, Hanski E, Salomon Y, Lancet D (1985) Odorant-sensitive adenylate cyclase may mediate olfactory reception. Nature 316: 255-258

-Pawley JB (1995) Handbook of biological confocal microscopy – 2nd ed. (Pawley JB, ed). New York and London: Plenum Press

-Pelosi P (1996) Perireceptor events in olfaction. J Neurobiol 30: 3-19.

-Petti MA, Matheson SF, Burd GD (1999) Differential antigen expression during metamorphosis in the tripartite olfactory system of the African clawed frog, *Xenopus laevis*. Cell Tissue Res 297: 383-396.

-Pritchard JB, Miller DS (1993) Mechanisms mediating renal secretion of organic anions and cations. Physiol Rev 73: 765-796

-Reisert J, Matthews HR (2001). Responses to prolonged odour stimulation in frog olfactory receptor cells. J Physiol (Lond) 534: 179-191

-Renes J, De Vries EG, Jansen PL, Muller M (2000) The (patho)physiological functions of the MRP family. Drug Resist Updat 3: 289-302

-Ressler KJ, Sullivan SL, Buck LB (1994) Information coding in the olfactory system: evidence for a steratyped and highly organized epitope map in the olfactory bulb. Cell 79: 1245-1255

-Restrepo D, Miyamoto T, Bryant BP, Teeter JH (1990) Odor stimuli trigger influx of calcium into olfactory neurons of the channel catfish. Science 249: 1166-1168

-Ronnett GV, Moon C (2002) G proteins and olfactory signal transduction. Annu Rev Physiol 64: 189-222

-Schild D (1985) A computer-controlled device for the application of odours to aquatic animals. J Electrophysiol Techn 12: 71-79

-Schild D (1989) Whole-cell currents in olfactory receptor cells of *Xenopus laevis*. Exp Brain Res 78: 223-232

-Schild D, Jung A, Schultens HA (1994) Localization of calcium entry through calcium channels in olfactory receptor neurones using a laser scanning microscope and the calcium indicator dyes Fluo-3 and Fura-Red. Cell Calcium 15: 341-348

-Schild D (1996) Laser scanning microscopy and calcium imaging. Cell Calcium 19: 281-296

-Schild D, Gennerich A, Schultens HA (1996) Microcontrollers as inexpensive pulse generators and parallel processors in electrophysiological experiments. Med Biol Eng Comput 34: 305-307.

-Schild D, Restrepo D (1998) Transduction mechanisms in vertebrate olfactory receptor cells. Physiol Rev 78: 429-466

-Scott JW (1986) The olfactory bulb and central pathways. Experientia 42: 223-232

-Shipley MT, Ennis M (1996) Functional organization of olfactory system. J Neurobiol 30: 123-176

-Simmonds MP (1985) African Clawed toad survey. British Herpetological Society Bulletin No. 13

-Sklar PB, Anholt RR, Snyder SH (1986) The odorant-sensitive adenylate cyclase of olfactory receptor cells. Differential stimulation by distinct classes of odorants. J Biol Chem 261: 15538-15543

-Smetters D, Majewska A, Yuste R (1999) Detecting action potentials in neuronal populations with calcium imaging. Methods 18: 215-221

-Speca DJ, Lin DM, Sorensen PW, Isacoff EY, Ngai J, Dittman AH (1999) Functional identification of a goldfish odorant receptor. Neuron. 23: 487-498

-Sun H, Johnson DR, Finch RA, Sartorelli AC, Miller, DW, Elmquist WF (2001) Transport of fluorescein in MDCKII-MRP1 transfected cells and mrp1-knockout mice. Biochem Biophys Res Commun 284: 863-869

-Szakacs G, Jakab K, Antal F, Sarkadi B (1998) Diagnostics of multidrug resistance in cancer. Pathol Oncol Res 4: 251-257

-Thévenod F, Friedmann JM, Katsen AD, Hauser IA (2000) Up-regulation of multidrug resistance P-glycoprotein via nuclear factor-κB activation protects kidney proximal tubule cells from cadmium- and reactive oxygen species-induced apoptosis. J Biol Chem 275: 1887-1896

-Tinsley RC, Loumont C, Kobel HR (1996) Geographical distribution and ecology. The biology of *Xenopus* (Tinsley RC, Kobel HR, eds), pp 35-59. Oxford, England: Clarendon Press

-Vernhet L, Allain N, Bardiau C, Anger JP, Fardel O (2000) Differential sensitivities of MRP1-overexpressing lung tumor cells to cytotoxic metals. Toxicology 142: 127-134

-Versantvoort CH, Bagrij T, Wright KA, Twentyman PR (1995) On the relationship between the probenecid-sensitive transport of daunorubicin or calcein and the glutathione status of cells overexpressing the multidrug resistance-associated protein (MRP). Int J Cancer 63: 855-862

-Vogl A, Noe J, Breer H, Boekhoff I (2000) Cross-talk between olfactory second messenger pathways. Eur J Biochem 267: 4529-4535

-Vogler C, Schild D (1999) Inhibitory and excitatory responses of olfactory receptor neurons of *Xenopus laevis* tadpoles to stimulation with amino acids. J Exp Biol 202: 997-1003

-Wong ST, Trinh K, Hacker B, Chan GC, Lowe G, Gaggar A, Xia Z, Gold GH, Storm DR (2000) Disruption of the type III adenylyl cyclase gene leads to peripheral and behavioral anosmia in transgenic mice. Neuron 27: 487-97

-Zhainazarov AB, Ache BW (1995) Odor-induced currents in *Xenopus* olfactory receptor cells measured with perforated-patch recording. J Neurophysiol 74: 479-483

-Zufall F, Leidners-Zufall T, Greer CA (2000) Amplification of odor-induced Ca^{2+} transients by store-operated Ca^{2+} release and its role in olfactory signal transduction. J Neurophysiol 83: 501-512

-Zufall F, Munger SD (2001) From odor and pheromone transduction to the organization of the sense of smell. Trends Neurosci 24: 191-193

6. Acknowledgements

7. Curriculum Vitae

Personal data

Name: Ivan Manzini

Date of birth: 26. 04. 1974

Place of birth: Bolzano, Italy

Nationality: Italian

School education

1980-1985   Primary School J. H. Pestalozzi, Bolzano

1985-1988   Secondary School A. Schweitzer, Bolzano

1988-1993   Secondary High School H. Kunter, Bolzano

University education

October 1993-September 1999   University of Modena and Reggio Emilia, Modena
Diploma in Biological Sciences
Diploma work in the laboratory of Prof. Pier Cosimo
Magherini, Department of Biomedical Sciences
Subject: Synaptic activity mediated by glutamatergic
receptors in the substantia gelatinosa in rat spinal
cord

October 1999-January 2003   University of Göttingen, Göttingen
PhD in the laboratory of Prof. Dr. Dr. Detlev Schild,
Department of Molecular Neurophysiology
Subject: Diversity of transduction mechanisms in
receptor neurons of the main olfactory epithelium in
Xenopus laevis tadpoles